

The Late Quaternary Evolution of the Southern Vietnamese Continental Shelf

Dissertation
zur Erlangung des Doktorgrades
der Mathematisch-Naturwissenschaftlichen Fakultät
der Christian-Albrechts-Universität zu Kiel

Vorgelegt von

Bui Viet Dung

2011

Referent: Prof. Dr. Karl Stattegger

Koreferent: Prof. Dr. Gert Jan Weltje

Tag der mündlichen Prüfung: 13.04.2011

Zum Druck genehmigt: Ja

Der Dekan: Prof. Dr. Lutz Kipp

Contents

Contents	i
List of figures	iv
List of tables	ix
Acknowledgements	x
Abstract.....	xi
Zusammenfassung	xiii
1. Introduction	1
1.1 Objectives and approach.....	3
1.2 Structure of the thesis	3
1.3 Geological setting of study area	4
1.4 Climate and oceanographic conditions of study area	5
1.5 Late Quaternary sea-level changes in study area.....	6
1.6 Data and general method	7
1.6.1 Seismic stratigraphy	8
1.6.2 Numerical modeling	11
References	12
2. Late Pleistocene-Holocene seismic stratigraphy on the South East Vietnam Shelf	
Abstract	15
2.1 Introduction	17
2.2 Regional setting	18
2.3 Methods and available data	20
2.4 Results	22
2.4.1 Seismic units and bounding surfaces.....	22
2.4.2 Sedimentary characteristics and ages of deposits.....	24
2.4.3 Continental shelf architecture.....	24
2.4.4 Late Pleistocene-Holocene sequence stratigraphic model for the SE Vietnam Shelf and controlling factors	34
2.5 Discussion and conclusions	40
References	42

3. Late Pleistocene-Holocene seismic stratigraphy of the Nha Trang Shelf, Central Vietnam

Abstract	47
3.1 Introduction	49
3.2 Regional setting	49
3.3 Methods and available data	52
3.4 Results	54
3.4.1 Sequence stratigraphic analysis	54
3.4.2 Sedimentary characteristics and ages of deposits.....	59
3.4.3 Sequence stratigraphic interpretation	64
3.5 Proposed sequence stratigraphic model for the Nha Trang Shelf	69
3.6 Discussion and conclusions	74
References	76

4. Flux and fate of sediments on the Nha Trang Shelf (central Vietnam) since the Last Glacial Maximum (LGM): field measurements and process-based modeling

Abstract	81
4.1 Introduction	83
4.2 Regional setting	84
4.3 Numerical modeling	86
4.3.1 The 3D Simclast model	86
4.4 Input data	90
4.4.1 Sediment and water discharge	90
4.4.2 Sediment thickness data from seismic profiles	93
4.4.3 Sea-level data.....	96
4.4.4 Initial bathymetry from seismic profiles	97
4.5 Results and discussion	98
4.5.1 Sensitivity experiments	98
4.5.2 Predicted sediment supply to the shelf during HST and TST period	104
4.5.3 Final simulation of sedimentation on the Nha Trang Shelf.....	105
4.5.3.1 Input data	105
4.5.3.2 Sedimentation over 19.6 ky (deglaciation/Holocene)	106
4.6 Discussion.....	109
4.7 Conclusions	110
References	112

5. General conclusions.....	115
References	118

List of figures

- Fig 1.1** Map of the SCS and two studied areas on the southern Vietnam shelf: SE shelf (a) and Central Shelf off Nha Trang (b).....2
- Fig 1.2** Shaded elevation map with major tectonic faults (red line) and Cenozoic basins on the study area. Locations of Cenozoic basins and faults are adapted from Longman (1993) and Clift et al. (2008). 4
- Fig 1.3** Monsoon-driven surface current system in the SCS in June (left) and December (right) (Wyrтки 1961). 6
- Fig 1.4** Sea-level curves over the past 130 ky (a) and LGM/deglacial period for SE Asia (Hanebuth et al., 2004; Shackleton 1987; Chappell et al 1996; Fleming et al 1998; Statterger et al., in prep)..... 7
- Fig 1.5** Map of the southern Vietnam Shelf and seismic profiles used in this thesis. 8
- Fig 1.6** Classification of seismic facies and related depositional environments adapted from Badley (1985), Vail (1987) and Veenken (2007). Types of seismic strata terminations are modified after Catuneanu (2002). 9
- Fig 1.7** Sequence stratigraphic systems tracts as defined by the interplay between base level changes and sedimentation rate (modified from Catuneanu 2002). For simplicity, the sedimentation rate is kept constant during the base level fluctuations. 10
- Fig 2.1** Map of the South East Vietnam Shelf with seismic profiles. Lower small map shows locations of seismic profiles (black lines) and sediment cores (blue circles) used in this research. Elevation data of the land part is extracted from Shuttle Radar Topography Mission (SRTM) digital elevation models (<http://srtm.usgs.gov>). 19
- Fig 2.2** Classification of seismic facies and related depositional environments adapted from Badley (1985), Vail (1987) and Veenken (2007). 21
- Fig 2.3** Sequence stratigraphic systems tracts as defined by the interplay between base level changes and sedimentation rate (modified from Catuneanu 2002). For simplicity, the sedimentation rate is kept constant during the base level fluctuations. 22
- Fig 2.4** Seismic profiles (a) and sequence stratigraphic interpretation (b) of the LGM lowstand wedge deposits. The upper part of the wedge was probably reworked and eroded taking the LGM sea-level (Hanebuth et al., 2009) as reference. Core ages are cited from Schimanski and Statterger (2005). For abbreviations see Table 2-1. 28
- Fig 2.5** Seismic profiles (a) and sequence stratigraphic interpretation (b) of northern incised-valley with different tributaries. Core results indicate a transition from fluvial (Te) in the lower to transition lithology (Tr) in the mid and fully marine

	influence (Ma) in the uppermost part (Tjallingii et al., 2010). For abbreviations see Table 2-1.....	30
Fig 2.6	Seismic profiles (a) and sequence stratigraphic interpretation (b) of northern incised-valley with point-bar structure. For abbreviations see Table 2-1.	31
Fig 2.7	Seismic profiles (a) and sequence stratigraphic interpretation (b) of southern incised-valley off modern Mekong Delta. Top of the channel is covered by numerous active sandwaves. For abbreviations see Table 2-1.....	32
Fig 2.8	Part of seismic profile showing thick highstand wedge deposits (U5) of the modern Mekong Delta. Seismic profiles (a) and sequence stratigraphic interpretation (b). For abbreviations see Table 2-1.....	33
Fig 2.9	The last glacial lowstand surface-morphology with reference to the present sea-level. Red numbers indicate depth below present sea-level of the lowstand surface identified from sediment cores on land (Hoang 2002; Ta et al., 2002b).....	35
Fig 2.10	Thickness map of deglacial/Holocene sediments. The sediment depocentres are located mostly within the incised-valleys, the modern Mekong subaqueous delta and the narrow outer shelf off Phu Quy Island. Thickness of the eastern Mekong subaqueous delta is roughly calculated from sediment cores on land and bathymetry.....	36
Fig 2.11	Thickness of modern highstand sediments (last 8 ky) constructed from seismic profiles. The northern part of the HST is not shown on the map. The HST sediments depocentre locates off Cape Camau and the wedge tends to develop toward the Gulf of Thailand to the west.	37
Fig 2.12	Distribution of late Pleistocene-Holocene depositional systems on the SE Vietnam Shelf constructed from seismic profiles. Red line shows the HST boundary indentified from seismic profiles and the northern boundary of the HST wedge is roughly indicated from thickness map shown on Fig 2.9.....	38
Fig 2.13	Late Pleistocene-Holocene sequence stratigraphic model for the SE Vietnam Shelf (a) with regional sea-level curve (b) (Stattegger et al, in prep) and comparison to theoretical models of Vail (c) and Zaitlin (d).....	39
Fig 3.1	Map of Nha Trang Shelf with modern bathymetry and available data (seismic profiles and sediment cores). Locations of geological faults adapted from Fyhn et al. (2009) and Clift et al. (2008). Elevation data of the land part is extracted from Shuttle Radar Topography Mission (SRTM) digital elevation models (http://srtm.usgs.gov).....	51

Fig 3.2	Classification of seismic facies and related depositional environments adapted from Badley (1985), Vail (1987) and Veenken (2007).....	53
Fig 3.3	Sequence stratigraphic systems tracts as defined by the interplay between base level changes and sedimentation rate (modified from Catuneanu 2002). For simplicity, the sedimentation rate is kept constant during the base level fluctuations.....	54
Fig 3.4	Seismic profile (a) and sequence stratigraphic interpretation (b) of the transition from inner to outer shelf on the northern part off Hon Gom Peninsula. AMS dating indicates very young highstand deposits (0.42 and 0.86 ky BP). Core data adapted from Wiesner et al., (2006). For abbreviations see Table 3-1.....	58
Fig 3.5	Seismic profile (a) and sequence stratigraphic interpretation (b) of the outer shelf off Hon Gom Peninsula with the complete record of systems tracts. Core data adapted from Wiesner et al., (2006). For abbreviations see Table 3-1.....	60
Fig 3.6	Seismic profile (a) and sequence stratigraphic interpretation (b) of the inner shelf of Van Phong Bay with aggradational stacking patterns of deglacial deposits. Discrimination between HST and TST is hardly resolved. For abbreviations see Table 3-1.....	61
Fig 3.7	Seismic profile (a) and sequence stratigraphic interpretation (b) of the mid and outer shelf of Van Phong Bay. For abbreviations see Table 3-1.....	62
Fig 3.8	Seismic profile (a) and sequence stratigraphic interpretation (b) of the transition from the inner to outer shelf of Nha Trang Bay. For abbreviations see Table 3-1...	63
Fig 3.9	Seismic profile (a) and sequence stratigraphic interpretation (b) offshore Nha Trang Bay. Regressive unit (U1) is toplap truncated by the lowstand surface (SB1) and overlain by deglacial/Holocene deposits (U3 and U4). Core data adapted from Schimanski and Statterger (2005).....	64
Fig 3.10	Total sediment thickness map of sequence 2 (U0, U1 units) and U2 unit. Thick deposits on the outer shelf resulted from well developed regressive units (U1 and U2) which are pinching out landward at water depth of 100-120 m.....	65
Fig 3.11	Contour map of the LGM surface (depth below the modern sea-level) constructed from seismic profiles. Basically the lowstand surface was blocked at the LGM sea-level around -125 to -140 m and its seaward extension was merged with the transgressive surface (TS).....	66
Fig 3.12	Total deglacial/Holocene sediment thickness (sequence 1) including U3 and U4 units. The sediment depocentre is located on the mid shelf.	68
Fig 3.13	Sediment thickness map of HST (a) and TST (b) of sequence 1. HST depocentre is located on the mid shelf in front of Van Phong and Nha Trang Bay. HST deposits	

are probably transported along-shore southward. The TST deposits develop over the shelf without significant sediment depocentre.	69
Fig 3.14 Late Pleistocene-Holocene sequence stratigraphic model for the Nha Trang Shelf (a) with regional sea-level curve (b) (Hanebuth et al., 2004; Shackleton 1987; Chappell et al., 1996; Fleming et al., 1998) and comparison to theoretical models of Zaitlin (c) and Vail (d).....	73
Fig 4.1 Map of the Nha Trang Shelf with modern bathymetry and available seismic profiles. Elevation data of the land part is extracted from Shuttle Radar Topography Mission (SRTM) digital elevation models (http://srtm.usgs.gov).....	85
Fig 4.2 Flow chart of the fluvial module (Dalman 2009).....	87
Fig 4.3 Flow chart of the continental shelf module (Dalman 2009).....	89
Fig 4.4 Rivers and streams of three main local basins draining into the Nha Trang Shelf...	90
Fig 4.5 Rating curve for sediment load to discharge conversion.....	92
Fig 4.6 Total deglacial sediment thickness and its frequency distribution histogram on the Nha Trang Shelf derived from seismic data (Fig 3.12, Chapter 3, Bui et al., in prep).....	93
Fig 4.7 Sediment thickness map of HST (a) and TST (b) on the Nha Trang Shelf. Thickness frequency distributions are derived from seismic data (Fig 3.13, Chapter 3, Bui et al., in prep).	95
Fig 4.8 Sea-level data and deglacial sea-level curve for the Sunda and Southern Vietnam Shelf (Hanebuth et al., 2000; Hanebuth et al., 2009; Statterger et al., in prep.).....	96
Fig 4.9 The model grid of the LGM lowstand surface with 87 rows and 57 columns of 1 km ² cell size and LGM coastline.....	97
Fig 4.10 Net sediment preservation (a) and erosion/deposition with morphology of the coastline after 1 ky simulation (b) with different coarse fraction of fluvial and sub-surface sediment. Red arrows indicate river entries.	99
Fig 4.11 Net sediment preservation (a) and erosion/deposition with morphology of the coastline after 1 ky simulation (b) with different deep water wave heights. Red arrows indicate river entries.	100
Fig 4.12 Erosion/deposition during HST (8.0-0 ky BP) and morphology of the coastline at 0 ky BP with different percentage of sediment supply from the north. Red arrows indicate river entries.	102
Fig 4.13 Erosion/deposition during TST (19.6-8.0 ky BP) and morphology of the coastline at 8.0 ky BP with different percentage of sediment supply from the north. Red arrows indicate river entries.	103

Fig 4.14 Correlation between percentage of sediment supply from the north and net sediment preserved on the shelf.	104
Fig 4.15 Sediment thickness distribution at different periods from 19.6-0 ky BP (Deglaciation/Holocene) with reference to the coastline evolution (Fig 4.16).	107
Fig 4.16 Coastline (yellow color) evolution over 19.6 ky (Deglaciation/Holocene) from final simulation. The real modern coastline is shown by red line. Negative values indicate the elevation on land and positive values indicate water depth at sea.	108
Fig 4.17 Sediment thickness distribution over 19.6 ky (Deglaciation/Holocene) from final simulation with reference to modern coastline.	110
Fig 5.1 Late Pleistocene-Holocene sequence stratigraphic model for the SE and Central Vietnam Shelf.	115

List of tables

Table 2.1	Systems tracts, seismic units and facies, bounding surfaces and reflection patterns on the SE Vietnam Shelf. Abbreviations: LST = Lowstand systems tract, TST = Transgressive systems tract, HST = Highstand systems tract.	27
Table 3.1	Systems tracts, seismic units and facies, bounding surfaces and reflection patterns on the Nha Trang Shelf. Abbreviations: FSST = Falling state systems tract, LST = Lowstand systems tract, TST = Transgressive systems tract, HST = Highstand systems tract.	56
Table 4.1	Input parameters and sediment load of three main basins from denudation rate. Average denudation rate adapted from Einsele (2000).	91
Table 4.2	Input parameters and sediment load of three main basins from BQART equation.	92
Table 4.3	Parameters of sensitivity experiments	98
Table 4.4	Simulation scenarios and percentage of sediment preserved on the shelf.....	101
Table 4.5	Input parameters of the final simulation.....	106

Acknowledgements

First of all, I would like to express my deep gratitude to my supervisor Prof. Dr. Karl Stattegger for a lot of guidance and supports during the period of working and writing the thesis.

Secondly, I would like to thank Prof. Dr. Gert Jan Weltje for constructive discussions and help about sequence stratigraphy and numerical modeling.

Dr. Rory Dalman is thanked for supporting the work with Simclast model.

I thank Nguyen Trung Thanh, Nguyen Cong Thanh, Daniel Unverricht, Dr. Rik Tjallingii and Dr. Tran Tuan Dung for numerous useful discussions. I thank Christoph Heinrich for English-German translation of the abstract.

I am grateful to the DFG and MOST for funding the project. I would like to thank Dr. Phung Van Phach for excellent organization of the project.

Also, I would like to thank all of the crew and scientists who were involved in SO 140, SO 187, VG5, VG9, Mekong 2007 and Mekong 2008 cruises on the Vietnam shelf for excellent collected data.

Last but not least I thank my dear parents for their love, encouragement and standing by me during my PhD studies. I will always wish them all the best.

Abstract

The late Pleistocene-Holocene sedimentary architecture on two different geological setting areas on the Southern Vietnam Shelf has been investigated on the basis of shallow seismic data, sediment core data, sequence stratigraphic concepts and numerical modeling.

The Southeast (SE) Vietnam Shelf architecture since the Last Glacial Maximum (LGM) to present (25 ky) is composed of three systems tracts and a lowstand surface which has probably experienced multi-phases of the sea-level fall (regression stage), sea-level lowstand and was reworked again during transgression. The incised-channels of the paleo-Mekong river are found at modern water depths between 20 to 60 m with W-E to N-S orientation and show a clear change from north to south. The northern incised-channel branch off Vung Tau appears as narrow and deep V-shape in cross-section (<5 km wide and tens of meters deep) which probably resulted from the steep and more accentuated morphology of the shelf. By contrast, the southern incised-channels show an N-S orientation with a trend of decreasing in depth of incision (< 15 m deep) in comparison to the northern ones due to the lower gradient of shelf. LST deposits on the SE Vietnam Shelf consist of a prograding delta wedge and a lowstand erosional surface. TST was dispersed across the shelf as a layer overlying the sequence boundary SB1. The TST was mostly sheltered from marine erosional processes in the incised-valley depressions. The HST is primarily composed of thick prograding mud clinoforms of the modern Mekong subaqueous delta and it is pinching out at modern water depths of 20-30 m.

Evolution of the Nha Trang Shelf over 120 ky includes four systems tracts: FSST, LST, TST and HST. FSST and LST are well preserved on the modern outer shelf and they were pinching out landward at water depth of around 100-120 m. The LST wedge deposits on the central shelf are only recorded in the steep gradient shelf off Hon Gom Peninsula and they are almost absent in the other parts of study area. The relict beach-ridge deposits identified at water depth of about ~ 130 m below present sea-level indicate that the LGM sea-level lowstand in this area was lower than on the Sunda Shelf in the South. The difference probably resulted from subsidence due to high deglacial Holocene sedimentation and/or neotectonic movements of the East Vietnam Fault System. The LGM lowstand surface can be traced by seismic profiles across the shelf. This surface shows a relatively high gradient in the middle part and becomes gentler toward the inner and outer shelf as well as from northern to the southern part of study area. TST deposits on the Nha Trang Shelf were accumulated across the shelf with significant thickness. The TST shows a clear transition from backstepping to aggradational

stacking patterns from outer to inner shelf. HST is formed as a shore-parallel mid-shelf clinoform and its thickness decreases toward the inner and outer shelf.

The late Pleistocene-Holocene sequence stratigraphic models of the SE Vietnam and Nha Trang Shelf show distinctive features which result from the differences in sediment supply regime, shelf morphology and hydrodynamic conditions between the two areas. On the SE Vietnam Shelf, the thick HST wedge is confined to the inner shelf leaving the mid and outer shelf in starving condition. The HST depocentre on the Nha Trang Shelf is located on the mid shelf forming a clinoform and it is thinning toward the inner and outer shelf. TST deposits on the SE Vietnam Shelf are often thin and widely dispersed over the shelf. By contrast, TST deposits on the Nha Trang Shelf were stacked much thicker than their counterparts on the low-gradient shelf of the SE Vietnam Shelf. Incised-channels are almost absent on the Nha Trang Shelf but they are very well recorded on the SE Vietnam Shelf. LST wedge deposits are recorded in both areas below 100 m water depth on the outer shelf. The LST wedge deposits on the SE Vietnam Shelf are thicker than on the Nha Trang Shelf.

Sedimentation on the Nha Trang Shelf (Central Vietnam) from the end of the LGM to present has been investigated on the basis of process-based numerical modeling simulations and shallow seismic data. The results show that the annual sediment supply to the Nha Trang Shelf during HST period (8.0-0 ky BP) ranges from: 4.1 to 5.1 million tons of sediment per year (Mt/y). 42 to 59 % of supplied sediments during HST period are accumulated on the shelf and the rest are mostly transported alongshore southward. The annual sediment supply to the Nha Trang Shelf during TST period (19.6-8.0 ky BP) ranges from: 10.9 to 19.8 Mt/y. 27 to 50 % of supplied sediments during TST period were stored on the shelf and significant amount of sediments escaped from the shelf to the continental slope during early transgression and were transported alongshore to the south. During HST and TST period, 50-80 % of total supplied sediment was contributed by three local river basins (Cai, Dinh and Van Phong) and the rest was transported alongshore from the north. Cai River was the most important local sediment source which contributed 2 to 6 times more sediment than Dinh and Van Phong River, respectively. Sedimentation on the Nha Trang Shelf from the end of the LGM to present has been estimated by modeling simulation. In general, the results of the model simulation are quite compatible to the field data. Some differences between these two approaches suggest that an improvement of input database as well as model calibration is needed.

Zusammenfassung

Auf der Basis von Flachwasser-Seismik, Sedimentkernen, sequenzstratigraphischen Konzepten und numerischen Modellsimulationen wurde der spätpleistozäne bis holozäne sedimentäre Aufbau zweier, von der Genese unterschiedlicher Gebiete des südvietnamesischen Schelfs untersucht.

Die Entwicklung des südvietnamesische Schelfs zeigt seit dem letzten glazialen Maximum (LGM) bis in die Gegenwart (25 ky) drei Systemtrakte und eine Grenzfläche des Meeresspiegeltiefstandes, welche vermutlich mehre Stadien der Absenkung des Meeresspiegels (Regression) und Aufarbeitung während der Transgression erfuhren. Man findet eingeschnittenen Kanäle des Paläo-Mekong, die bei heutigen Wassertiefen von 20 m bis 60 m liegen und welche eine klare Veränderung von Nord nach Süd zeigen.

Der nördliche Arm des eingeschnittenen Mekong-Tals bei Vung Tau ist schmal und im Querschnitt v-förmig ausgebildet (< 5 km breit und mehrere 10er-Meter tief), was vermutlich an einer steilen und stark akzentuierten Morphologie des trocken gefallen Schelfs liegt. Im Gegensatz zu den nördlichen Kanälen zeigen die weiter südlich und mit N-S Orientierung gelegenen Paläo-Kanäle aufgrund einer flacheren Morphologie des Schelfes einen Trend zu geringeren Einschnittstiefen (< 15 m). Die Ablagerungen des Meeresspiegeltiefstandes (lowstand, LST) auf dem südvietnamesischen Schelf sind aus einem progradierenden Delta und einer erosiven Tiefstand-Oberfläche aufgebaut. Der transgressive Systemtrakt (TST) ist über den gesamten Schelf verteilt und liegt als Schicht über der Sequenzgrenze SB1 und ist dabei zum Großteil innerhalb der eingeschnittenen Täler von marinen Errosionsprozessen verschont geblieben. Dazu ist der Hochstand-Systemtrakt (HST) primär aus mächtigen progradierenden sigmoidalen Sedimentkörpern (Kliniform, cliniform) im Silt-/Tonbereich des modernen subaquatischen Mekong-Deltas aufgebaut und läuft in Wassertiefen von 20 m bis 30 m aus. Die Entwicklung des Nha Trang Schelfs über die letzten 120 ky dagegen beinhaltet vier Systemtrakte: FSST (Systemtrakt des fallenden Meeresspiegels, falling state system tract), LST, TST und HST. FSST und LST sind auf dem heutigen äußeren Schelf sehr gut erhalten und laufen landwärts bei einer Wassertiefe von ca. 100 m bis 120 m aus. Die keilförmigen LST Ablagerungen auf dem zentralen Schelf wurden nur in den steilen Schelfregionen bei der Insel Hon Gom aufgenommen und traten nicht in anderen Bereichen des Untersuchungsgebiets auf. Die fossilen Strandwallablagerungen, welche in Wassertiefen von ca. 130 m unter dem heutigen Meeresspiegel gefunden wurden, deuten darauf hin, dass während des LGM der Meeresspiegeltiefstand in dieser Region niedriger als am Sunda-Schelf im Süden war. Ein Grund für diese Differenz könnten etwa eine durch hohe postglaziale

Sedimentation verstärkte Subsidenz sein und/oder neotektonische Bewegungen des ostvietnamesischen Störungssystems. Die LGM Oberfläche des Tiefstandes (Sequenzgrenzfläche SB1) kann sehr gut auf dem Schelf entlang der seismischen Profile verfolgt werden. Diese zeigt einen starken Gradienten im mittleren Teil und wird deutlich flacher in Richtung des inneren und äußeren Schelfs, ebenso im nördlichen und südlichen Teil des Untersuchungsgebiets. Auf dem Nha Trang Schelf wurden 10er-Meter mächtige TST Ablagerungen mit abgelagert, wobei dieser Systemtrakt einen klaren Übergang von schrittweise retrogradierenden zu aggradierenden Mustern vom äußeren zum inneren Schelf zeigt. Der HST ist als küstenparallele Klinoform ausgebildet dessen Mächtigkeit zum inneren und äußeren Schelf abnimmt.

Das spätpleistozän-holozäne sequenzstratigraphische Modell des südvietnamesischen und des Nha Trang Schelfs zeigen deutliche Unterschiede in ihren Merkmalen, deren Ursache in den unterschiedlichen Randbedingungen, wie zum Beispiel Sedimentverfügbarkeit, Morphologie und Hydrodynamik liegen. Auf dem südvietnamesischen Schelf ist der mächtige HST auf den inneren Schelf hin begrenzt und blockiert dadurch die Sedimentzufuhr auf den mittleren und äußeren Schelf. Der Ablagerungsraum des HST auf dem Nha Trang Schelf liegt auf dem mittleren Schelf und bildet dort eine Klinoform welche zum inneren und äußeren Schelf hin ausläuft. Die Ablagerungen des TST auf dem südvietnamesischen Schelfs sind meist gering mächtig und weiträumig verteilt. Deutlich mächtiger dagegen sind die TST Ablagerungen auf dem engeren Nha Trang Schelf. Paläo- Kanäle sind auf dem südvietnamesischen Schelf gut ausgebildet, fehlen aber fast komplett auf dem Nha Trang Schelf.

In beiden Gebieten findet man auf dem Schelf keilförmige LST Ablagerungen unterhalb einer Wassertiefe von 100 m, wobei deren Mächtigkeit auf den dem südvietnamesischen Schelf deutlich größer sind als auf dem Nha Trang Schelf.

Die Sedimentation auf dem Nha Trang Schelf (Zentral-Vietnam) vom LGM bis in die Gegenwart wurde auf der Basis von prozessbasierten numerischen Modellsimulationen und Flachwasser-Seismik untersucht. In den Ergebnissen zeigt sich, dass die jährliche Sedimentzufuhr auf den Nha Trang Schelf während der HST-Periode zwischen 4.1 und 5.1 Million Tonnen pro Jahr liegt. Davon werden 42 bis 59 % auf dem Schelf akkumuliert und der restliche Anteil küstenparallel nach Süden abtransportiert. Die jährliche Sedimentzufuhr auf den Nha Trang Schelf während der TST-Periode dagegen erreicht Raten von 10.9 bis 19.8 Millionen Tonnen pro Jahr, wovon 27 bis 50.0 % auf dem Schelf abgelagert wurden. Ein signifikanter Anteil an Sediment aber wurde während des Frühstadiums der Transgression aus dem System in Richtung Kontinentalhang und dort küstenparallel nach Süden transportiert. 50 bis 80 % des zur Verfügung stehenden Sediments kommt aus den drei Flüssen (Cai, Dinh und

Van Phong). Das restliche Material wird von Norden her küstenparallel eingetragen. Der Cai-Fluss ist hier die größte Quelle für Sediment. Er liefert 2 bis 6 mal so viel Fracht wie die anderen Zuflüsse Dinh und Van Pong. Die Sedimentation auf dem Nha Trang Schelf vom Ende des LGM bis heute wurde mit Hilfe von Modellrechnungen simuliert. Die Ergebnisse sind gut mit den Felddaten vergleichbar. Einige Diskrepanzen zeigen jedoch, dass weitere Untersuchungen nötig sind, um die Datenbasis zu erweitern und eine bessere Kalibrierung des Modells vorzunehmen.

Chapter 1

General introduction

1 Introduction

The South China Sea (SCS) is largest marginal sea located on the western margin of the Pacific Ocean. It is bordered to the north and west by the passive continental margin of south China and Vietnam, to the east by the Pacific Ocean (Fig 1.1). The total area of the SCS is about 3.6 million km², the average depth of SCS is about 1140m and the maximum deep is about 5560 m (Pham 2003). During the late Quaternary period, the continental shelves around the SCS experienced different phases of exposure and flooding corresponding to regressive and transgressive periods as a result of relative sea-level change (interactions between eustasy, tectonics and sediment compaction). Variations in continental shelf's sedimentary architecture were particularly marked through these periods, reflecting the interplay of local sediment supply, hydrodynamic conditions and sea-level fluctuations. Investigation the sedimentary architecture of the shelf will therefore reveal the characteristics of these specific governed processes which are crucial for predicting their future behavior. On the other hand, this can also improve the understanding of land-ocean interactions since the continentals shelf lies at the interface of these two environments. This PhD thesis is a part of the Vietnamese-German cooperation project in marine research "*Land-ocean-atmospheric interactions in the coastal zone of Southern Vietnam*" that was launched in 2003. In the framework of several sub-projects, high resolution seismic profiles and sediment samples have been collected on the Vietnam Shelf. Those data allow us to have a deep insight into the late Pleistocene-Holocene evolution of the Vietnam Continental Shelf.

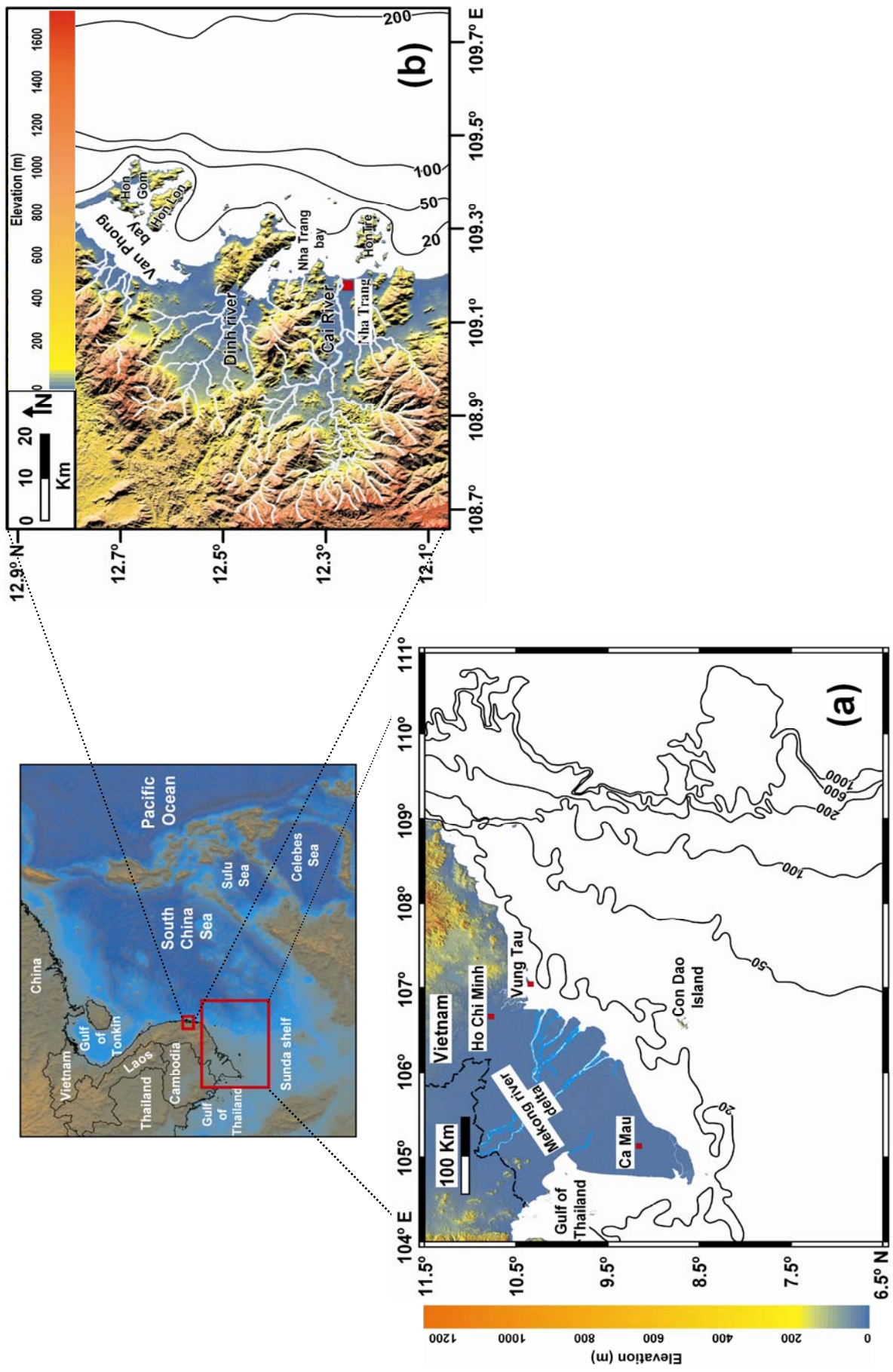


Fig 1.1. Map of the SCS and two studied areas on the southern Vietnam Shelf: SE Shelf (a) and Central Shelf off Nha Trang (b).

1.1 Objectives and approach

Normally, seismic data are viewed as two-dimensional time sections which supply two-way travel time (TWT) maps of sub-surface reflectors. In combination with sediment core data, seismic profiles can be used to indicate temporal as well as spatial changes within the subsurface sediments. Besides, information from regional sea-level curves can provide a general framework of continental shelf evolution for the seismic interpretation processes. The major purposes of this PhD thesis are to investigate and reconstruct the evolution of the southern Vietnam Continental Shelf during the late Pleistocene-Holocene period. Hence, our approach will combine high-resolution seismic profiles, sediment cores, surrounded regional area sea-level curves and numerical modeling. Seismic interpretation processes are carried with respect to sequence stratigraphic concepts. The specific aims of this thesis are:

- To analyze the late Pleistocene-Holocene seismic stratigraphic architecture on two different geological setting areas along the southern Vietnam Continental Shelf.
- To construct a sequence stratigraphic evolution model for the investigated areas as well as to evaluate the effects of the main local controlling factors.
- To hindcast the flux discharge and fate of sediments on the shelf by numerical modeling and comparison to field data.

1.2 Structure of the thesis

The thesis consists of 5 chapters. The contents of each chapter are described as following:

Chapter 1: short introduction to the study area, overall aims of the thesis, available data and general method.

Chapter 2: seismic-sequence stratigraphy of the broad and low-gradient shelf on the SE Vietnam since the Last Glacial Maximum (LGM).

Chapter 3: seismic-sequence stratigraphy of the high-gradient shelf off Nha Trang, southern central Vietnam for the last 120 ky.

Chapter 4: flux discharge and accumulation of sediments on the Nha Trang Shelf, southern central Vietnam since the LGM by numerical modeling and field data.

Chapter 5: general conclusions.

1.3 Geological setting of study area

The Vietnam Continental Shelf is situated at the western margin of the SCS and covers an area of $700 \times 10^3 \text{ km}^2$ (Pham 2003). Its general geometry consists of an asymmetric shape. The southern and northern parts are characterized by a wide and low gradient shelf. In contrast, the central part is marked by a narrow shelf (Fig 1.1). Our study area includes two different areas on the southern Vietnam Shelf: the southeast (SE) and southern Central Vietnam Shelf (Fig 1.1 and Fig 1.2). The continental shelf of the southern central part off Nha Trang is very narrow (40 km wide) with a high gradient ($\sim 0.3^\circ$). This area is surrounded by high mountains of Truong Son (Annamite) chain on the hinterland which supply sediments directly to the shelf via numerous small rivers (Fig 1.1). In contrast, the SE Shelf is much wider (80-450 km) with a very low gradient ($0.01\text{-}0.1^\circ$). On the hinterland, the Mekong River Delta plain covers most of area and is the major sediment supply for the SE Shelf (Fig 1.1).

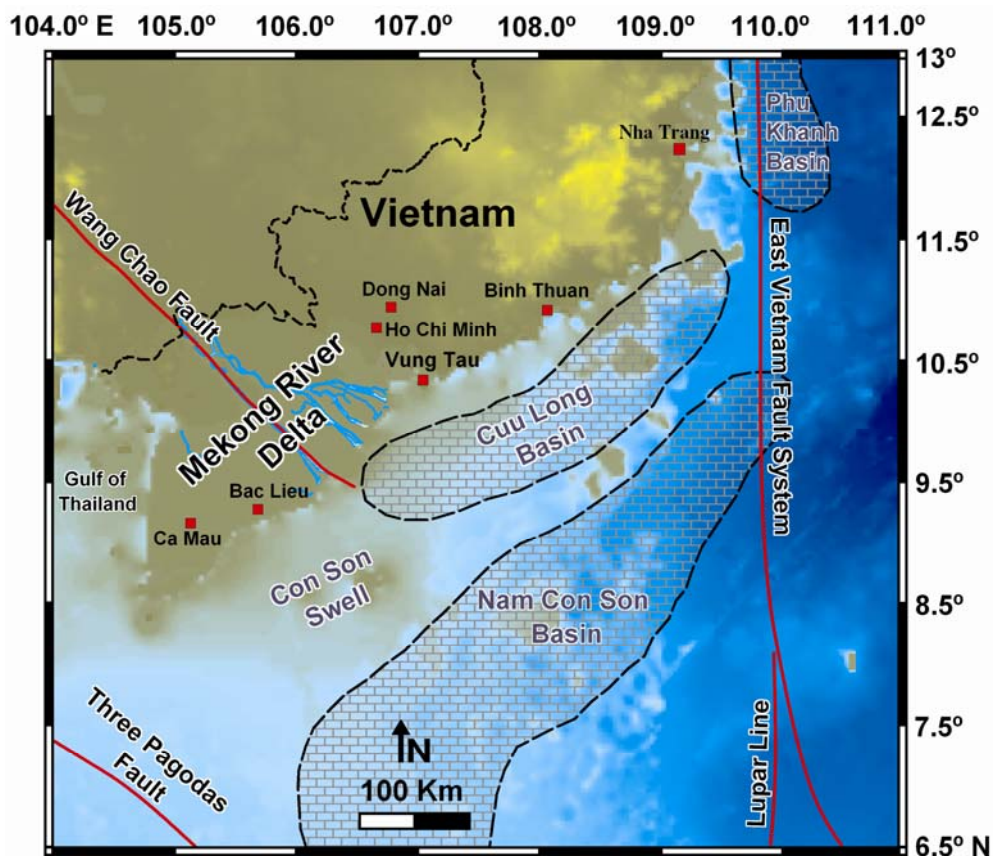


Fig 1.2. Shaded elevation map with major tectonic faults (red line) and Cenozoic basins on the study area. Locations of Cenozoic basins and faults are adapted from Longman (1993) and Clift et al. (2008).

Geological setting of the study area is generally controlled by the SCS evolution which was characterized by Cenozoic rifting phases that are suggested to be related to the opening of the

SCS around 32 to 15.5 Ma as a result of the India-Eurasia plate collision (Taylor and Hayes 1983; Briais et al., 1993). During the post rifting period (mid-Miocene to present), the study area was dominated by regional subsidence due to sediment loading and thermal cooling (Lee and Watkins 1998). Rifting phases during Cenozoic formed major subsiding and uplifting blocks in this area. Among them, Con Son Swell, Cuu Long and Nam Con Son Basins in the south and Phu Khanh Basin in the north are the most remarkable ones (Fig 1.2). The strike-slip East Vietnam Fault System running almost parallel to the shoreline along the 110⁰-Longitude, separates the continental shelf from the deep SCS areas (Fig 1.2). The NW-SE oriented Wang Chao Fault subdivided the modern Mekong Delta plain into two different parts with the uplift block in the southwest and subsidence in the northeast (Fig 1.2).

1.4 Climate and oceanographic conditions of study area

The climate and hydrodynamic conditions of the SCS including our study area are driven by the East Asian monsoon which is a part of the Asian monsoon system (An 2000). The East Asian monsoon is mainly controlled by temperature differences between the Asian continent and the Pacific Ocean. During winter monsoon, cold and dry air from high latitudes flows southward through the eastern margin of Tibetan Plateau to the SCS. During summer monsoon, warm and humid air from the low latitude of Indian Ocean flows northward through SCS to the Asian continent. In our study area, the sea surface circulation (Fig 1.3) is driven by seasonally reversing winds that blow stronger from northeast during winter (November to April) and weaker from southwest during summer (June to September). The transitional periods are marked by highly variable winds. Tide regime is quite complicated and varies along the southern Vietnam Shelf. Semi-diurnal tides govern the northeast (Vung Tau to Ca Mau Peninsula) with amplitudes of 2.5-3.8 m (Nguyen et al., 2000, Pham 2003). Diurnal tides develop in the western part (Ca Mau Peninsula and Gulf of Thailand) with amplitudes of 0.5-1 m (Nguyen et al., 2000, Pham 2003). The central shelf off Nha Trang is dominated by semi-diurnal to diurnal tide regime with amplitudes between 0.4 m in neap and 2.5 m in spring tide condition (Pham 2003, Szczuciński et al., 2005).

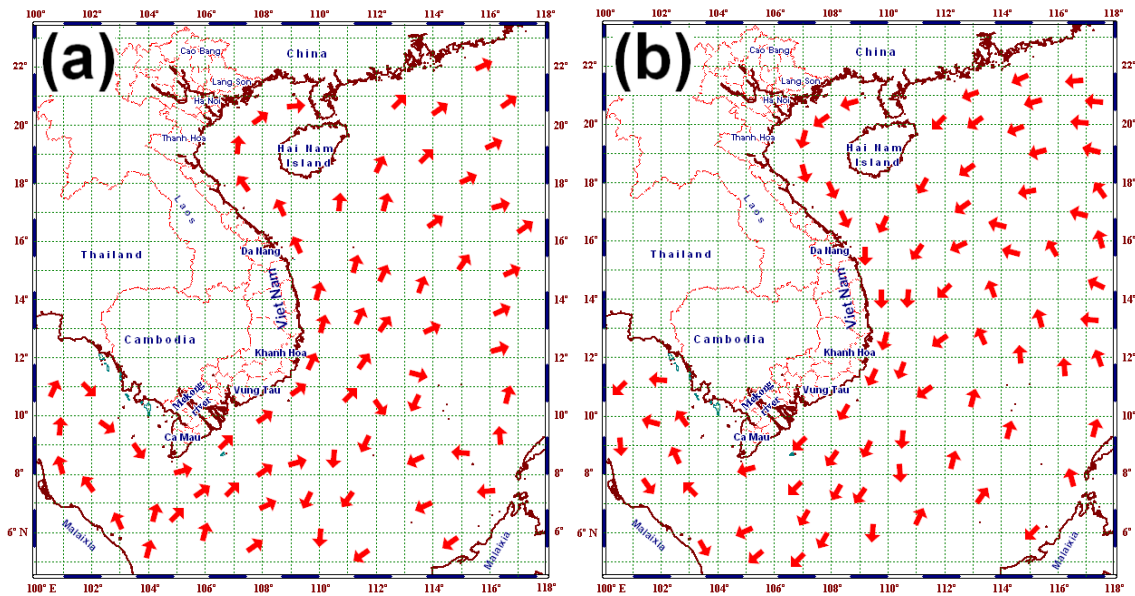


Fig 1.3. Monsoon-driven surface current system in the SCS in June (a) and December (b) (Wyrтки 1961).

1.5 Late Quaternary sea-level changes in study area

From the penultimate sea-level highstand during Marine Isotopic Stage (MIS) 5e, sea level dropped to the lowstand during MIS 2 (Fig 1.4). During the LGM period, the Vietnam Continental Shelf was subaerially exposed and became part of the SE Asia land as a result of the sea-level lowstand. The northern and southern continental shelves of Vietnam were significantly reduced in their size due to their broad and low-gradient shelf (Fig 1.1). River incision and subaerial erosion were the dominant processes on the shelf during the lowstand period. Sediment supplied from the continent was transported to the outer shelf via numerous incised-channels (Schimanski and Stattegger 2005). The minimum sea-level lowstand during the LGM in the SE Asian area was identified at 123 ± 2 m below the modern sea-level and it happened around 26-20 ky BP (Hanebuth et al., 2009). The LGM period was terminated by first sea-level rise pulse at 19.6 ky BP (Hanebuth et al., 2009) (Fig 1.4). The post-glacial sea-level rise period was marked by a linear tendency interfered by two major melt water pulses (MWP) (Hanebuth et al., 2000; Tjallingii et al., 2010) (Fig 1.4). The sea-level highstand positions varied along the Vietnam Shelf depending on local hydro-isostatic conditions. The maximum sea-level rise recorded on the Mekong Delta (southern part) was 2.5 m at 6.0-5.5 ky BP (Ta et al., 2002), 2-3 m at 6-4 ky BP on the Red River Delta (northern part) (Tanabe et al., 2003) and 1.5 m at 6.0-5.5 ky BP on the central Vietnam Shelf (Michelli 2008). After having reached the maximum position, sea-level started dropping linearly to its present-day position.

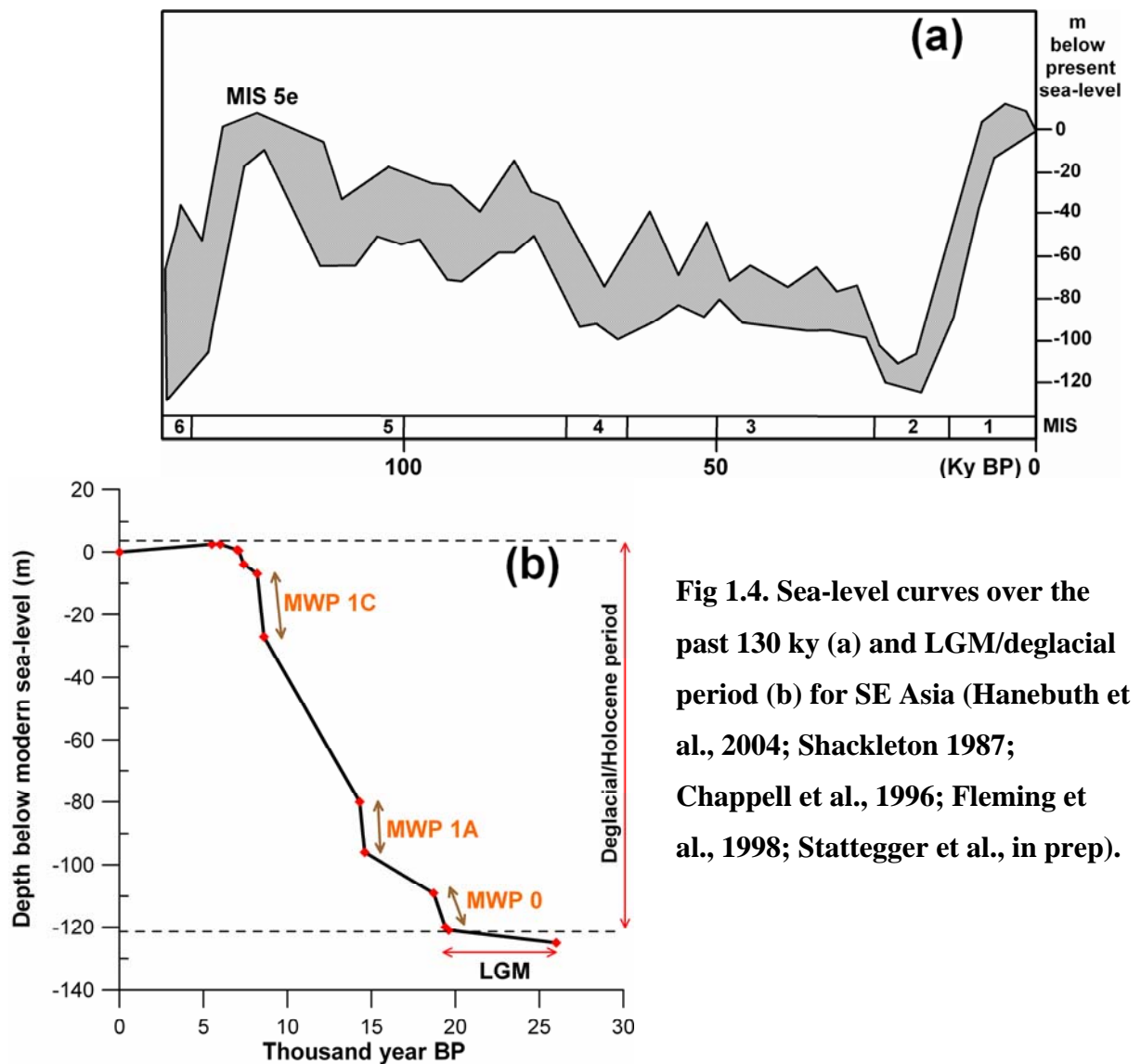


Fig 1.4. Sea-level curves over the past 130 ky (a) and LGM/deglacial period (b) for SE Asia (Hanebuth et al., 2004; Shackleton 1987; Chappell et al., 1996; Fleming et al., 1998; Stattegger et al., in prep).

1.6 Data and general method

High-resolution 2D seismic reflection data have been collected during different cruises along Southern Vietnam Shelf in the framework of the Vietnam-German cooperation project: SO 140 (Wiesner et al., 1999), VG5 (2004), VG9 (2005), SO187 (Wiesner et al., 2006) and Mekong (2007, 2008) (Fig 1.5). Since the objectives of the research concentrate on the continental shelf, seismic profiles were acquired mostly at water depths between 0 and 200 m (Fig 1.5). The collected seismic data were then processed to identify the principal seismic units. Sequence stratigraphic principles were applied to interpret the seismic architecture. In addition, the shelf sedimentation after the LGM was simulated by numerical modeling. Detailed characteristics of the applied methods and collected data are explained in three individual articles in chapter 2, chapter 3 and chapter 4:

- **Late Pleistocene-Holocene seismic stratigraphy on the South East Vietnam Shelf**
- **Late Pleistocene-Holocene seismic stratigraphy of Nha Trang Shelf, Central Vietnam**

➤ **Flux and fate of sediments on the Nha Trang Shelf (central Vietnam) since the Last Glacial Maximum (LGM): field measurements and process-based modeling**

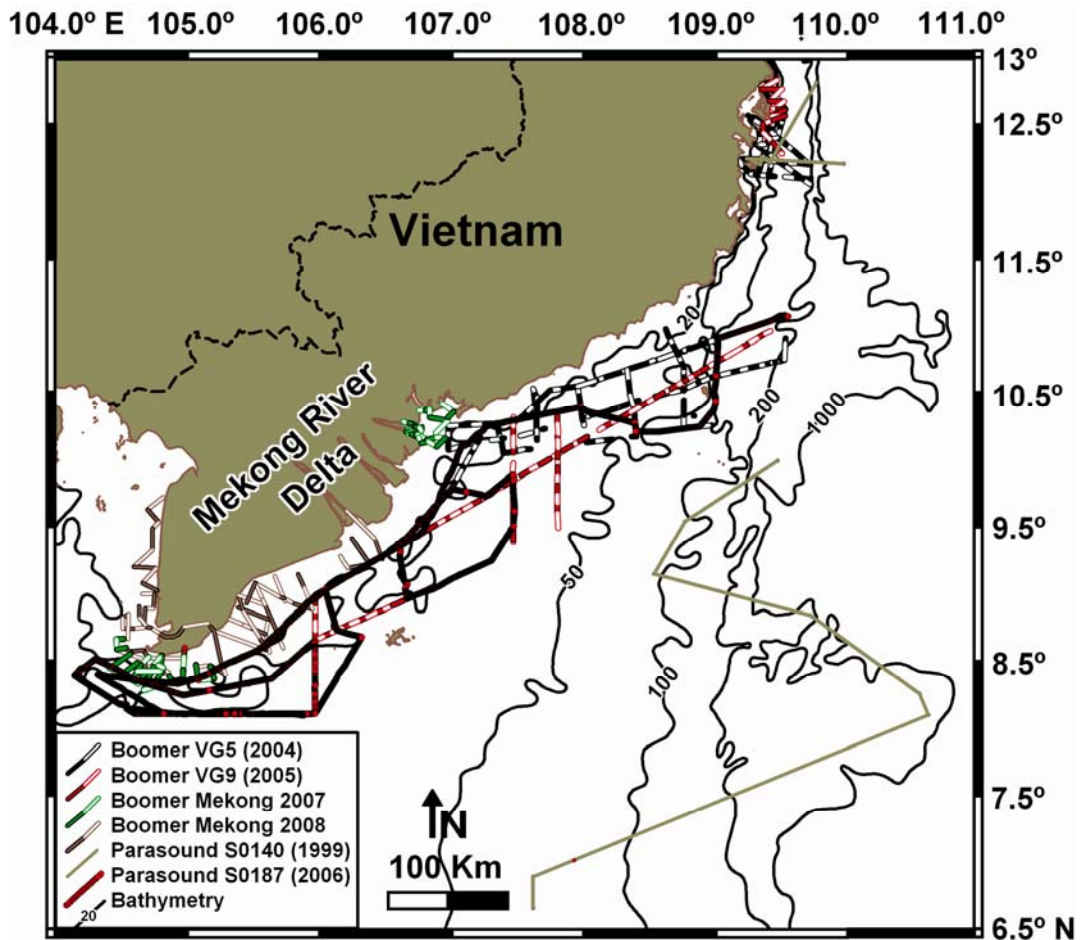


Fig 1.5. Map of the southern Vietnam Shelf and seismic profiles used in this thesis.

1.6.1 Seismic stratigraphy

Seismic data are interpreted on the basis of sequence stratigraphic concepts (Vail 1987). The seismic units are basically distinguished from each other by their reflection continuity, amplitude, frequency and configuration (Fig 1.6). Reflection continuity is associated with the continuity of strata and continuous reflections indicate uniform depositional processes. Reflection amplitude depends primarily on the acoustic impedance contrast along reflecting surfaces. In general, the amplitude of the reflected signal indicates the vertical impedance contrast in lithology. The reflection frequency relates to the vertical spacing between the zero-crossings on seismic trace (Veenken 2007). It can provide information on the spacing and possibly fluid content (occurrence of gas) of the bed. The configuration of seismic unit within the sequence is indicative of the depositional environments setting and processes (Fig 1.6).

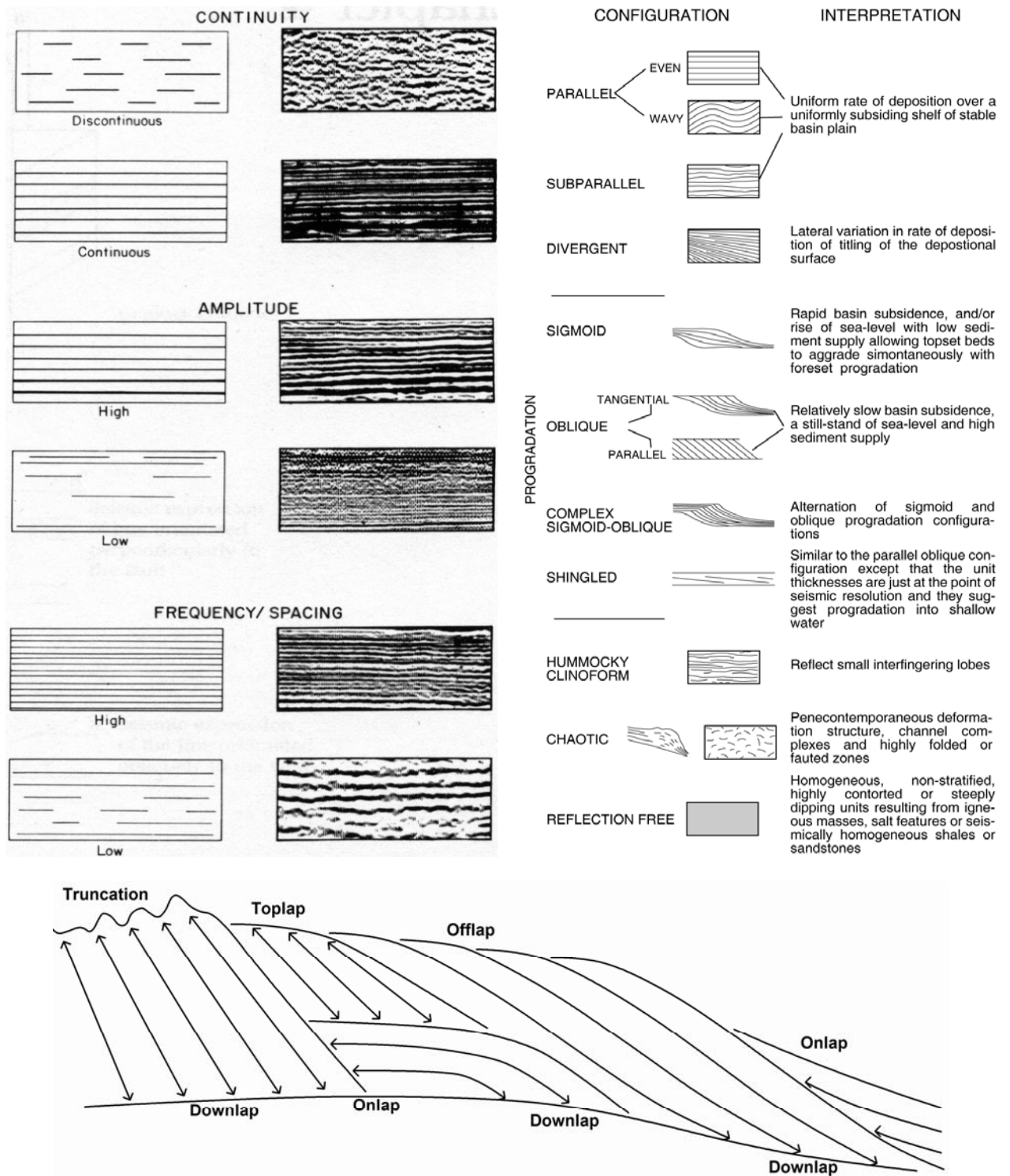


Fig 1.6. Classification of seismic facies and related depositional environments adapted from Badley (1985), Vail (1987) and Veenken (2007). Types of seismic strata terminations are modified after Catuneanu (2002).

Besides, the termination patterns of the seismic reflectors at the bounding surface as toplap, onlap, offlap, downlap and truncation (Fig 1.6) are also important criteria for identifying architecture of systems tracts (Catuneanu 2002). Downlap is often recognized at the base of prograding clinoforms and usually represents progradation of the basin margin. Onlap is identified by termination of low angle reflections against a steeper surface. Toplap is the termination of inclined reflections against an overlying lower angle surface. Truncation is termination of strata against an overlying erosional surface. Offlap is progressive offshore digression of the updip terminations of the sedimentary units within a conformable sequence of rocks (Catuneanu 2002). The interplay between base level changes (combined effect of eustasy, tectonics, sediment compaction, and environmental energy) and sedimentation rate controls the formation of sequence systems tract (Fig 1.7).

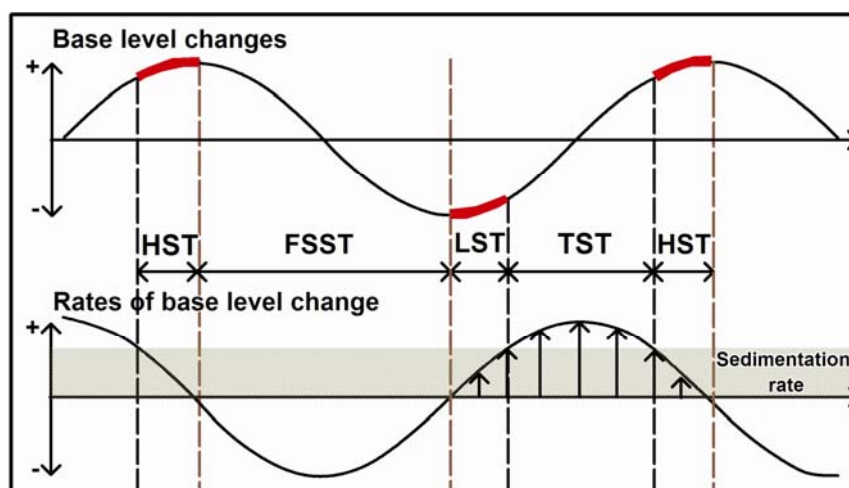


Fig 1.7. Sequence stratigraphic systems tracts as defined by the interplay between base level changes and sedimentation rate (Catuneanu 2002). For simplicity, the sedimentation rate is kept constant during the base level fluctuations.

For simplicity (by neglecting the energy of waves and currents), the base level is equated with the sea level (Catuneanu 2002). Hence, the concept of base level change is identical with the relative sea-level change. Accommodation is defined as the space available for sediments to accumulate and its variations depend on base level changes. In this research, we apply the four-fold division of systems tract to divide the sedimentary architecture into different stages in relation to sea-level fluctuations (Catuneanu 2002):

- **The falling stage systems tract (FSST)** was formed entirely during the stage of relative sea-level fall (forced regression), and it occurs independent of the ratio between the sedimentation rate and accommodation spaces.

- **The lowstand systems tract (LST)** was formed during the sea-level lowstand and slow sea-level rise when the rate of rise was lower than the sedimentation rate (normal regression).
- **The transgressive systems tract (TST)** was formed during the stage of relative sea-level rise when the rate of rise was higher than the sedimentation rate.
- **The highstand systems tract (HST)** was formed during the late stage of relative sea-level rise when the rate of rise was lower than the sedimentation rate.

1.6.2 Numerical modeling

In this research, we use the SimClast numerical modeling. It is a basin-scale 3D stratigraphic model, which was developed from 2004 to 2008 at Delft University of Technology, Holland (Dalman 2009). SimClast is a fully plan view 2D, depth-averaged model, which allows us to study the interaction between fluvial and marine processes. The principal characteristic of the model lies on its multi-scale simulation capacity. In which, the short-term and high-resolution processes model are coupled with the long-term stratigraphic model by implementing sub-grid scale processes into a large-scale basin-filling model. This parameterization refines morphodynamic behaviour and the resulting stratigraphy, while maintaining the computational efficiency. For the purpose of our research, the model uses 1 km scale grid-cell and time steps of 1 year. The model consists of two independent modules: the fluvial and continental shelf module. *The Fluvial Module* calculates fluvial discharge and sediment load along the river from the morphology and hydrodynamic conditions. Finally, the evolution of river channel is determined by comparing sediment load to transport capacity. The *Continental Shelf Module* calculates first hydrodynamic and sedimentation of the sediment plume released by the river. Then deep and shallow water wave celerity and orbital velocity are simulated. From the wave action reworking of the already settled sediment is determined. Finally, a transport algorithm calculates sediment movement and fallout.

References

- An ZS, Porter SC, Kutzbach JE, Wu X, Wang S, Liu X, Li X and Zhou W (2000). Asynchronous Holocene optimum of the East Asian monsoon. *Quaternary Science Reviews* 19, 743–762.
- Badley ME (1985). *Practical seismic interpretation*: International Human Resources Development Corporation, Boston, 266 pp.
- Briais A, Patriat P and Tapponnier P (1993). Updated interpretation of magnetic anomalies and seafloor spreading stages in the South China Sea: implications for the Tertiary tectonics of Southeast Asia. *Journal of Geophysical Research* 98, 6299-6328.
- Catuneanu O (2002). Sequence stratigraphy of clastic systems: concepts, merits, and pitfalls. *J.Afr. Earth Sci* 35, 1–43.
- Chappell J, Omura A, Esat T, McCulloch M, Pandolfi J, Ota Y and Pillans B (1996). Reconciliation of late Quaternary sea-levels derived from coral terraces at Huon Peninsula with deep sea oxygen isotope records. *Earth Planetary Science Letters* 141, 227–236.
- Clift P, Lee GH, N Anh Duc, Barckhausen U, H Van Long, and Sun Z (2008). Seismic reflection evidence for a Dangerous Grounds miniplate: No extrusion origin for the South China Sea. *Tectonics* 27, TC3008.
- Dalman R (2009). Multi-scale simulation of fluvio-deltaic and shallow marine stratigraphy. PhD thesis. University of Delft, 156 pp.
- Fleming K, Johnston P, Zwartz D, Yokoyama Y, Lambeck K and Chappell J (1998). Refining the eustatic sea-level curve since the Last Glacial Maximum using far- and intermediate-field sites. *Earth Planetary Science Letters* 163, 327–342.
- Hanebuth TJJ, Statterger K and Grootes PM (2000). Rapid flooding of the Sunda Shelf; A Late Glacial Sea-Level record. *Science* 288, 1033-1035.
- Hanebuth TJJ and Statterger K (2004). Depositional sequences on a late Pleistocene-

Holocene tropical siliciclastic shelf (Sunda Shelf, (SE Asia). *Journal of Asian Earth Sciences* 23, 113-126.

Hanebuth TJJ, Stattegger K and Bojanowski A (2009). Termination of the Last Glacial Maximum sea-level lowstand: The Sunda-Shelf data revisited. *Global and Planetary Change* 66, 76-84.

Lee GH and Watkins JS (1998). Seismic stratigraphy and hydrocarbon potential of the Phu Khanh Basin, offshore Central Vietnam, South China Sea. *AAPG Bulletin* 82, 1711–1735.

Longman MW (1993). Future bright for Tertiary carbonate reservoirs in Southeast Asia: *Oil & Gas Journal* 91(51), 107– 112.

Michelli M (2008). Sea-level changes, coastal evolution and paleoceanography of coastal waters in SE - Vietnam since the mid - Holocene. PhD thesis. University of Kiel, 160 pp.

Nguyen VL, Ta TKO and Tateishi M (2000). Late Holocene depositional environments and coastal evolution of the Mekong River Delta, Southern Vietnam. *Journal of Asian Earth Sciences* 18(4), 427-439.

Pham VN (Editor) (2003). *Bien Dong Monograph. Vol. II –Meteorology, Marine Hydrology and Hydrodynamics*, Hanoi National University Publisher, Hanoi, 565 pp (in Vietnamese).

Schimanski A and Stattegger K (2005). Deglacial and Holocene Evolution of the Vietnam Shelf: Stratigraphy, Sediments and Sea-level change. *Marine Geology* 214, 365-387.

Shackleton NJ (1987). Oxygen isotopes, ice volume and sea-level. *Quaternary Science Reviews* 6, 183–190.

Stattegger K, Tjallingii R, Phung VP and Wetzel A (in prep). Holocene sea-level history of SE Asia and its global implications. To be submitted to *Global and Planetary Change*.

Szczuciński W, Jagodziński R, Nguyen TT, Kubicki A and Stattegger K (2005). Sediment dynamics and hydrodynamics during a low river discharge conditions in Nha Trang Bay, Vietnam. *Meyniana* 57,117-132.

Tanabe S, Hori K, Saito Y, Haruyama S, Vu VP and Kitamura A (2003). Song Hong (Red River) delta evolution related to millennium-scale Holocene sea-level changes. *Quaternary Science Reviews* 22, 2345-2361.

Ta TKO, Nguyen VL, Tateishi M, Kobayashi I, Tanabe S and Saito Y (2002). Holocene delta evolution and sediment discharge of the Mekong River, southern Vietnam. *Quaternary Science Reviews* 21(16-17), 1807-1819.

Taylor B and Hayes DE (1983). Origin and history of the South China Sea basin. In: D.E. Hayes (Editor). *The tectonic and geologic evolution of Southeast Asian seas and islands; Part 2: Geophysical Monograph*, 23-56.

Tjallingii, R, Stattegger K, Wetzel A and Van Phach P (2010). Infilling and flooding of the Mekong River incised valley during deglacial sea-level rise. *Quaternary Science Reviews* 29 (11-12), 1432-1444.

VAIL PR (1987). Seismic stratigraphy interpretation using sequence stratigraphy, Part 1: seismic stratigraphy interpretation procedure, *in* Bally, A.W., ed., *Atlas of Seismic Stratigraphy*, Vol. 1: American Association of Petroleum Geologists, *Studies in Geology* 27, 1–10.

Veenken P C H (2007). *Seismic Stratigraphy, Basin Analysis and Reservoir Characterisation*, vol. 37, 1st ed., 509 pp., Elsevier, Oxford.

Wiesner M, Stattegger K, Kuhnt W, et al. (1999). Cruise Report SONNE 140 SÜDMEER III, Reports Institut für Geowissenschaften 7, 157 pp.

Wiesner M, Stattegger K., Voß M, et al. (2006). Reports Institut für Geowissenschaften 23, 99 pp.

Wyrtki K (1961). Physical oceanography of the South Asian waters. Scientific results of marine investigations of the South China Sea and the Gulf of Thailand. NAGA Report. Scripps Institute of Oceanography, CA, 115 pp.

Chapter 2

Late Pleistocene-Holocene seismic stratigraphy on the South East Vietnam Shelf

Bui Viet Dung¹, Karl Stattegger¹, Phung Van Phach², Nguyen Trung Thanh²

¹*Institute of Geosciences, Kiel University, D-24118, Kiel, Germany*

²*Institute for Marine Geology and Geophysics, 18 Hoang Quoc Viet, Hanoi, Vietnam*

To be submitted to *Global and Planetary Change*.

Abstract

The late Pleistocene-Holocene sedimentary architecture of the Southeast (SE) Vietnam Shelf has been investigated by means of high resolution seismic profiles and core samples. Three systems tracts and a prominent seismic reflection surface at the base of the sequence are revealed. This surface (SB1) is widely recorded in seismic profiles, and it is interpreted as sequence boundary formed by subaerial processes during the late Pleistocene sea-level fall and subsequent marine reworking during transgression. Surface map of the lowstand surface is compiled from seismic profiles and sediment cores revealing the W-E to N-S oriented incised-valley system of the paleo-Mekong River. The incised-valleys can only be traced from 20 to 60 m of modern water depths and they show a clear change in morphology from north to south of study area. The northern incised-valley branch off Vung Tau appears as narrow and deep V-shape in cross-section (<5 km wide and tens of meters deep) which probably resulted from the high-gradient morphology of the shelf. By contrast, the wide and low-gradient shelf off the modern Mekong Delta and Ca Mau Peninsula created shallow incised-valleys (5-15 km wide and < 15 m deep) on the exposed self.

The lowstand systems tract (LST) consists of a prograding outer shelf delta-wedge which was formed during the Last Glacial Maximum (LGM) sea-level lowstand period. The transgressive systems tract (TST) is well preserved in the incised-valleys where its thickness reaches up to 15-25 m. As revealed by sediment cores and seismic facies, the TST deposits within incised-channels mark a transition from fluvial facies at the base to fully marine deposits in the upper part of the channels. On the exposed shelf and the interfluvial of the incised-channels, TST is presented as a layer mostly consisting of sand overlying directly the sequence boundary SB1 with variable thickness (0-15 m). The highstand systems tract (HST)

is primarily consisting of thick mud clinoforms of the modern Mekong subaqueous delta that prograded onto the shelf after the mid-Holocene sea-level highstand about 6.0-5.5 ky BP ago. The HST wedge tends to extend along-shore to the southwestern part with maximum thickness (30 m) recorded in Cape Ca Mau area. Seaward, it is pinching out at modern water depths of 20-30 m resulting in a veneer HST layer on the middle and outer shelf which is locally mixed with the lower transgressive deposits.

The proposed post-Pleistocene sequence-stratigraphic model for the SE Vietnam Shelf is different from the theoretical model of Vail (1987) in the sense that the thick highstand wedge is confined to the inner shelf due to the broad and low-gradient shelf morphology and strong local hydrodynamic conditions driven by the monsoon system. The TST tends to disperse on the shelf instead of forming a thick backstepping unit since accommodation space was created faster than sediment supply during the rapid transgression.

2.1 Introduction

The Southeast (SE) Vietnam Shelf is situated on the south western continental margin of the South China Sea (SCS) (Fig 2.1). During the Last Glacial Maximum (LGM) and deglacial periods, the SE Vietnam Shelf has experienced differential states of exposure and flooding corresponding to regressive and transgressive cycles as a result of sea-level fluctuations. Such variations gave strong influences on the sedimentary architecture of the continental shelf, reflecting the interactions between sediment supply, hydrodynamic conditions and sea-level change. Study of the sedimentary architecture of the shelf will therefore reveal the characteristics of the governing factors and paleo-processes, and improve our understanding of land-ocean interactions. Previous research on the late Quaternary sedimentation on the SE Vietnam Shelf mainly focused on the Mekong Delta plain with its Holocene evolution (Nguyen et al., 2000; Ta et al., 2001a; Ta et al., 2001b; Ta et al., 2002a; Ta et al., 2002b; Hori and Saito 2007; Tamura et al., 2007; Tamura et al., 2009). These studies conclude that the modern Mekong Delta has initiated around 8 ky Before Present (BP), prograding seaward ~250 km from Cambodia to the SCS during the last 6 ky and switching from a tide dominated to a mixed tide-wave dominated delta during the last 3 ky. Recent study on the SE Vietnam Shelf has focused on the Holocene sedimentation and suggest that the modern sediment accumulation rate on the SE Vietnam Shelf is in the range of 5-10 or 25-40 cm/ky at low hydrodynamic regime areas (Schimanski and Stattegger 2005). New results derived from hydro-acoustic surveys on the SE Vietnam Shelf have revealed numerous asymmetric NE-SW oriented bedforms (few meters high and hundreds meters long) found at water depths of 20-40 m (Kubicki 2008; Bui et al., 2009). Detailed studies on the late Quaternary sequence stratigraphy of the nearby continental shelf were concentrated on the central Sunda Shelf in the south (Hanebuth et al., 2000; Hanebuth et al., 2002; Hanebuth et al., 2003; Hanebuth and Stattegger 2004). Numerous results of sequence stratigraphy on the SE Vietnam Shelf focus only on the Cenozoic basin evolution and oil&gas potential. Research of the late Quaternary sequence stratigraphy on this shelf remains poorly published so far (Tjallingii et al., 2010). In this study, we will present results of the seismic-sequence stratigraphy analysis on the SE Vietnam Shelf with special regard to the post-Pleistocene period. The specific aims of this study are to:

- Investigate the late Pleistocene-Holocene seismic-sequence stratigraphic architecture on the SE Vietnam Shelf
- Reconstruct and propose a sequence stratigraphic model framework for the SE Vietnam Shelf since the LGM to present

- Compare the Vietnamese to other sequence stratigraphic models to infer local controlling factors

2.2 Regional setting

The SE Vietnam Shelf is bordered by a 600 km long coastline to the west, the SCS to the east, the Gulf of Thailand to the southwest and the Sunda Shelf to the south (Fig 2.1). Geological setting of the SE Vietnam Shelf is characterized by Cenozoic rifting phases that are suggested to be related to the opening of the SCS around 32 to 15.5 Ma as a result of the India-Eurasia plate collision (Taylor and Hayes 1983; Briaais et al., 1993). The SE Vietnam Continental Shelf (between 0-200 m deep) is narrow in the north (~80 km wide) and widens to the south and southwest (~450 km wide) (Fig 2.1). This transition is inherited from the hinterland morphology where it is dominated by high rocky mountain in the north and low-gradient area of the modern Mekong Delta plain in the south (Fig 2.1). The climate and hydrodynamic conditions of study area are driven by the East Asian monsoon which blow from northeast during winter (November to April) and from the southwest during summer (June to September) (Pham 2003). Tide regime on the SE Vietnam Shelf is generally considered to be non-uniform. From Vung Tau to Ca Mau Peninsula, semi-diurnal tides are well developed, whereas the southwestern part off Ca Mau Peninsula and Gulf of Thailand is dominated by diurnal tides. Tide amplitude varies from 2.5-3.8 m in the northeastern part off Vung Tau and reduces to 0.5-1 m toward Ca Mau Peninsula and Gulf of Thailand (Wolanski et al., 1996, Nguyen et al., 2000, Pham 2003). The Mekong River is most important sediment source for the SE Vietnam Shelf. It is initiated from the Tibetan Plateau and runs through six other countries upstream before reaching the sea in Vietnam, The river has annually suspended sediment discharges of about 160 million tons/y, with the highest proportion is from August to October (rainy season) and it significant reduces during February to May (dry season) (Milliman and Syvitski 1992; Nguyen et al., 2000, Pham 2003).

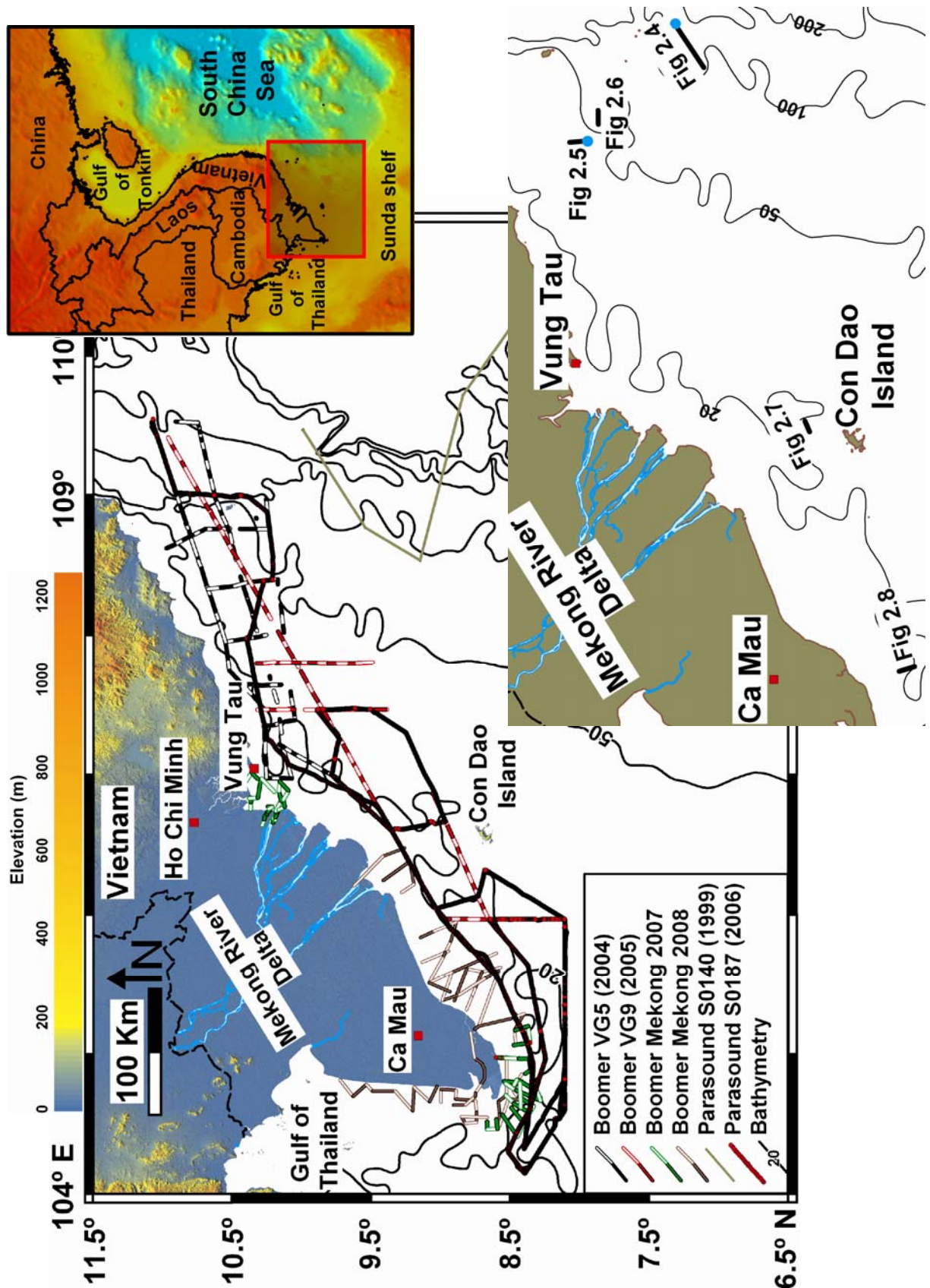


Fig 2.1. Map of the South East Vietnam Shelf with seismic profiles. Lower small map shows locations of seismic profiles (black lines) and sediment cores (blue circles) used in this research. Elevation data of the land part is extracted from Shuttle Radar Topography Mission (SRTM) digital elevation models (<http://srtm.usgs.gov>).

2.3 Methods and available data

For the present study, data of high resolution 2D seismic reflection are performed. Those data have been obtained during different cruises along Vietnam Shelf in the framework of the Vietnam-German cooperation project: SO 140 (Wiesner et al., 1999), VG5 (2004), VG9 (2005), SO187 (Wiesner et al., 2006) and Mekong (2007, 2008). Seismic data were acquired using two different sound-sources: boomer and parasound. Since the objective of the research concentrate on the shelf, seismic profiles are located mostly at water depths between 0 and 200 m (Fig 2.1).

Parasound is a hull-mounted system which combines a narrow beam echosounder with a sub-bottom profiler. The system is operated with a fix primary frequency of 18 kHz and a secondary primary frequency variable from 20.5–23.5 kHz. Both primary frequencies are transmitted simultaneously in a narrow beam ($\sim 4^\circ$) and the constructive interference of these frequencies (parametric effect) allows to generate a working frequency (secondary frequency) within the beam of 2.5–5.5 kHz (Grant and Schreiber 1990). In our research, the parasound data was collected with secondary primary frequency of 22 kHz resulting in secondary working frequency of 4 kHz. The data was digitally recorded and sampled at frequency of 40 kHz. Navigation data was supplied by the ship's GPS (Global positioning system).

The boomer system (EG&G Uniboom) is a single channel system which includes an electrical energy supplier and an electromagnetic transducer that transforms the discharged energy to electro-dynamic acoustic pulses. During the surveys, the transducer of the boomer source was employed in a catamaran that was towed along with a hydrophone-streamer receiver (with 8 hydrophones) astern of the vessel. The average speed of the vessel was 4 knots. The boomer source produces a wide bandwidth working frequency with the main range of 0.3 to 11 kHz resulting in a typical penetration of 20 to 100 m below the seabed depending on the acoustic impedance (product of velocity and density) of the sediments. The boomer source regularly produced from 2 to 3.67 shots per second. The sound waves were reflected when reaching the reflection surfaces which are regarded as acoustic-impedance contrast boundaries. The hydrophone-streamer received the pressure reflection signals and converted them into voltage responses before transmitting them to the computer. Seismic traces were digitally recorded and displayed by using NWC software. A GPS was used to guarantee the accurate positions of the recorded seismic traces. During the final cruise (Mekong 2008), we deployed a C-Boom boomer system which has similar working mechanism to the EG&G Uniboom boomer. The dominant working frequency of the C-Boom system was 1.76 kHz.

For data processing, the frequency high/low pass filtering has been applied for the recorded data. Highpass filter is set to keep all frequencies higher than the selected frequency. In

contrast, lowpass filter is set to keep all frequencies lower than the selected frequency. The frequency band-pass filtering of 2.5-6 kHz for parasound and 0.5-7 kHz for boomer data are applied for all seismic profiles on the SE Vietnam Shelf. The interpreted seismic surfaces are then picked with the software Kingdom Suite SMT 8.4. Average sound velocity of 1500 m/s in sea water and 1550 m/s in subsurface sediments has been assumed for Two-way travel time (TWT)-depth conversion.

Seismic data are interpreted on the basis of sequence stratigraphic concept which was initiated by Mitchum and Vail (1977) and Vail (1987), and then further refined by numerous authors. The seismic units are basically distinguished from each other by their reflection continuity, amplitude, frequency and configuration (Fig 2.2, see chapter 1).

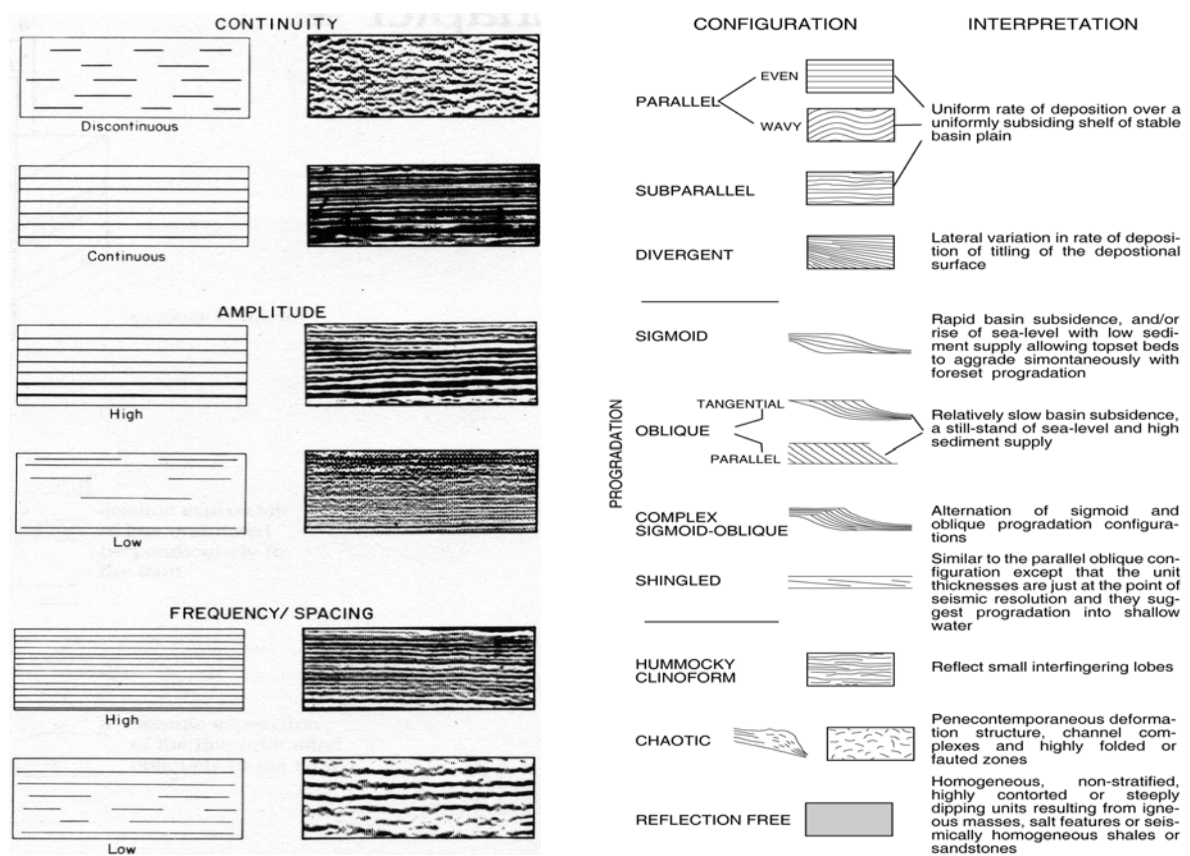


Fig 2.2. Classification of seismic facies and related depositional environments adapted from Badley (1985), Vail (1987) and Veenken (2007).

The interplay between base level changes (combined effect of eustasy, tectonics, sediment compaction, and environmental energy) and sedimentation rate controls the formation of sequence systems tract (Fig 2.3). For simplicity (by neglecting the energy of waves and currents), the base level is equated with the sea level (Catuneanu 2002). Hence, the concept of base level change is identical with the relative sea-level change. Accommodation is defined as

the space available for sediments to accumulate and its variations depend on base level changes. In this research, we apply the four-fold division of systems tract to divide the sedimentary architecture into different stages in relation to sea-level fluctuations (Catuneanu 2002; Catuneanu et al., 2009):

- **The falling stage systems tract (FSST)** was formed entirely during the stage of relative sea-level fall (forced regression), and it occurs independent of the ratio between the sedimentation rate and accommodation spaces.
- **The lowstand systems tract (LST)** was formed during the sea-level lowstand and slow sea-level rise when the rate of rise was lower than the sedimentation rate (normal regression).
- **The transgressive systems tract (TST)** was formed during the stage of relative sea-level rise when the rate of rise was higher than the sedimentation rate.
- **The highstand systems tract (HST)** was formed during the late stage of relative sea-level rise when the rate of rise was lower than the sedimentation rate.

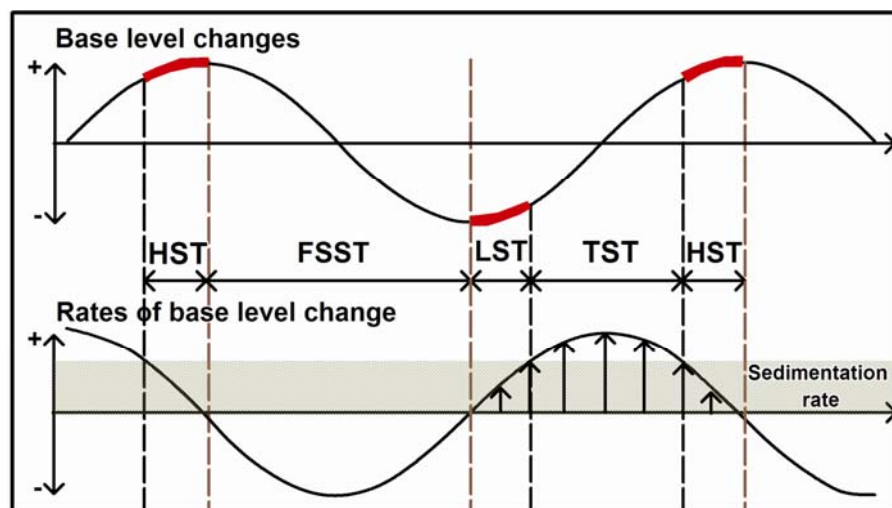


Fig 2.3. Sequence stratigraphic systems tracts as defined by the interplay between base level changes and sedimentation rate (modified from Catuneanu 2002). For simplicity, the sedimentation rate is kept constant during the base level fluctuations.

2.4 Results

2.4.1 Seismic units and bounding surfaces

In general, five seismic units and three major bounding surfaces are identified on the seismic profiles (Table 2.1).

Major bounding surfaces:

- SB1 is marked by highly continuous and strong amplitude reflector on all seismic profiles (Fig 2.4, Fig 2.5, Fig 2.7 and Fig 2.8). It can be traced across the shelf from water depths between 20 to 150 m. Further landward (0-20 m deep), the appearance of shallow gas effects have prevented its detection (Fig 2.8).
- RS1 surface mostly occurs within the incised-valley systems where it is characterized by moderate-amplitude and continuous reflectors on seismic profiles (Fig 2.5, Fig 2.6 and Fig 2.7). In the upper edge of incised-valley systems, it is almost merged with the lower SB1 surface (Fig 2.5 and Fig 2.6). RS1 surface is recorded on seismic profiles as boundary between the lower strong-chaotic reflector unit and the upper planar transparent reflector unit.
- RS2 is first surface which appears below the modern seabed (Fig 2.5 and Fig 2.8). In seismic profiles on the mid and outer shelf, it is characterized by medium to low amplitude but highly continuous reflectors. To the inner shelf around the modern Mekong subaqueous delta (0-30 m deep), it is clearly recorded on seismic sections as high amplitude and continuous surface which formed the boundary between the lower sheet-like transparent reflector unit and the overlying seaward dipping reflector unit (Fig 2.8).

Seismic units:

- U1 is characterized by seaward dipping reflectors with tangential oblique shape which is flattening toward the top (Fig 2.4). It is recorded only on the modern outer shelf at water depths of ~150 m. Estimated thickness of this unit on seismic profiles is approximately 50 m (Fig. 2.4).
- U2 is recorded only within the incised-valley systems. Its deposits prevail in the basal part of the channels. It is represented by high amplitude and low continuity reflectors (Fig 2.5 and Fig 2.6). Top of this unit is overlain by a smooth and continuity surface (RS1). In some channels, U2 unit occupies the whole channel and it is overlain directly by RS2 surface (Fig 2.5). Maximum thickness of this unit reaches up to ~30 m in northern incised-channel branch off Vung Tau where the incised-valleys cut deeply into the underlying sediments (Fig 2.5 and Fig 2.6). By contrast, its thickness reduces to around 10 m toward the southern part off Mekong Delta and Ca Mau Peninsula (Fig 2.7).
- U3 shows low to moderate amplitude unit with transparent reflectors developing across the shelf (Fig 2.4, Fig 2.5, Fig 2.7 and Fig 2.8). Within the incised-valleys, it occurs at the top of incised-valleys overlying the U2 unit with a clear boundary (RS1 surface). Out of the incised-valley system, this unit is composed of transparent layer overlying directly the SB1 surface (Fig 2.8). This unit is bounded on the top by a continuous and low amplitude

surface (RS2) (Fig 2.5). Thickness of this unit is highly variable. In some incised-valleys or in the inner shelf, its thickness reaches up to 15 m (Fig 2.7 and Fig 2.8), but it reduces very fast to few meters or is almost absent on the interfluvial of the incised-valleys and to the mid and outer shelf (Fig 2.5 and Fig 2.6).

- U4 is the uppermost unit recorded on seismic profiles. It represents a very thin layer developing only on the mid and outer shelf. It is characterized by transparent seismic reflectors overlying the U3 unit (Fig 2.5). This unit is occasionally absent on the seismic profile where its thickness is thin (less than seismic system resolution) and mixed with the lower U3 unit (Fig 2.6 and Fig 2.7).
- U5 is well recorded on the inner shelf off the modern Mekong subaqueous delta (0-30 m). It appears as strong amplitude, high continuity and seaward dipping reflectors. It forms tangential downlap to the lower RS2 surface (Fig 2.8). This unit shows seaward thinning trend with an average thickness of 15-20 m. This unit is almost pinched out at modern water depths of around 20-30 m and (Fig 2.8, Fig 2.10 and Fig 2.11). Further seaward, it is connected with the U4 unit.

2.4.2 Sedimentary characteristics and ages of deposits

Radiocarbon datings of sediment core taken in the upper part of the outer shelf wedge (Fig 2.4) provide ages of 24.3 ky BP in the lower part of the core and 0.6 to 1.2 ky BP in the upper part of the core (Schimanski and Stattegger 2005). These ages correspond to the LGM sea-level lowstand and deglacial period according to the regional sea-level curve (Hanebuth et al., 2000; Hanebuth et al., 2009). Results of X-ray fluorescence (XRF) core scanning of sediment cores taken from the incised-valleys at water depths between 29 and 60 m on the SE Vietnam Shelf show a clear boundary between the lower fluvial mud and the upper marine sand within the sediment cores (Fig 2.5; Tjallingii et al., 2010). Ages of deposits of six sediment cores taken at water depth between 29 and 155 m on the SE Vietnam Shelf range from 0.3 to 13.3 ky BP (Tjallingii et al., 2010). The uppermost parts of eight sediment cores taken at modern water depths between 50 to 150 m on the SE Vietnam Shelf show high content of sand fraction up to 97% and carbonate content up to 19% (Schimanski and Stattegger 2005).

2.4.3 Continental shelf architecture

In general, the sedimentary architecture on the SE Vietnam Shelf from LGM to present is composed of three systems tracts: Lowstand systems tract (LST), Transgressive systems tract (TST) and Highstand systems tract (HST). Those systems tracts are bounded by the sequence

boundary at the base and are separated by flooding surfaces. Summary of systems tracts and bounding surfaces is listed in Tab 1.

➤ **Sequence boundary and flooding surfaces**

The seismic reflection SB1 surface is interpreted as sequence boundary forming the base of the sequence. This surface has probably experienced multi-phases of the sea-level fall (regression stage), sea-level lowstand and was reworked again during transgression. No direct dating is available for this surface on the SE Vietnam Shelf, however the formation of SB1 surface in our research can be correlated to the late Pleistocene soil surface dated as 25-30 ky BP on the outer Sunda Shelf (Hanebuth and Stattegger 2004). An interpolation map of this surface derived from seismic profiles and sediment cores on land is shown on Fig 2.9. In the nearshore areas, depth of the lowstand surface is around 20 m and it is submerged seaward following the modern bathymetry. The most interesting feature of this map is the incised-channel system, which was probably formed during the relative sea-level fall period. Channels can be traced by seismic profiles from 20 to 60 m of modern water depths and show W-E to N-S orientation (Fig 2.5, Fig 2.6 and Fig 2.7). The formation of the incised-valley systems seems to be controlled by the shelf morphology showing a clear change from northern to southern part of study area. The northern incised-valley branch off Vung Tau shows narrow and deep incised V-shape (<5 km wide and tens meter in depth) which resulted from the narrow and high-gradient morphology of the shelf (Fig 2.5 and Fig 2.6). By contrast, the southern incised-channels show an N-S orientation with a trend of decreasing in deep of incision (< 15 m deep) in comparison to the northern ones due to the lower gradient of shelf morphology (Fig 2.7).

The deposits of the U2 and U3 units are bounded above by RS1 surface showing clear transition from fluvial to marine sediments (Tjallingii et al., 2010). ¹⁴C dating values of U2 and U3 units at water depth of 60 m range from 13.3 to 11.9 ky BP (Fig 2.5) which are corresponding to the transgressive period according to regional sea-level curve (Hanebuth et al., 2000; Hanebuth et al., 2009). RS1 surface is therefore interpreted as a ravinement surface resulted from eroding the lower fluvial deposits by shallow marine hydrodynamic activities during the transgression.

The maximum flooding surface (Mxfs) is normally defined as downlapping surface formed at the top of transgressive deposits (Catuneanu 2002). The RS2 surface in our research acting as boundary of the upper downlapping clinoforms and lower sheet-like deposits is interpreted as Mxfs marking the boundary between TST and HST.

➤ **Lowstand systems tract (LST)**

U1 unit consists of reflectors with progradational oblique wedge-shape which can be attributed to the depositions of the LST. The thick tangential oblique-shape clinoforms are often associated with period of sea-level stillstand or little rise with substantial sediment supply (Vail 1987). Sediment core dating result (~ 24.3 ky BP) on the upper part of the wedge (Fig 2.4) suggest that it was probably formed during the sea-level lowstand period. U1 unit is therefore interpreted as the depositions of the paleo- Mekong Delta in response to the falling stage and slow sea-level rise during the latest sea-level lowstand. As documented by large time gap of dating results along the sediment core and the absence of topset reflectors on top of the wedge (Fig 2.4), we speculate that the lowstand wedge was probably reworked and eroded during the early following transgressive phase. Numerous relict sandwaves found at water depth of 120 m on the northernmost part of the shelf (Fig 2.12) confirms the strong bottom current activities during early transgression (Bui et al., 2009) and their migration could probably erode the upper part of the LST wedge. The boundary between the LST and TST within the lowstand wedge is not resolved under the resolution of seismic data (Fig 2.4). However, age control by core SO 140 93-3 suggests the LST wedge was overlain by a veneer layer of TST and HST deposits.


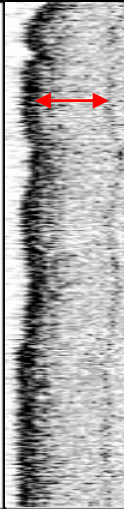
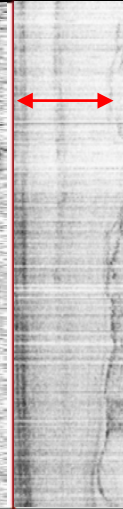

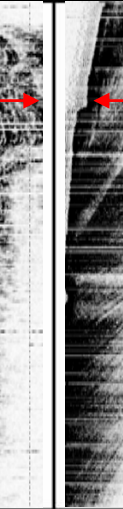

Systems tract	Seismic unit	Acoustic facies and configuration	Occurrence	Thickness (m)	Seismic image
HST	U5	High to moderate amplitude, low frequency, high continuity, oblique tagential downlap	Inner shelf	0-25	
	U4	Transparent, parallel	Mid-outer shelf	0-1	
TST	RS2				
	U3	Low to moderate amplitude, transparent, parallel	The entire shelf	0-15	
	RS1				
LST	U2	Moderate to high amplitude, variable frequency, low continuity, locally transparent, parallel to oblique, infill	Incised-channels	0-30	
	U1	High amplitude, high frequency, high continuity, oblique tagential downlap, toplap	Outer shelf	50	
	SB1				

Table 2.1. Systems tracts, seismic units and facies, bounding surfaces and reflection patterns on the SE Vietnam Shelf. Abbreviations: LST = Lowstand systems tract, TST = Transgressive systems tract, HST = Highstand systems tract.

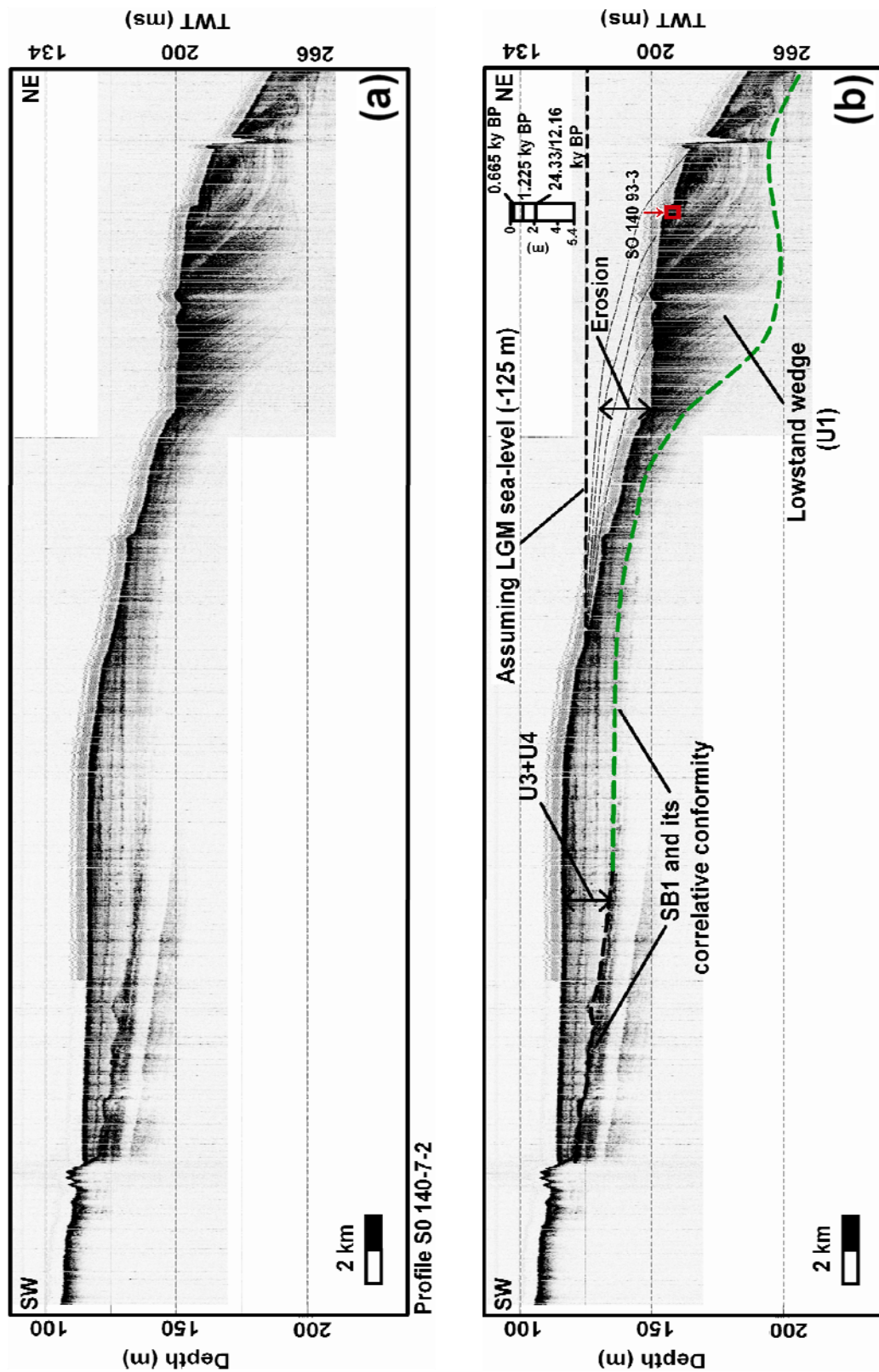


Fig 2.4. Seismic profile (a) and sequence stratigraphic interpretation (b) of the LGM lowstand wedge deposits. The upper part of the wedge was probably reworked and eroded taking the LGM sea-level (Hanebuth et al., 2009) as reference. Core ages are cited from Schimanski and Statteger (2005). For abbreviations see Table 2-1.

➤ **Transgressive systems tract (TST)**

The U2 and U3 units are recorded within the incised-valleys and on the exposed shelf. The deposits of the U2 and U3 units show a clear transition from terrigenous to marine deposits as documented by XRF core analyze (Fig 2.5; Tjallingii et al., 2010). From sediment cores taken at modern water depths between 29 and 155 m on the SE Vietnam Shelf, ages of U2 and U3 units were deduced from 13.3 to 9 ky BP (Tjallingii et al., 2010). Therefore U2 and U3 units were probably formed during succeeding periods of transgression. U2 is recorded at the base of incised-valley with strong and low continuity seismic reflectors with point-bar geometry indicating formation in fluvial environment. Sediment cores can only reach the upper part of this unit with the oldest age of around 13.3 ky BP (Fig 2.5), though the lower deposits might have been formed during the lowstand period (Zaitlin et al., 1994). U2 unit is interpreted as lowstand to transgressive fluvial deposits. The planar-transparent seismic reflectors of U3 unit suggest that it might have been formed in a low energy depositional environment. The uppermost parts of sediment cores taken at modern water depths between 50 and 150 m on the SE Vietnam Shelf show dominance of sand fraction and high content of carbonate (Schimanski and Stattegger 2005) which are probably corresponding to the formation of U3 deposits in our research. Similarly, a marine carbonate sand layer has been identified on top of all sediment cores taken from the incised-valleys on the SE Vietnam Shelf (Tjallingii et al., 2010). U3 is interpreted as transgressive estuarine to shallow marine sand deposits. Out of the incised-valley, U3 unit mostly appears as a parallel and transparent layer overlying the lowstand erosional surface (Fig 2.5, Fig 2.6, Fig 2.7 and Fig 2.8).

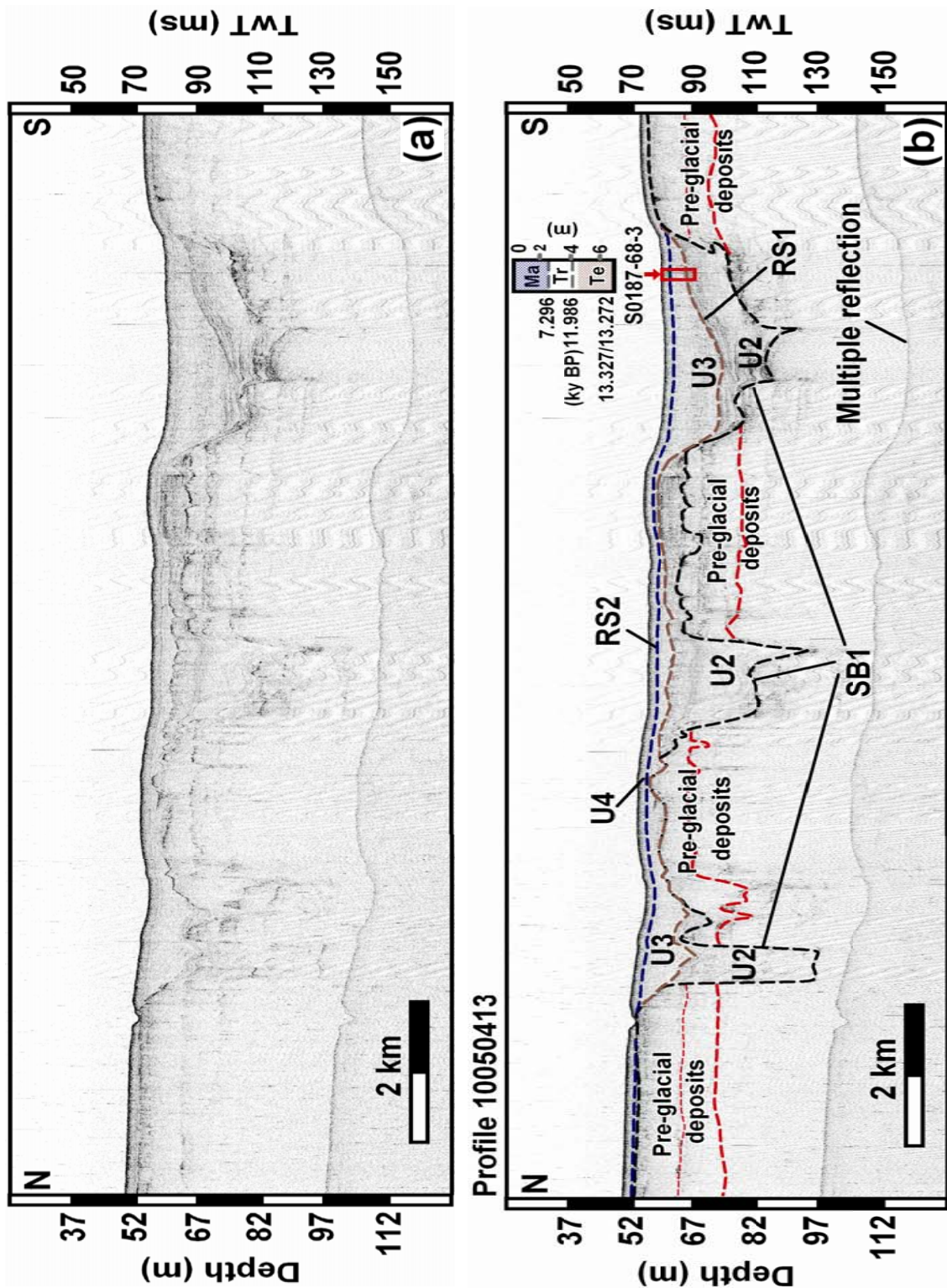


Fig 2.5. Seismic profile (a) and sequence stratigraphic interpretation (b) of northern incised-valley with different tributaries. Core results indicate a transition from fluvial (Te) in the lower to transition (Tr) in the mid and fully marine influence (Ma) in the uppermost part (Tjallingii et al., 2010). For abbreviations see Table 2-1.

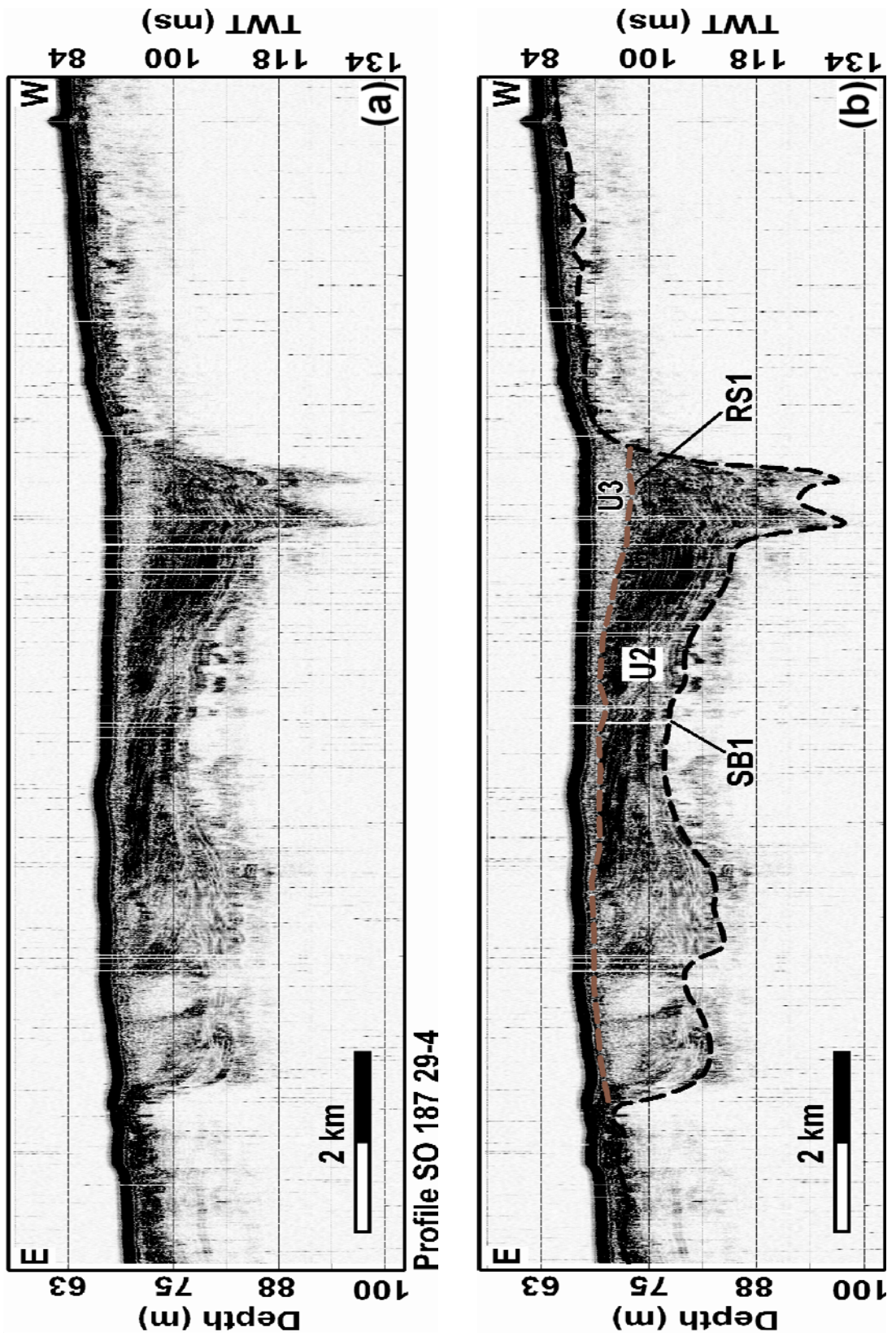


Fig 2.6. Seismic profile (a) and sequence stratigraphic interpretation (b) of northern incised-valley with point-bar structure. For abbreviations see Table 2-1.

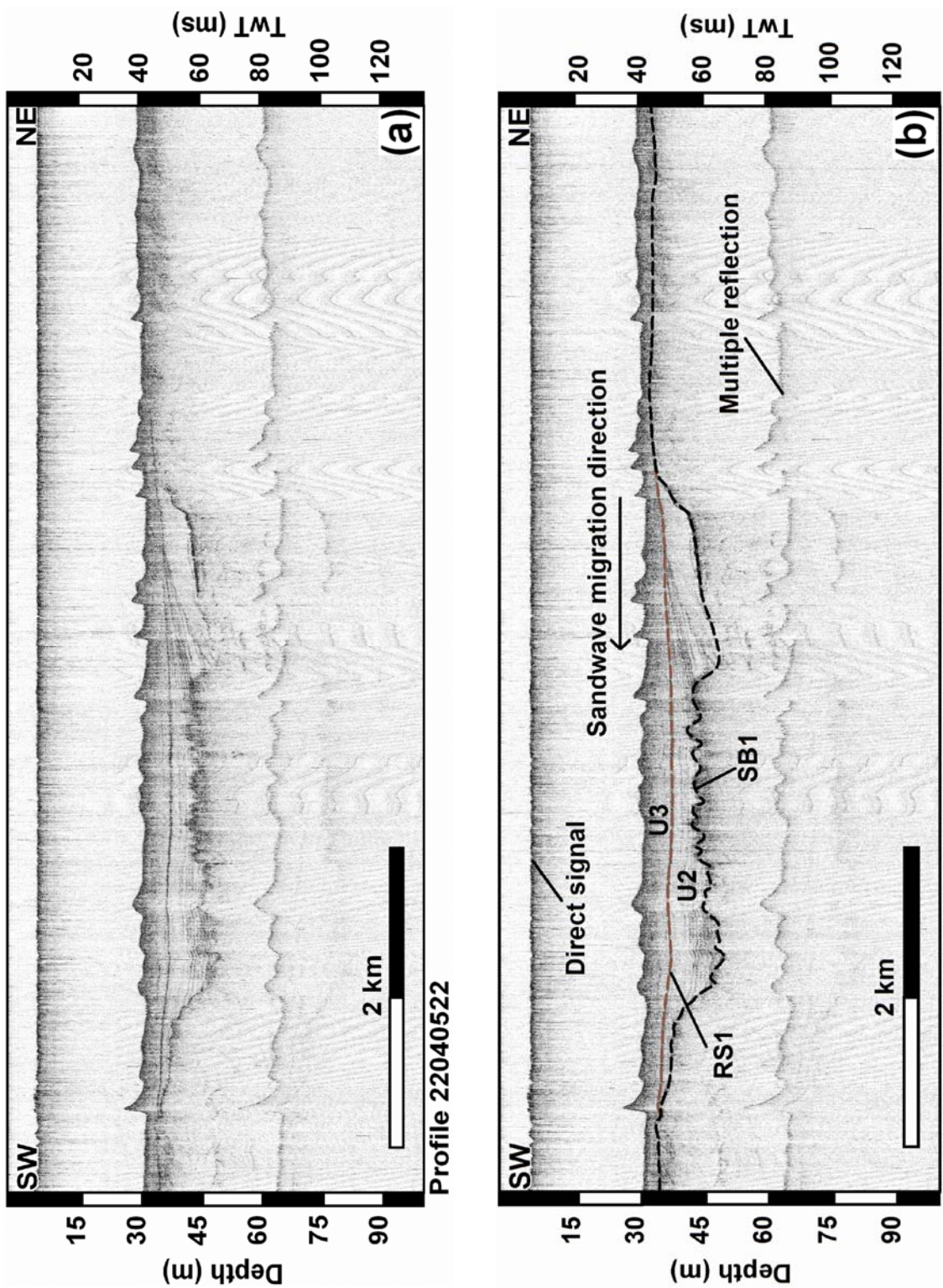


Fig 2.7. Seismic profile (a) and sequence stratigraphic interpretation (b) of southern incised-valley off modern Mekong Delta. Top of the channel is covered by numerous active sandwaves. For abbreviations see Table 2-1.

➤ **Highstand systems tract (HST)**

The U5 unit is recorded on seismic profiles as prograding clinoforms downlapping onto the maximum flooding surface (Mxfs RS2 surface) (Fig 2.8). In the lower part, a horizontal and transparent layer is observed covering directly the SB1 surface. Recent studies on the delta plain near Cambodia lowland have provided age of the Mxfs of around 8.0 ky BP which preceded the formation of the modern Mekong Delta (Hori and Saito 2007; Tamura et al., 2007; Tamura et al., 2009).

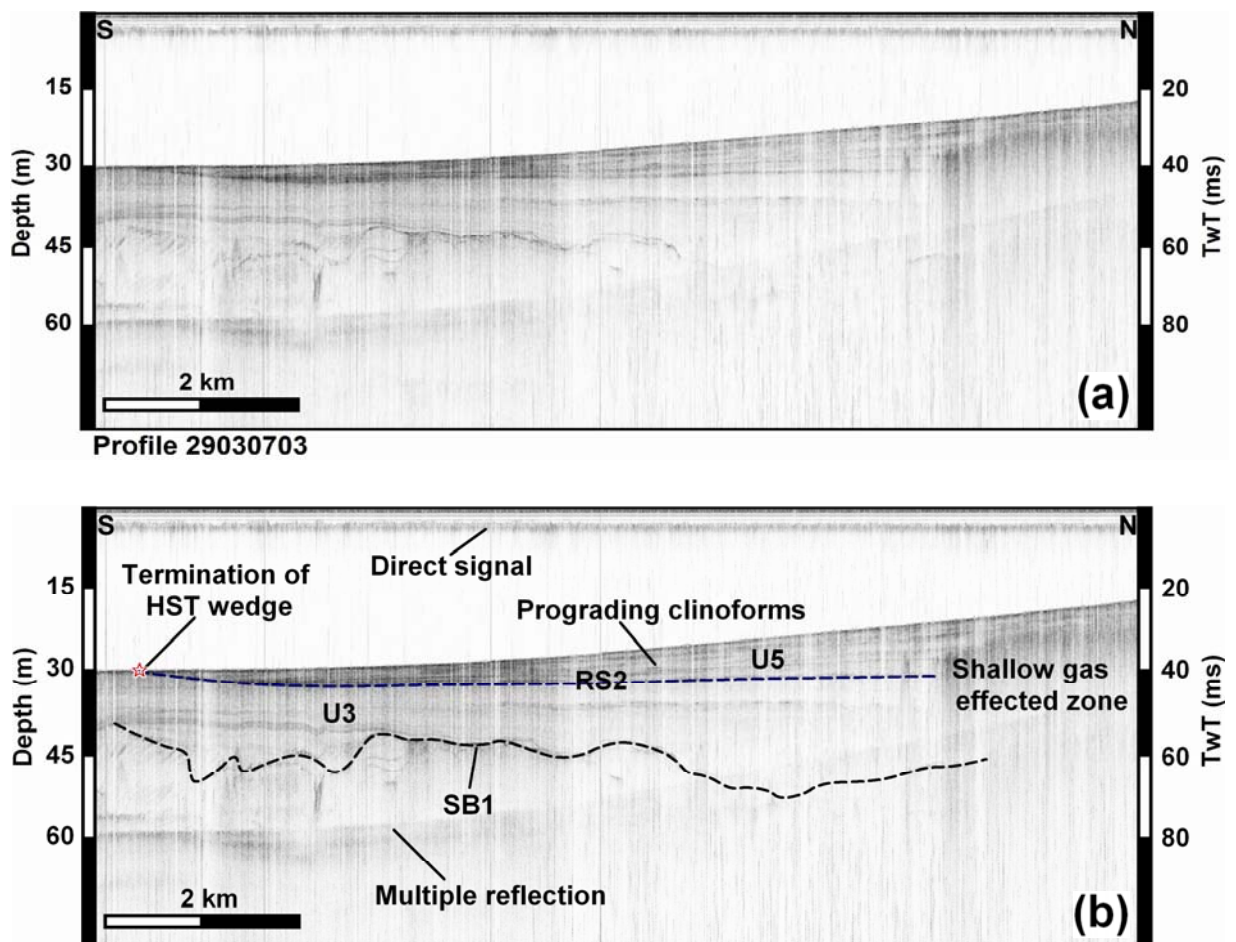


Fig 2.8. Part of seismic profile showing highstand wedge deposits (U5) of the modern Mekong Delta. Seismic profile (a) and sequence stratigraphic interpretation (b). For abbreviations see Table 2-1.

No core dating results are available for U5 unit so far. Nevertheless, comparison to the similar prograding clinoforms found in other regions (Liu et al., 2004) suggests that unit U5 represents the modern Mekong Delta clinoforms which developed after the maximum mid-Holocene sea-level highstand about 6-5.5 ky on the SE Vietnam Shelf (Ta et al., 2002a; Ta et

al., 2002b). This clinoform wedge is confined to the inner shelf with an offshore extension is approximately 20 km (Fig 2.11). Out of the highstand wedge, the HST appears as a very thin transparent layer (U4 unit) (Fig 2.4 and Fig 2.5). U4 unit is often mixed with the lower U3 unit or absent on seismic profiles (Fig 2.4, Fig 2.6 and Fig 2.7). U4 unit was documented in the uppermost parts of all sediment cores on the SE Vietnam shelf as fully marine deposits with age of 0.3 to 8.0 ky BP (Fig 2.5; Tjallingii et al., 2010). The formation of U4 unit can be correlated to the thin marine mud (condensed section) on the Sunda Shelf which was dated as 11.0-4.0 ky BP (Hanebuth and Stattegger 2004). U4 unit is therefore interpreted as a condensed section which resulted from sediment starvation.

2.4.4 Late Pleistocene-Holocene sequence stratigraphic model for the SE Vietnam Shelf and controlling factors

In general, the evolution of the SE Vietnam Shelf over the last 25 ky from LGM to present time can be divided to three periods corresponding to three systems tracts: LST, TST and HST.

As a result of the falling sea-level initiated from Marine Isotope 5e (~120 ky BP) to LGM (~20 ky BP) (Hanebuth and Stattegger 2004), most of the SE Vietnam Shelf has been exposed to subaerial processes and river incision. During the LGM period, the lowstand erosional surface and incised-valleys (paleo-Mekong River) were developed on the exposed shelf as a result of the base level adjustment. In this research, the incised-valleys can only be traced from 20 to 60 m of modern water depths. On the other parts of the shelf, the incised-valleys were probably reworked and erased during the following transgression. The development of the LGM surface on the SE Vietnam Shelf correlated well to the modern bathymetry with a high gradient in the north and gentle surface toward the southern part (Fig 2.9). The river mouths at LGM period were located around 123 ± 2 m deep (Hanebuth et al., 2009) and they formed a thick prograding wedge (U1 unit) on the outer shelf (Fig 2.4). As discussed in the previous section, the LST wedge was partly eroded during the onset of transgression that might significantly reduced its original thickness (Fig 2.4). The LST wedge thickness of ~50 m recorded on seismic profile evidences the stability of sea-level for considerable of time and huge sediment supply from the paleo-rivers to the outer shelf during LGM period. The LST deposits on the SE Vietnam Shelf consist of a prograding delta wedge and partly the lowermost fluvial deposits in the incised-channels.

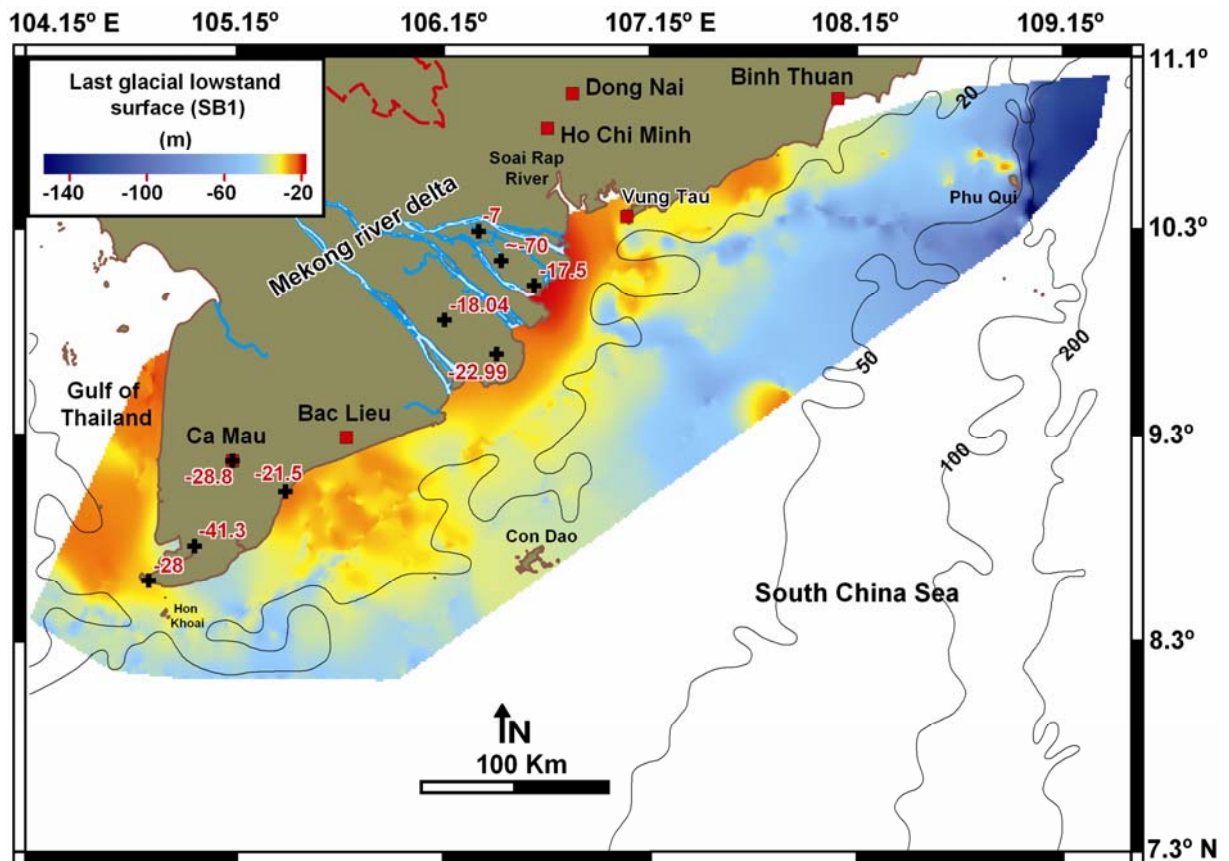


Fig 2.9. The last glacial lowstand surface-morphology with reference to the present sea-level. Red numbers indicate depths below present sea-level of the lowstand surface identified from sediment cores on land (Hoang 2002; Ta et al., 2002b).

The termination of the LGM is complex and remains a subject of discussion. In general, a slight rise of sea-level from 26 to 20 ky BP (Peltier and Fairbanks 2006) and the first significant sea-level rise starting from 19.6 ky BP (Fig 2.13) mark the final phase of the LGM (Hanebuth et al., 2009). The maximum flooding surface on the Mekong Delta plain was dated around 8.0 ky BP (Hori and Saito, 2007, Tamura et al., 2007, Tamura et al., 2009). Hence, we deduce that the TST on the SE Vietnam Shelf took place from 19.6-8.0 ky BP. Different surfaces within the TST as ravinement surface (RS1) can be clearly observed within the incised-valleys marking the transition from fluvial to marine environment (Fig 2.5 and Fig 2.6). The TST on the SE Vietnam Shelf mostly appears as a thin (0 - 5 m in thickness), sheet-like layer overlying the lowstand erosional surface (Fig 2.5, Fig 2.6 and Fig 2.8). However, its thickness locally increases up to around 15 m with aggradational stacking patterns in sheltered areas with increasing sediment supply (Fig 2.8). Thick TST deposits are well recorded only within the incised-valley system at water depths between 20-60 m since they were well preserved in valley depressions from the succeeding marine erosional

processes (Fig 2.5, Fig 2.6 and Fig 2.10). In all seismic profiles of our research, the transgressive surface acting as boundary between LST and TST deposits documented on the standard incised-valley model (Zaitlin et al., 1994) is not visible. The preservation potential of this facies is normally low due to the erosional processes during transgression period (Catuneanu 2002).

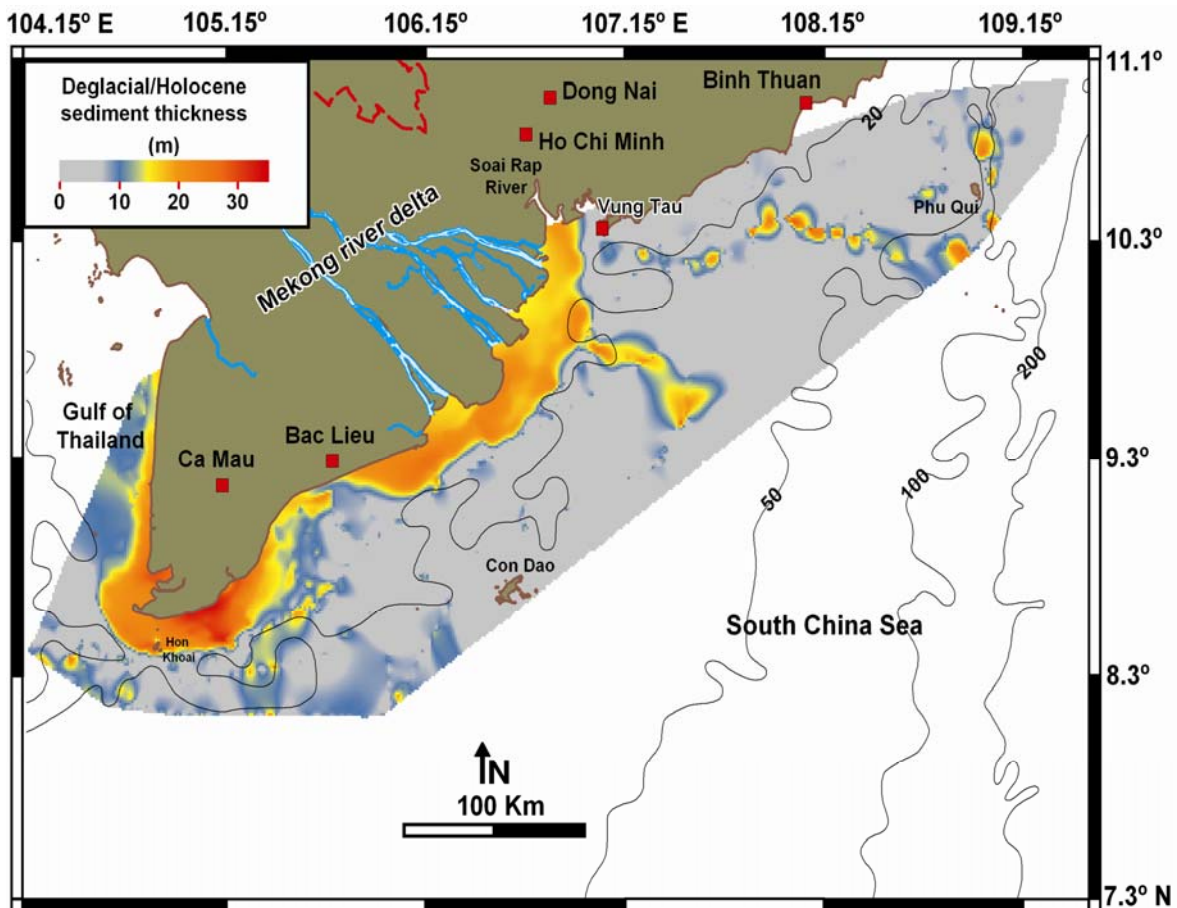


Fig 2.10. Thickness map of deglacial/Holocene sediments. The sediment depocentres are located mostly within the incised-valleys, the modern Mekong subaqueous delta and the narrow outer shelf off Phu Quy Island. Thickness of the eastern Mekong subaqueous delta is roughly calculated from sediment cores on land and bathymetry.

As mentioned above, the maximum flooding surface on the SE Vietnam Shelf has been established around 8.0 ky BP coincident with the initiation of the modern Mekong Delta. After the initiation phase of aggradation, the modern Mekong Delta has prograded rapidly following the mid-Holocene sea-level highstand of about 1.5 to 2.5 m above the modern level reached between 6.0 and 5.5 ky BP (Ta et al., 2002a; Ta et al., 2002b; Michelli 2008). The highstand wedge (U5) recorded in our research is the modern Mekong subaqueous delta. This wedge is

mostly developed around the modern coastline and pinched out seaward at water depths of 20-30 m (Fig 2.8 and Fig 2.11).

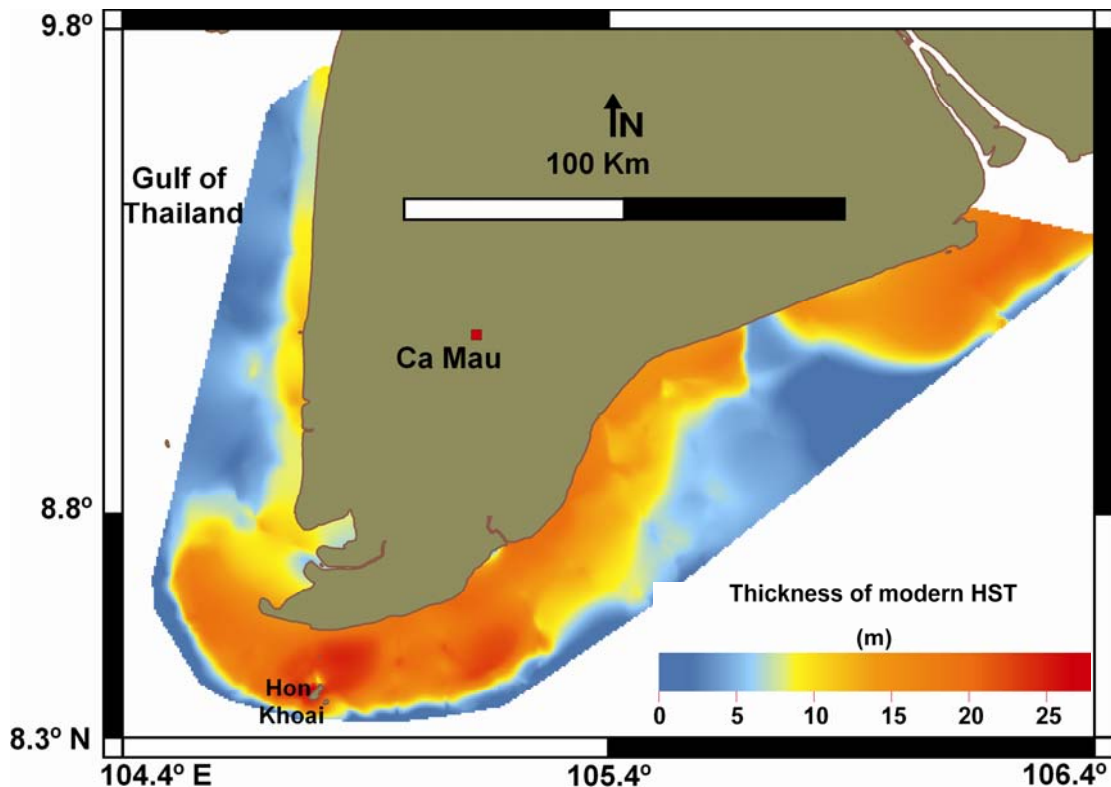


Fig 2.11. Thickness of modern highstand sediments (last 8 ky) constructed from seismic profiles. The northern part of the HST is not shown on the map. The HST sediment depocentre locates off Cape Camau and the wedge tends to develop toward the Gulf of Thailand to the west.

On the mid and outer shelf, the HST appears as thin layer overlying the TST deposits (Fig 2.4 and Fig 2.5). The distribution of modern HST deposits can be explained by two controlling factors: shelf morphology and modern hydrodynamic conditions on the SE Vietnam Shelf. The southward widening of the SE Vietnam Shelf area has increased the distance (average about 200 km) between sediment sources (Mekong River) to the middle and outer shelf and therefore reduces the modern sediment supply to this area. Moreover, numerous NE-SW oriented sandwaves found at modern water depths of 20-40 m suggest the activities of strong modern bottom currents (0.6-0.7 m/s) which can prevent the deposition of fine sediments (Kubicki 2008; Bui et al., 2009). Numerous modern sandwaves on the mid-shelf (Fig 2.12) indicate the dominance of sand-sized fractions in the surface sediments as well as the limited extension of modern fine sediments to this area of the shelf. The double-effect of shelf morphology and strong currents driven by the local monsoon system (NE-SW)

may have prevented the HST mud wedge in developing further offshore. In addition, the along-shore transport of supplied sediments from Mekong River mouths in the southwestward direction was promoted. The sediment isopach map of the HST constructed from seismic profiles indicates that the sediment depocentre of the HST wedge is located off Cape Ca Mau and tends to develop further westward into the Gulf of Thailand (Fig 2.11).

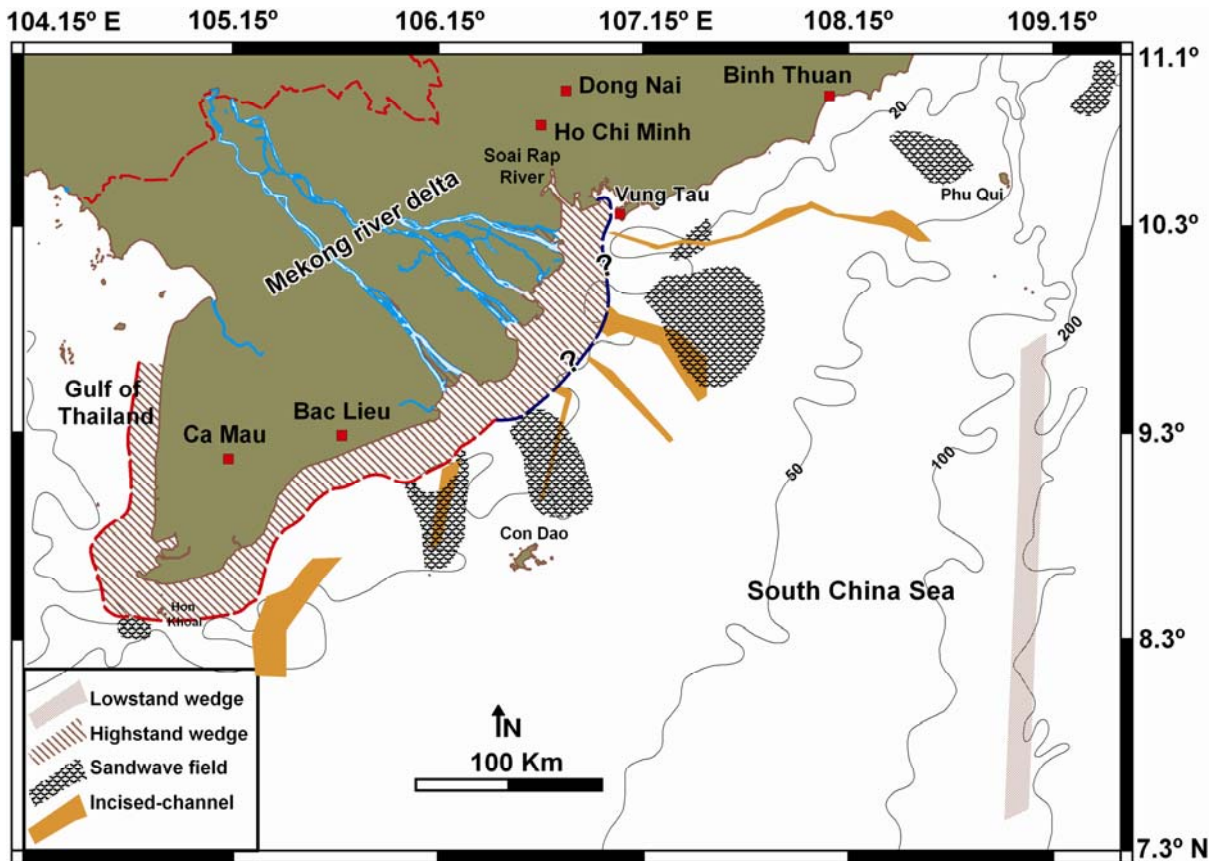


Fig 2.12. Distribution of late Pleistocene-Holocene depositional systems on the SE Vietnam Shelf constructed from seismic profiles. Red line shows the modern HST wedge boundary indentified from seismic profiles and the northern boundary of the HST wedge is roughly indicated from thickness map shown on Fig 2.9.

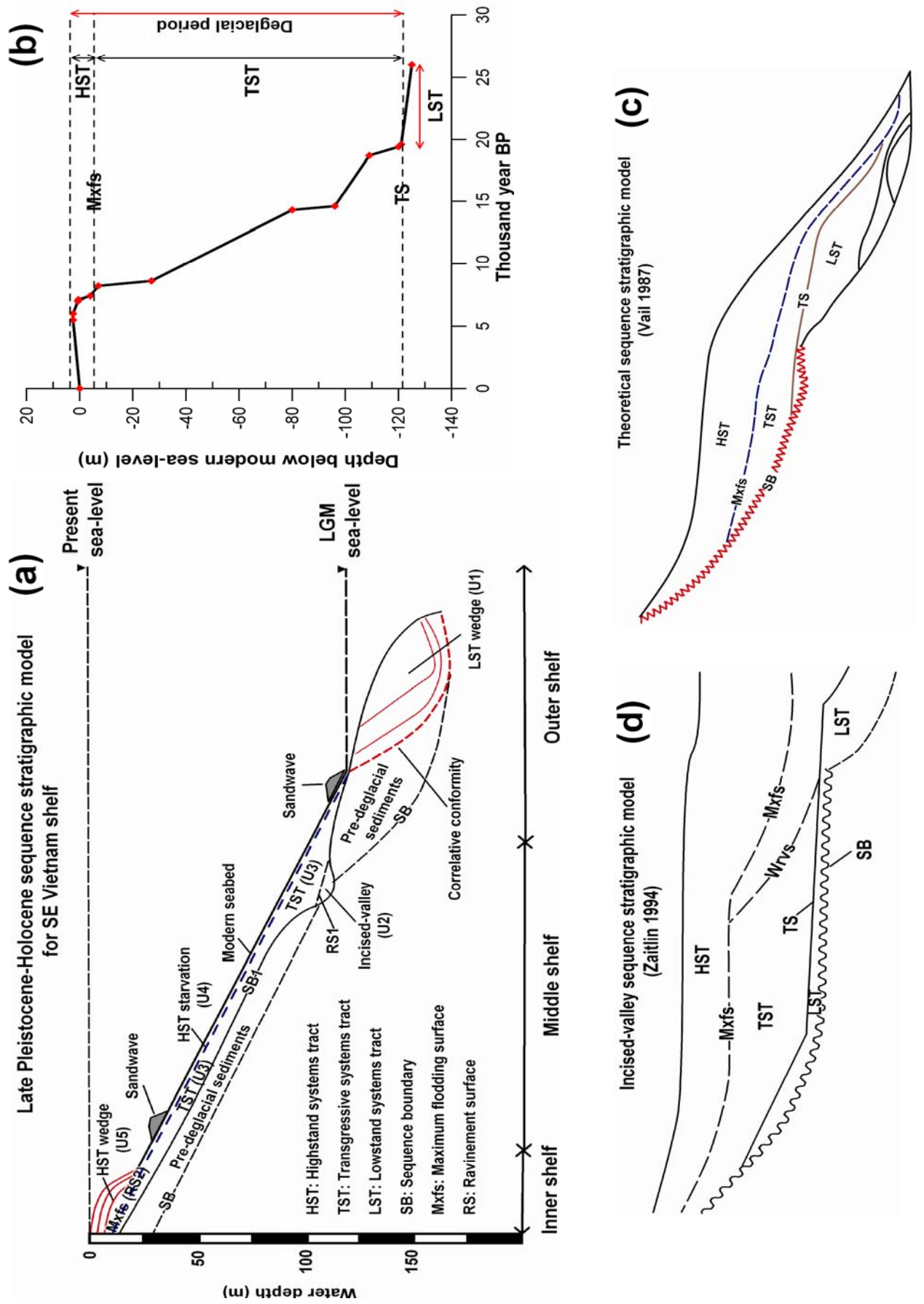


Fig 2.13. Late Pleistocene-Holocene sequence stratigraphic model for the SE Vietnam Shelf (a) with regional sea-level curve (b) (Stattegger et al, in prep) and comparison to theoretical models of Vail (c) and Zaitlin (d).

2.5 Discussion and conclusions

Proposed sequence-stratigraphic model for the SE Vietnam Shelf basically follows the main features of the theoretical model of Vail (1987) (Fig 2.13). Nevertheless, there still exist some differences between these two models reflecting the local controlling factors. In general, sedimentation on the SE Vietnam Shelf reflects the interactions between sea-level change, shelf gradient and hydrodynamic conditions.

On the SE Vietnam Shelf, the thick highstand wedge is confined to the inner shelf instead of extending to the middle and outer shelf as proposed on the Vail model. Sediment depositions on the middle and outer shelf of the SE Vietnam Shelf are typical for the modern HST starvation shelves which were observed as well on the neighboring Sunda Shelf (Hanebuth and Stattegger 2004) and on the shelf of the East China Sea (Dong and Soo 2000). In general, no clear backstepping stacking patterns of the TST deposits is recorded on the SE Vietnam Shelf. We deduce the high dispersion of the transgression deposits on the SE Vietnam Shelf as a result of a high accommodation space/sediment supply ratio which resulted from the rapid transgression over very low-gradient shelf. In such cases, the TST deposits tend to disperse widely over the shelf instead of forming thick stack of backstepping layers (Cattaneo and Steel 2003). Therefore, the model of thick backstepping TST observed in Vail model cannot be applied to the SE Vietnam Shelf. This is similar to the sequence stratigraphic model for the Sunda Shelf (Hanebuth and Stattegger 2004), North Yellow Sea (Liu et al., 2004) and East China Sea (Dong and Soo 2000). The transgressive surface (TS) separating the LST and TST was not clearly documented on the SE Vietnam Shelf since it was often reworked and amalgamated with the lowstand sequence boundary during the transgression (Cattaneo and Steel 2003). Besides, the LST fluvial deposits which are predicted of being preserve in the lowermost part of the incised-channels (Zaitlin et al., 1994) are neither clearly distinguished on seismic profiles nor documented from sediment cores.

The late Pleistocene-Holocene sedimentary architecture of the SE Vietnam Shelf has been revealed on the basis of seismic-sequence stratigraphic concepts. Five seismic units and three main bounding surfaces are indentified in forming the uppermost sequence on the SE Vietnam Shelf.

- The LST with unit U1 consists of a prograding outer shelf delta wedge with lowstand erosional basal surface. The lowstand surface is widely recorded over the shelf forming the base of the sequence. An interesting feature of the lowstand surface is the incised-valley system formed by incision of the paleo-Mekong River during the falling sea-level. These channels are traced by seismic profiles from 20 to 60 m of modern water depths and they seem to be governed by the shelf morphology. The northern incised-valley

branch off Vung Tau shows narrow and deep V-shape in cross-section, which has probably resulted from the high-gradient morphology of the shelf. By contrast, the wide and low-gradient shelf off the modern Mekong Delta and Ca Mau Peninsula created shallow incised-valleys on the exposed self.

- The TST is mostly preserved from marine erosional processes in the incised-valley depressions which are filled up by unit U2. It shows an upward transition from fluvial to fully marine conditions as a result of marine transgression. On the exposed shelf and the interfluvial, the TST shows a thin layer mostly consisting of sand (unit U3) overlying directly the sequence boundary SB1.
- The HST is primarily composed of the thick prograding mud clinoforms of the modern Mekong subaqueous delta forming unit U5. This unit is limited to modern water depths of 0-30 m. After escaping from the river mouth, the HST mud is transported along-shore to the southwestern part and forms a sediment depocentre off Cape Ca Mau. Toward the mid and outer shelf, the HST sediments form the condensed section with unit U4 as a very thin layer locally mixing with the lower transgressive sediments without clear boundary.
- The interactions between shelf morphology, local hydrodynamic conditions and sea-level change are important controlling factors of depositional systems on the SE Vietnam Shelf.

References

Badley ME (1985). Practical seismic interpretation: International Human Resources Development Corporation, Boston, 266 pp.

Briais A, Patriat P and Tapponnier P (1993). Updated interpretation of magnetic anomalies and seafloor spreading stages in the South China Sea: implications for the Tertiary tectonics of Southeast Asia. *Journal of Geophysical Research* 98, 6299-6328.

Bui VD, Schimanski A, Stattegger K, Van Phung P, Nguyen TT, Nguyen TH, Nguyen TT and Phi TT (2009). Sandwaves on the Southeast Vietnam Shelf recorded by high resolution seismic profiles: formation and mechanism. *Frontiers of Earth Science in China* 3 (1), 9-20.

Cattaneo A and Steel RJ (2003). Transgressive deposits: a review of their variability. *Earth-Science Reviews* 62 (3-4), 187-228.

Catuneanu O (2002). Sequence stratigraphy of clastic systems: concepts, merits, and pitfalls. *J.Afr. Earth Sci* 35, 1–43.

Catuneanu O et al. (2009). Towards the standardization of sequence stratigraphy, *Earth-Science Reviews* 92, 1–33.

Dong G and Soo CP (2000). High-Resolution Seismic Study as a Tool for Sequence Stratigraphic Evidence of High-Frequency Sea-Level Changes: Latest Pleistocene–Holocene example from The Korea Strait. *Journal of Sedimentary Research* 70 (2), 269-309.

Grant JA and Schreiber R (1990). Modern swath sounding and sub-bottom profiling technology for research applications: The Atlas Hydrosweep and Parasound Systems. *Mar.Geophys.Res* 12, 9-19.

Hanebuth TJJ and Stattegger K, Grootes PM (2000). Rapid flooding of the Sunda Shelf: A Late Glacial Sea-Level record. *Science* 288, 1033-1035.

Hanebuth TJJ, Stattegger K and Saito Y (2002). The stratigraphic architecture of the central Sunda Shelf (SE Asia) recorded by shallow-seismic surveying. *Geo-Marine Letters* 22, 86-

Hanebuth TJJ, Stattegger K, Schimanski A, Lüdmann T and Wong HK (2003). Late Pleistocene forced regressive deposits on the Sunda Shelf (SE Asia). *Marine Geology* 199 (1-2), 139-157.

Hanebuth TJJ and Stattegger K (2004). Depositional sequences on a late Pleistocene Holocene tropical siliciclastic shelf (Sunda Shelf, (SE Asia). *Journal of Asian Earth Sciences* 23, 113-126.

Hanebuth TJJ, Stattegger K, Bojanowski A (2009). Termination of the Last Glacial Maximum sea level lowstand: The Sunda-Shelf data revisited. *Global and Planetary Change* 66, 76-84.

Hoang VT (2002). Quaternary sedimentation on the South West Vietnam Shelf. PhD thesis Hanoi University of natural science, 127 pp (in Vietnamese).

Hori K and Saito Y (2007). An early Holocene sea-level jump and delta initiation, *Geophys. Res. Lett* 34, L18401.

Kubicki A (2008). Large and very large subaqueous dunes on the continental shelf off southern Vietnam, South China Sea. *Geo-Marine Letters* 28 (4), 229-238.

Liu JP, Milliman JD, Gao S and Cheng P (2004). Holocene development of the Yellow River's subaqueous delta, North Yellow Sea. *Marine Geology* 209, 45–67.

Michelli M (2008). Sea-level changes, coastal evolution and paleoceanography of coastal waters in SE - Vietnam since the mid - Holocene. PhD thesis. University of Kiel, 160 pp.

Mitchum JR and Vail PR (1977). Seismic stratigraphy and global changes of sea-level: Part 7. Seismic stratigraphy interpretation procedure. In: Payton, C.E. (Ed.), *Seismic Stratigraphy Applications to Hydrocarbon Exploration*. AAPG Memoirs 26, 63– 81.

Milliman JD and Syvitski PM (1992). Geomorphic/tectonic control of sediment discharge to the ocean: The importance of small mountainous rivers. *J. Geol* 100, 525-544

Nguyen VL, Ta TKO and Tateishi M (2000). Late Holocene depositional environments and coastal evolution of the Mekong River Delta, Southern Vietnam. *Journal of Asian Earth Sciences* 18(4), 427-439.

Peltier WR and Fairbanks RG (2006). Global glacial ice volume and Last Glacial Maximum duration from an extended Barbados sea level record. *Quaternary Science Reviews* 25 (23–24), 3322–3337.

Pham VN (Editor) (2003). *Bien Dong Monograph. Vol. II –Meteorology, Marine Hydrology and Hydrodynamics*, Hanoi National University Publisher, Hanoi, 565 pp (in Vietnamese).

Schimanski A and Stattegger K (2005). Deglacial and Holocene Evolution of the Vietnam Shelf: Stratigraphy, Sediments and Sea-level change. *Marine Geology* 214, 365—387.

Shuttle Radar Topography Mission (SRTM) digital elevation models (<http://srtm.usgs.gov>).

Stattegger K, Tjallingii R, Phung VP and Wetzel A (in prep). Holocene sea-level history of SE Asia and its global implications. To be submitted to *Global and Planetary Change*.

Ta TKO, Nguyen VL, Kobayashi I, Tateishi M and Saito Y (2001a). Late Pleistocene-Holocene Stratigraphy and Delta Progradation, the Mekong River Delta, South Vietnam. *Gondwana Research* 4 (4), 799-800.

Ta TKO, Nguyen VL, Tateishi M, Kobayashi I and Saito Y (2001b). Sedimentary facies, diatom and foraminifer assemblages in a late Pleistocene-Holocene incised-valley sequence from the Mekong River delta, Bentre Province, southern Vietnam; the BT2 core. *Journal of Asian Earth Sciences* 20(1), 83-94.

Ta TKO, Nguyen VL, Tateishi M, Kobayashi I, Saito Y and Nakamura T (2002a). Sediment facies and Late Holocene progradation of the Mekong River Delta in Bentre Province, southern Vietnam: An example of evolution from a tide-dominated to a tide- and wave-dominated delta. *Sedimentary Geology* 152 (3-4), 313-325.

Ta TKO, Nguyen VL, Tateishi M, Kobayashi I, Tanabe S and Saito Y (2002b). Holocene delta evolution and sediment discharge of the Mekong River, southern Vietnam. *Quaternary*

Science Reviews 21(16-17), 1807-1819.

Tamura T, Saito Y, Sieng S, Ben B, Kong M, Choup S and Tsukawaki S (2007). Depositional facies and radiocarbon ages of a drill core from the Mekong River lowland near Phnom Penh, Cambodia: evidence for tidal sedimentation at the time of holocene maximum flooding. *Journal of Asian Earth Sciences* 29, 585–592.

Tamura T, Saito Y, Sieng S, Ben B, Kong M, Sim I, Choup S and Akiba F (2009). Initiation of the Mekong River delta at 8 ka: evidence from the sedimentary succession in the Cambodian lowland. *Quaternary Science Reviews* 28 (3–4), 327–344.

Taylor B and Hayes DE (1983). Origin and history of the South China Sea basin. In: D.E. Hayes (Editor). *The tectonic and geologic evolution of Southeast Asian seas and islands; Part 2: Geophysical Monograph*, 23-56.

Tjallingii, R, Stattegger K, Wetzel A and Van Phach P (2010). Infilling and flooding of the Mekong River incised valley during deglacial sea-level rise. *Quaternary Science Reviews* 29(11-12), 1432-1444.

VAIL PR (1987). Seismic stratigraphy interpretation using sequence stratigraphy, Part 1: seismic stratigraphy interpretation procedure, *in* Bally, A.W., ed., *Atlas of Seismic Stratigraphy*, Vol. 1: American Association of Petroleum Geologists, *Studies in Geology* 27, 1–10.

Veenken P C H (2007). *Seismic Stratigraphy, Basin Analysis and Reservoir Characterisation*, vol. 37, 1st ed., 509 pp., Elsevier, Oxford.

Wiesner M, Stattegger K, Kuhnt W, et al. (1999). Cruise Report SONNE 140 SÜDMEER III, Reports Institut für Geowissenschaften 7, 157 pp.

Wiesner M, Stattegger K., Voß M, et al. (2006). Reports Institut für Geowissenschaften 23, 99 pp.

Wolanski E, Nguyen NH, Le TD, Nguyen HN and Nguyen NT (1996). Fine-sediment Dynamics in the Mekong River Estuary, Vietnam. *Estuarine Coastal and Shelf Science* 43,

565-582.

Zaitlin BA, Dalrymple RW and Boyd R (1994). The stratigraphic organization of incised-valley systems associated with relative sealevel changes. In: Dalrymple, R.W., Boyd, R., Zaitlin, B.A. (Eds.), *Incised-Valley System: Origin and Sedimentary Sequences*, SEPM Special Publications 51, 45–60.

Chapter 3

Late Pleistocene-Holocene seismic stratigraphy of Nha Trang Shelf, Central Vietnam

Bui Viet Dung¹, Karl Stattegger¹, Phung Van Phach²

¹*Institute of Geosciences, Kiel University, D-24118, Kiel, Germany*

²*Institute for Marine Geology and Geophysics, 18 Hoang Quoc Viet, Hanoi, Vietnam*

Abstract

The late Pleistocene-Holocene stratigraphic architecture on the steep and narrow shelf off Nha Trang, central Vietnam has been explored by high resolution seismic profiles integrated with sediment core data. Sequence stratigraphic results reveal five major seismic units and three bounding surfaces which are composed of two distinctive sequences. Those sequences are bounded by two regional unconformities (SB1, SB2) which have been formed in response to different sea-level regimes.

The lower sequence (sequence 2) consists of two seismic units (U0, U1) which are well developed on the outer shelf with maximum thickness of around 20-30 m and reduce to a thin or missing layer toward the middle and inner shelf. U1 and U2 units are mostly presented as seaward dipping clinoforms and pinch out landward at modern water depths of 100-120 m. Locations and internal patterns of the deposits suggest that the U1 and U2 units were primarily formed from the falling stage of sea-level to slow sea-level rise. U1 and U2 unit are interpreted as falling stage systems tract (FSST) and lowstand systems tract (LST), respectively. Ages of these units are deduced from Marine Isotope Stage (MIS) 3 to the Last Glacial Maximum (LGM) sea-level lowstand. The lowermost unit U0 is expressed as transparent and parallel layer overlying the SB2 surface, and is interpreted as deposits formed during the preceding highstand and transgression period (MIS 5e and older). The long gap between U0 and U1 unit is attributed to the erosional hiatus. The revealed relict beach-ridge deposits at water depth of about ~ 130 m below the present water depth indicate that the LGM sea-level lowstand in this area was lower than in neighboring areas and it probably resulted from subsidence due to high sedimentation rate and/or neotectonic movements of the East Vietnam Fault System. The LGM lowstand surface SB1 is traced by seismic profiles across the shelf. This surface shows relatively high gradient in the middle part (50-100 m

deep) and becomes gentler toward the inner and outer shelf as well as from northern to the southern part of study area.

The deglaciation/Holocene sequence following the LGM (U3 and U4 units) is separated from the lower units by the lowstand surface (SB1) and subdivided by the maximum flooding surface (Mxfs) RS1. The transgressive systems tract (TST) (U3 unit) consists of transgressive healing phase deposits on the outer shelf, backstepping onlap deposits on the mid shelf and aggradational deposits on the inner shelf. The TST deposits are well recorded across the shelf with average thickness of 25-30 m. The uppermost unit U4 is interpreted as modern highstand systems tract (HST) developing as seaward dipping clinofolds downlapping onto the Mxfs surface. The modern HST deposits form an along-shore mid-shelf sediment depocentre (average thickness ~15m) and its thickness decrease toward the inner and outer shelf.

The late Pleistocene high amplitude of sea-level change during a long fourth-order and superimposed by shorter fifth-order cycle is the principal factor in reorganizing the formation of the Nha Trang continental shelf sequence. Other local controlling factors as fluctuations in sediment supply, morphological variations of the lowstand surface, subsidence rate and hydrodynamic conditions provided the distinctive features of the Nha Trang Shelf sequence stratigraphic model in comparison with neighboring other areas.

3.1 Introduction

The Nha Trang Shelf is located on a passive continental margin, southernmost of the central Vietnam (Fig 3.1). Following the Last Glacial Maximum (LGM) about 20 ky BP (Before Present), the shelf was submerged rapidly due to its narrow and steep gradient during the post-glacial sea-level rise and therefore many older deposits were protected from erosion during the deglacial transgression. Well preserved relict deposits provide an excellent example for testing sequence stratigraphic concepts which were applied worldwide on continental shelves.

Previous studies on Holocene sedimentation on the Vietnamese Shelf has revealed high sediment accumulation rates off the Central Vietnam reaching up to 50-100 cm/ky (Schimanski and Stattegger 2005). It is also indicated that the surface sediments of the inner shelf in this area were dominated by relict sand (Allen 1967; Douglas et al., 1973; Szczuciński et al., 2005; Szczuciński et al., 2009). Different sand-barrier generations at Hon Gom Peninsula were dated between 8 to 0.2 ky BP (Dam 2010). Detailed studies on the late Quaternary sequence stratigraphy on the nearby shelf were concentrated on the central Sunda Shelf (Hanebuth et al., 2002; Hanebuth et al., 2003; Hanebuth and Stattegger 2004).

Results of sequence stratigraphy on the central Vietnam Shelf were mainly focused on the offshore Cenozoic basin evolution and hydrocarbon potential (Lee and Waltkin 1998; Fyhn et al., 2009), but research of the late Quaternary sequence stratigraphy on the Central Vietnam Shelf was not investigated in detail. In this research, we will apply the concept of sequence stratigraphy to the interpretation of shallow seismic high-resolution profiles on the Nha Trang Shelf (Fig 3.1). The general aims of this study are therefore to:

- Analyze the late Pleistocene-Holocene seismic stratigraphic architecture.
- Reconstruct the late Pleistocene-Holocene evolution of the shelf and propose a general sequence stratigraphic model.
- Compare the Nha Trang Shelf to other sequence stratigraphic models to distinguish local controlling factors

3.2 Regional setting

The Nha Trang Shelf is bordered by the Vietnamese coastline to the west and the South China Sea (SCS) to the east (Fig 3.1). The continental shelf is narrow and separated from the deep South China Sea by the N-S directed East Vietnam Fault System on the continental slope and rise (Fig 3.1). This fault system is generally considered to be the southward extension of the Red River strike-slip fault zone and runs almost parallel to the shoreline

along the 110⁰-Longitude (Lee and Watkins 1998; Clift et al., 2008; Fyhn et al., 2009). The continental shelf of study area is 40 km wide in average, steep in the middle and gentle in the inner and outer shelf (Fig 3.1). There are two bays in our study area: Van Phong in the northern and Nha Trang in the central part. The climate and hydrodynamic conditions of study area are driven by the East Asian monsoon system with winds mostly from NE during winter (October to March) and SW during summer (April to September) (Pham 2003). Most of sediments are supplied to the shelf by numerous small and short rivers which drain the high relief with maximum elevation of 2000 m (Fig 3.1). Estimated total suspended sediment load of all small rivers in study area ranges from $1.7-4 \times 10^6$ ton/year, of which Cai and Dinh River account for about 90 % of amount (Chapter 4, section 4.4.1; Bui et al., in prep). About 70 % of supplied sediments are transported to the shelf during short periods of the rainy season (September to December) and 30 % in the dry season (January to August) (National Project KC08.12 2004). Long-term monitoring data (1985-1995) collected in Nha Trang station indicate the average temperature of 27°C and the average rainfall of 96.7 mm/month (Emch 2008). The study area is dominated by semi-diurnal to diurnal tide regime with amplitude of 0.4 m in neap and 2.5 m in spring tides (Pham 2003, Szczuciński et al., 2005). Average wave height in this area ranges from 0.5 m and 2.0 m during fair-weather and they can reach up to 7.5 m during storm conditions (Thanh et al., 2004).

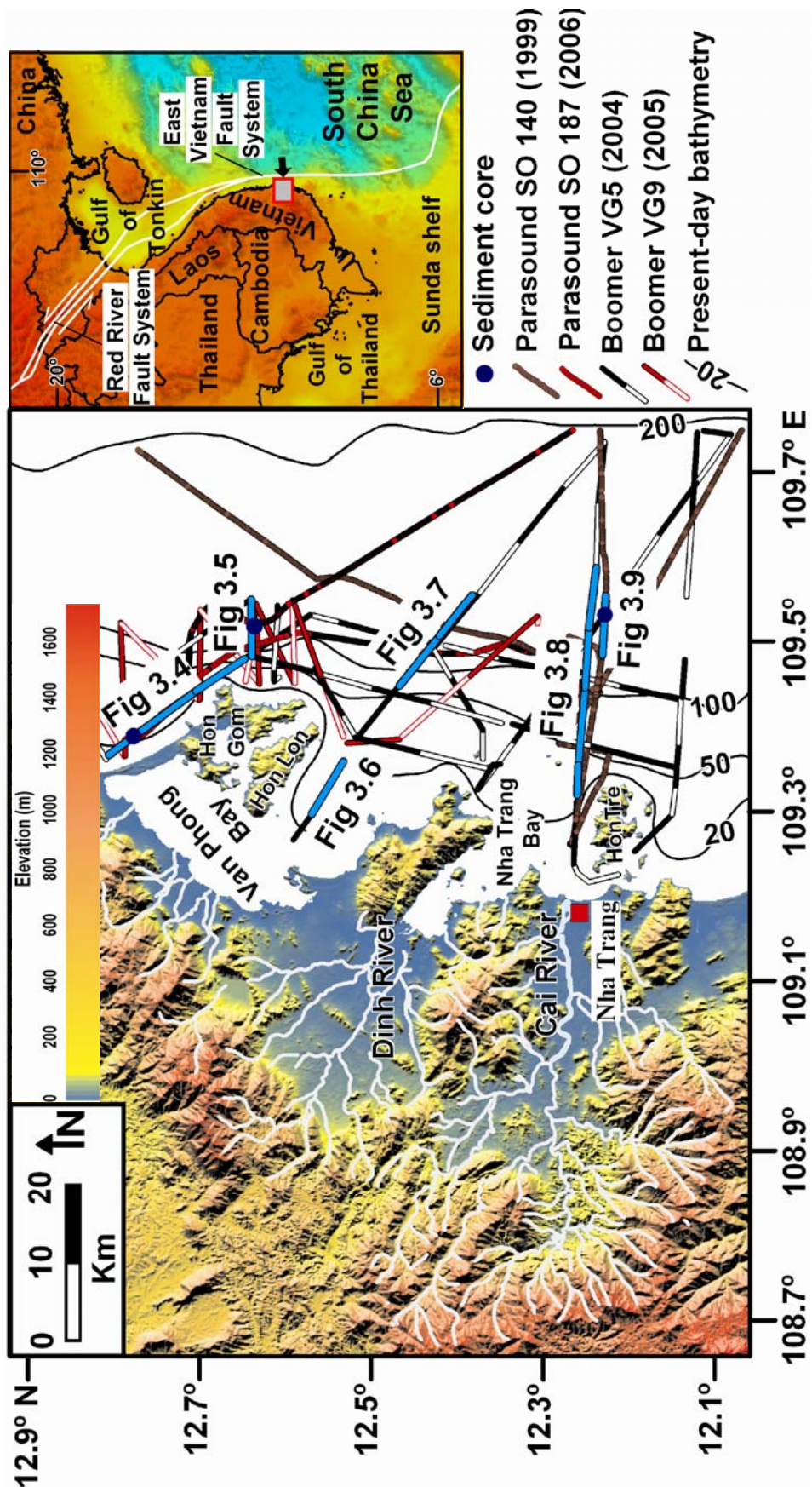


Fig 3.1. Map of Nha Trang Shelf with modern bathymetry and available data (seismic profiles and sediment cores). Locations of geological faults are adapted from Fyhn et al. (2009) and Clift et al. (2008). Elevation data of the land part is extracted from Shuttle Radar Topography Mission (SRTM) digital elevation models (<http://srtm.usgs.gov>).

3.3 Methods and available data

About 620 km of 2D high resolution seismic profiles have been analyzed on the Nha Trang Shelf (Fig 3.1). Those data have been collected at the beginning of the SW monsoon season (April and May) during different cruises in the framework of Vietnamese-German cooperation project: SO 140 (Wiesner et al., 1999), VG5 (2004), VG9 (2005), SO187 (Wiesner et al., 2006). Seismic data were acquired with two different sound-sources: boomer and parasound. Since the objective of the research concentrates on the continental shelf, most of profiles are located at water depth between 20 and 200 m (Fig 3.1). The boomer system (EG&G Uniboom) is a single channel system which includes an electrical energy supplier and an electromagnetic transducer that transforms the discharged energy to electro-dynamic acoustic pulses. During the surveys, the transducer of the boomer source was employed in a catamaran that was towed along with a hydrophone-streamer receiver (with 8 hydrophones) astern of the vessel. The average speed of the vessel was 4 knots. The boomer source produces a wide bandwidth working frequency with the main range of 0.3 to 11 kHz resulting in a typical penetration of 20 to 100 m below the seabed depending on the acoustic impedance (product of velocity and density) of the sediments. The boomer source regularly produced from 2 to 2.67 shots per second. The sound waves were reflected when reaching the reflection surfaces which are regarded as acoustic-impedance contrast boundaries. The hydrophone-streamer received the pressure reflection signals and converted them into voltage responses before transmitting them to the computer. Seismic traces were digitally recorded and displayed by using NWC software. A GPS (Global positioning system) was used to guarantee the accurate positions of the recorded seismic traces.

Parasound is a hull-mounted system which combines a narrow beam echosounder with a sub-bottom profiler. The system is operated with a fix primary frequency of 18 kHz and a secondary primary frequency variable from 20.5–23.5 kHz. Both primary frequencies are transmitted simultaneously in a narrow beam ($\sim 4^\circ$) and the constructive interference of these frequencies (parametric effect) allows to generate a working frequency (secondary frequency) within the beam of 2.5–5.5 kHz (Grant and Schreiber 1990). In our research, the parasound data was collected with secondary primary frequency of 22 kHz resulting in secondary working frequency of 4 kHz. The data was digitally recorded and sampled at frequency of 40 kHz. Navigation data was supplied by the ship's GPS.

For data processing, the frequency high/low pass filtering has been applied for the recorded data. Highpass filter is set to keep all frequencies higher than the selected frequency. In contrast, lowpass filter is set to keep all frequencies lower than the selected frequency. The frequency band- pass filtering of 2.5-6 kHz for parasound and 0.5-7 kHz for boomer data are

applied for all seismic profiles on the Nha Trang Shelf. The interpreted seismic surfaces are then picked with the software Kingdom Suite SMT 8.4. Average sound velocity of 1500 m/s in sea water and 1550 m/s in subsurface sediments has been assumed for Two-way travel time (TWT)-depth conversion.

Seismic data are interpreted on the basis of sequence stratigraphic concept which was initiated by Mitchum and Vail (1977) and Vail (1987), and then further refined by numerous authors. The seismic units are distinguished from each other by their reflection continuity, amplitude, frequency and configuration (Fig 3.2, see chapter 1).

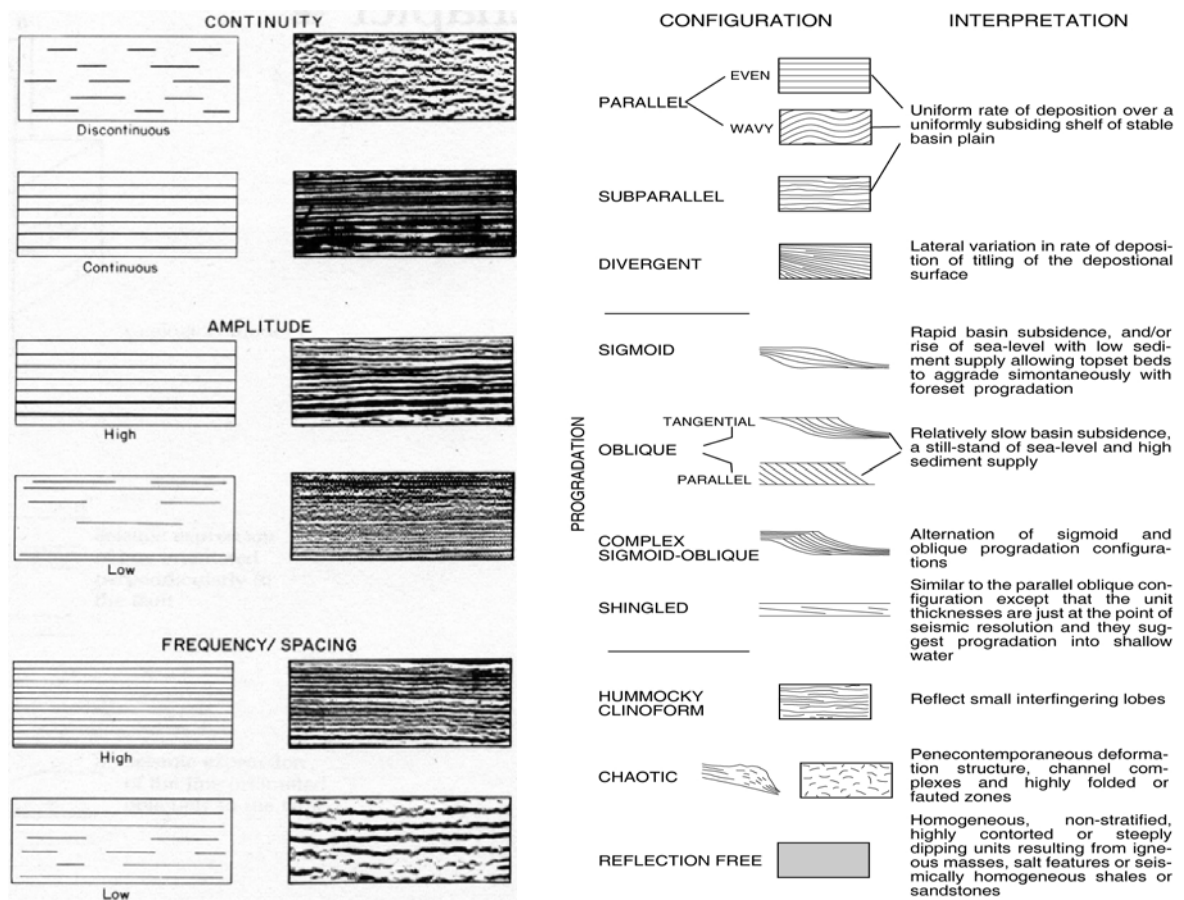


Fig 3.2. Classification of seismic facies and related depositional environments adapted from Badley (1985), Vail (1987) and Veenken (2007).

The interplay between base level changes (combined effect of eustasy, tectonics, sediment compaction, and environmental energy) and sedimentation rate controls the formation of sequence systems tract (Fig 3.3). For simplicity (by neglecting the energy of waves and currents), the base level is equated with the sea level (Catuneanu 2002). Hence, the concept of base level change is identical with the relative sea-level change. Accommodation is defined as the space available for sediments to accumulate and its variations depend on base

level changes. In this research, we apply the four-fold division of systems tract to divide the sedimentary architecture into different stages in relation to sea-level fluctuations (Catuneanu 2002; Catuneanu et al., 2009):

- **The falling stage systems tract (FSST)** was formed entirely during the stage of relative sea-level fall (forced regression), and it occurs independent of the ratio between the sedimentation rate and accommodation spaces.
- **The lowstand systems tract (LST)** was formed during the sea-level lowstand and slow sea-level rise when the rate of rise was lower than the sedimentation rate (normal regression).
- **The transgressive systems tract (TST)** was formed during the stage of relative sea-level rise when the rate of rise was higher than the sedimentation rate.
- **The highstand systems tract (HST)** was formed during the late stage of relative sea-level rise when the rate of rise was lower than the sedimentation rate.

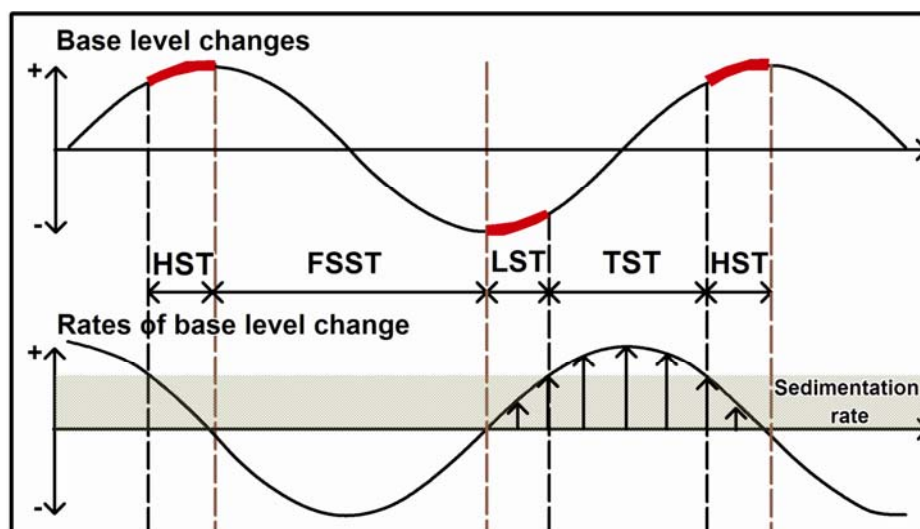


Fig 3.3. Sequence stratigraphic systems tracts as defined by the interplay between base level changes and sedimentation rate (modified from Catuneanu 2002). For simplicity, the sedimentation rate is kept constant during the base level fluctuations.

3.4 Results

3.4.1 Sequence stratigraphic analysis

In general, five seismic units and three major bounding surfaces are identified on the seismic profiles. The seismic units and their reflection configurations are summarized in Table 3.1.

Major bounding surfaces:

- SB1 is marked by high continuous and strong amplitude reflectors on seismic profiles (Fig 3.4 to Fig 3.9). This surface can be traced across shelf (20-140 m deep).
- The SB2 surface is the lowest reflection surface recorded on seismic profiles. It is presented as high continuous and strong amplitude reflectors (Fig 3.4 to Fig 3.9). Landward, it is mostly merged with the upper SB1 surface. However, this surface can be traced occasionally on the inner shelf where it is crossed by the SB1 surface as channel incision (Fig 3.6).
- RS1 is first surface which appears below the modern seabed (Fig 3.4, Fig 3.5, Fig 3.7 and Fig 3.8). It is characterized by medium amplitude but highly continuous reflectors on the mid and outer shelf. On the mid-shelf, RS1 surface is clearly defined on seismic profiles as boundary of the lower backstepping onlap and the upper seaward downlapping reflectors (Fig 3.8).

Seismic units:

- U0 is the lowest unit identified on seismic profiles. It is recorded across the shelf and bounded by the SB1 (upper) and SB2 (lower) surface (Fig 3.4 to Fig 3.8). This unit is characterized as horizontal and transparent reflectors on seismic profiles. Thickness of this unit shows strongly variable and ranges from 0-15 m.
- U1 is characterized by oblique parallel configuration with seaward dipping reflectors. It is truncated toplap by the overlying erosional surface SB1 and contacts tangential downlap with the lower U0 unit (Fig 3.9). On some seismic profiles (Fig 3.5, Fig 3.7 and Fig 3.8), U1 unit forms tangential downlap directly to the SB2 surface where U0 unit is absent. U1 unit is only recorded on the outer shelf and pinching out landward at water depths of 100-120 m. Estimated thickness of this unit on seismic profiles is approximate 20-25 m.

	Systems tract	Seismic units	Acoustic facies and configuration	Occurrence	Thickness (m)	Seismic image
Sequence 1	HST	U4	Low to moderate amplitude, variable frequency, medium continuity, locally transparent, parallel to sigmoid downlap	The entire shelf	0-25	
		RS1				
	TST	U3	Moderate to high amplitude, high frequency, high continuity, concave, backstepping onlap, aggradation	The entire shelf	0-50	
Sequence 2	LST	U2	Moderate to high amplitude, variable frequency, medium continuity, sigmoid downlap, toplap	Outer shelf	20	
		SB1	Moderate to high amplitude, high frequency, high continuity, oblique parallel downlap, toplap truncated	Outer shelf	20	
	FSST	U1				
		U0	Low to moderate amplitude, transparent, parallel	The entire shelf	0-15	
	HST+TST					
		SB2				

Table 3.1. Systems tracts, seismic units and facies, bounding surfaces and reflection patterns on the Nha Trang Shelf. Abbreviations: FSST = Falling stage systems tract, LST = Lowstand systems tract, TST = Transgressive systems tract, HST = Highstand systems tract.

- U2 unit is developed as seaward continuation of U1 unit and it is separated landward with the U1 unit by a concave surface (Fig 3.5). This unit is represented by sigmoid wedge shape with seaward dipping reflectors. On top of this unit, it forms toplap with the overlain smooth surface (Fig 3.5). Dipping angle of seismic reflectors of U2 unit is slightly smaller than those of U1 unit. Average thickness of this unit is about 20 m. The U2 unit is only detected on the northern shelf off Hon Gom Peninsula (Fig 3.5).
- U3 unit is recorded across the shelf (Fig 3.4 to Fig 3.9). This unit is bounded by the RS1 surface on top and SB1 surface at the base. U3 unit appears as thin transparent layer on the outer shelf. On the mid shelf, U3 unit is expressed as high amplitude reflectors with backstepping onlap configuration (Fig 3.4 to Fig 3.8). Toward the inner shelf, its seismic configuration becomes aggradational stacking patterns (Fig 3.6). Thickness of this unit shows low variability over the shelf with no significant depocenter.
- U4 is the uppermost unit on seismic profiles (Fig 3.4 to Fig 3.9). Its thickness is thin (average of 0-5 m) on the inner and outer shelf with parallel and transparent seismic reflectors. Thick deposits of this unit are mostly concentrated on the mid shelf where it appears on seismic profiles as thick seaward dipping reflectors (Fig 3.4 and Fig 3.8). Maximum thickness of this unit reaching up to 20-25 m on the mid shelf of Van Phong and Nha Trang Bay and it reduces toward the inner and outer shelf (Fig 3.8).

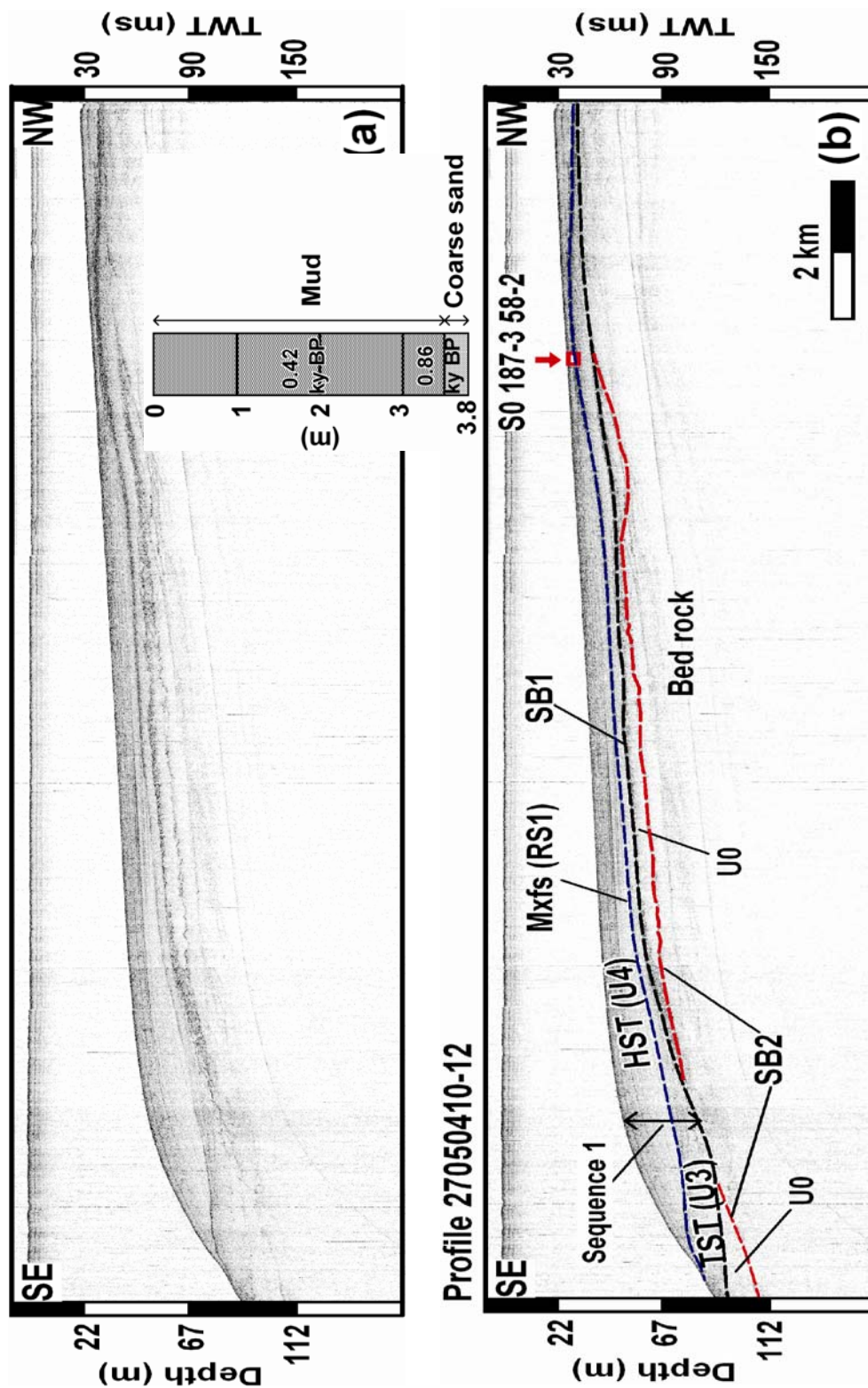


Fig 3.4. Seismic profile (a) and sequence stratigraphic interpretation (b) of the transition from inner to outer shelf on the northern part off Hon Gom Peninsula. Sediment core datings indicate very young highstand deposits (0.42 and 0.86 ky BP). Core data adapted from Wiesner et al., (2006). For abbreviations see Table 3-1.

3.4.2 Sedimentary characteristics and ages of deposits

Coring station at water depth of 29 m (core SO187-3 58-2) on the northern part off Hon Gom Peninsula shows a transition from coarse sand in the lowermost part to homogenous mud in the upper part of the sediment core (Fig 3.4). Two radiocarbon datings of this core provide ages of 0.42 and 0.84 ky BP (Fig 3.4). The 2.2 m long sediment core at water depth of 133 m off Hon Gom Peninsula shows homogenous muddy layer (Fig 3.5). Radiocarbon datings of sediment core at water depth of 134 m on the Nha Trang Shelf (core SO 140-C01, Fig 3.9) cover the age interval of 2.29 to 10.78 ky BP. The sediments have muddy composition, low sand content and abundant shell fragments along the core (Schimanki and Stattegger 2005). Earlier study on the outer Sunda Shelf indicated age of 25-30 ky BP of the late Pleistocene soil surface (Hanebuth and Stattegger 2004). The ages of the seaward dipping clinoforms (regressive unit) (at water depth of 80-126 m) below the LGM soils surface on the Sunda Shelf were dated as 50 to 30 ky BP (Hanebuth and Stattegger 2004; Hanebuth et al., 2003). Besides, a 6.2 m long core taken on the top of seaward dipping clinoforms (at water depth of 152 m) on the outer Sunda Shelf indicated age of 39-36 ky BP for the clinoform deposits and 4.0 ky BP for the overlying thin mud layer (Steinke et al., 2003). On the Southeast (SE) Vietnam Shelf, radiocarbon dating of sediment core at water depth of 156 m reaching the upper part of the lowstand wedge shows age of 24.33 ky BP (Schimanki and Stattegger 2005).

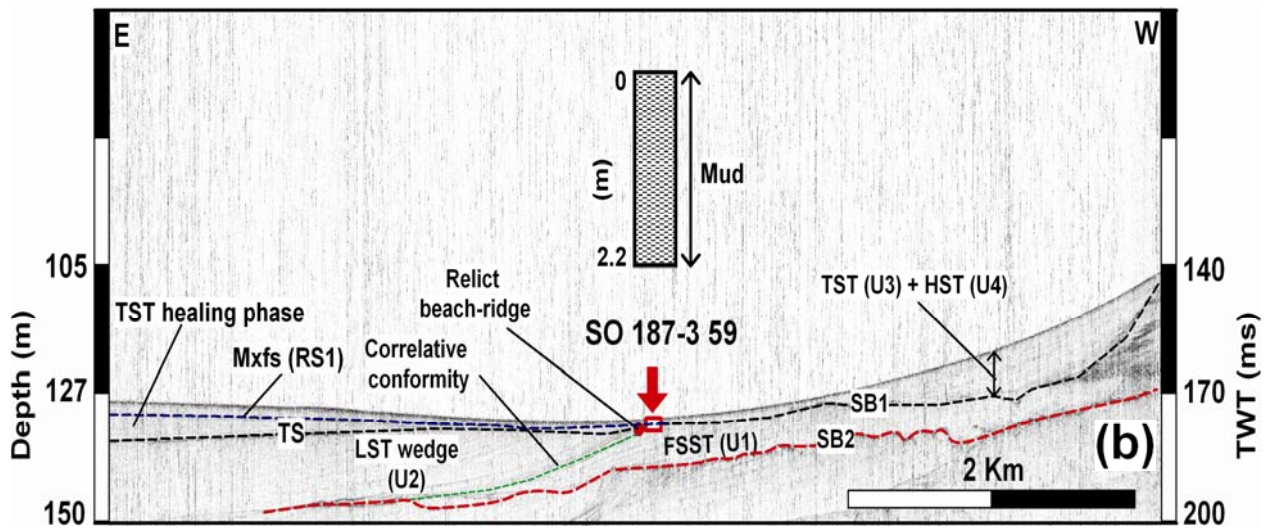
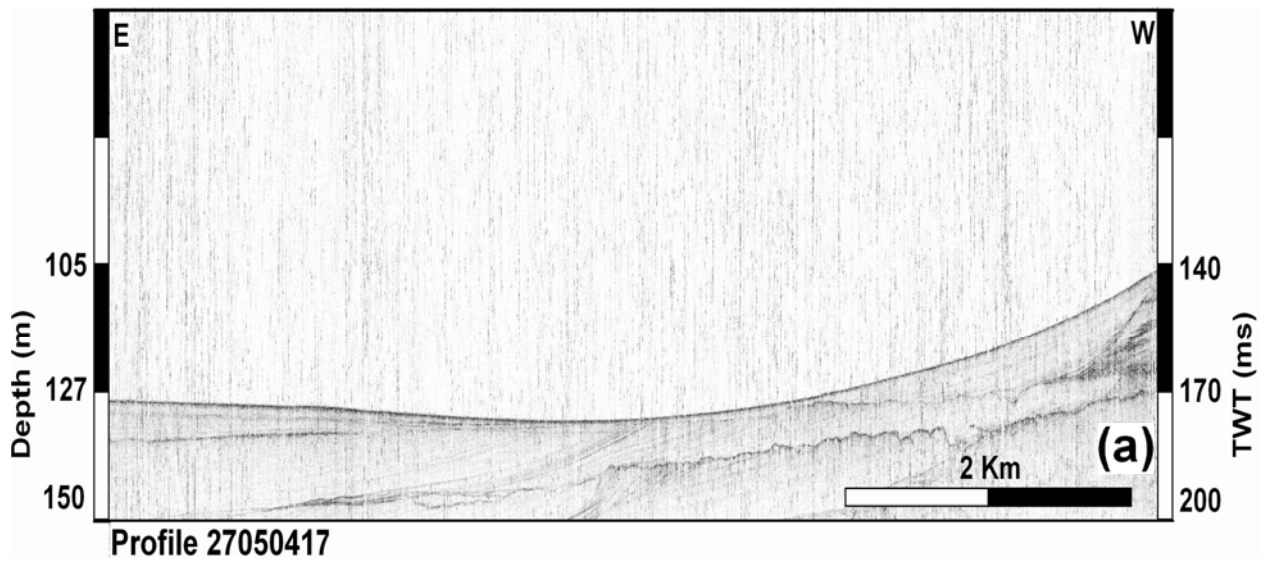


Fig 3.5. Seismic profile (a) and sequence stratigraphic interpretation (b) of the outer shelf off Hon Gom Peninsula with the complete record of systems tracts. Core data adapted from Wiesner et al., (2006). For abbreviations see Table 3-1.

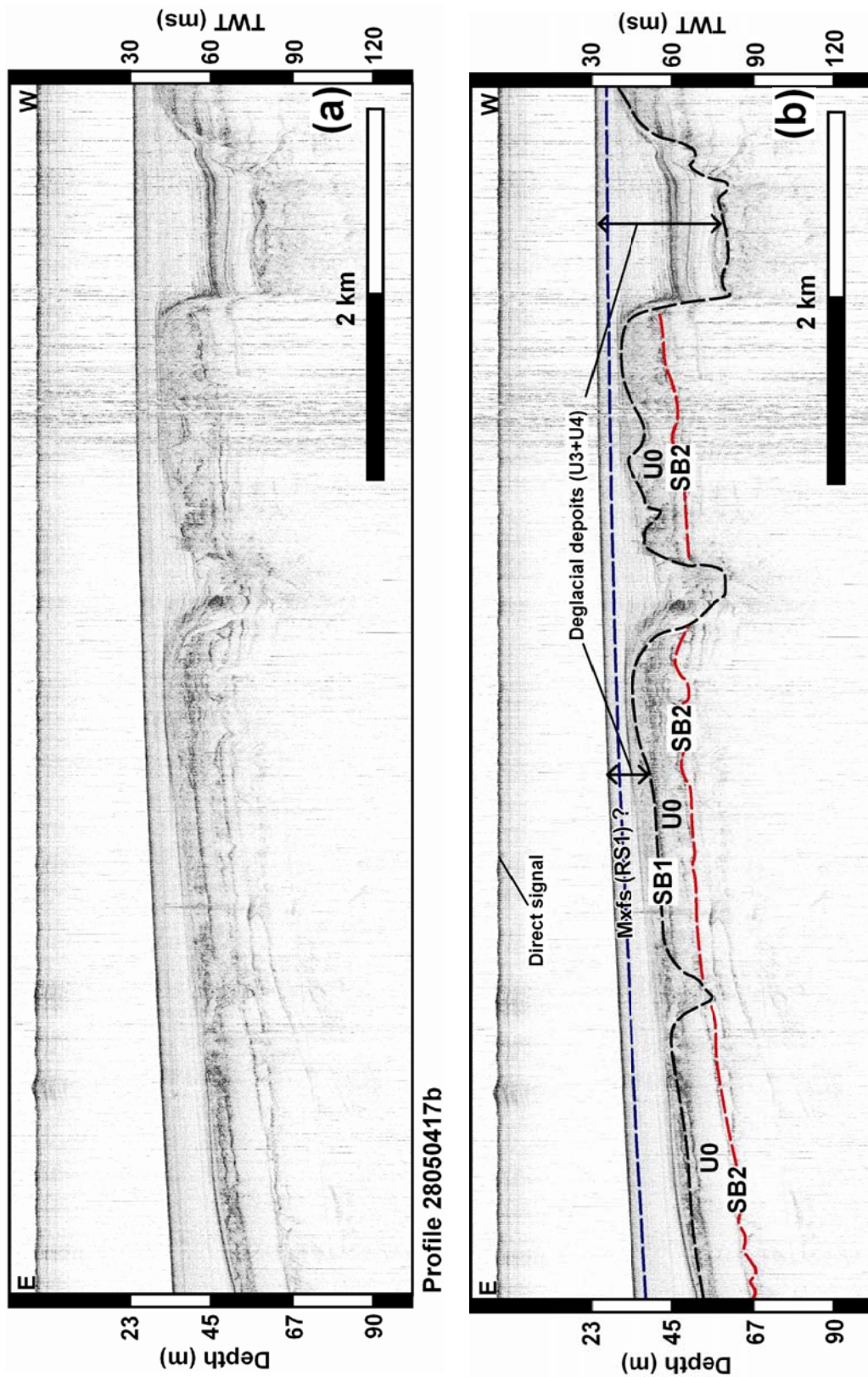


Fig 3.6. Seismic profile (a) and sequence stratigraphic interpretation (b) of the inner shelf of Van Phong Bay with aggradational stacking patterns of deglacial deposits. Discrimination between HST and TST is hardly resolved. For abbreviations see Table 3-1.

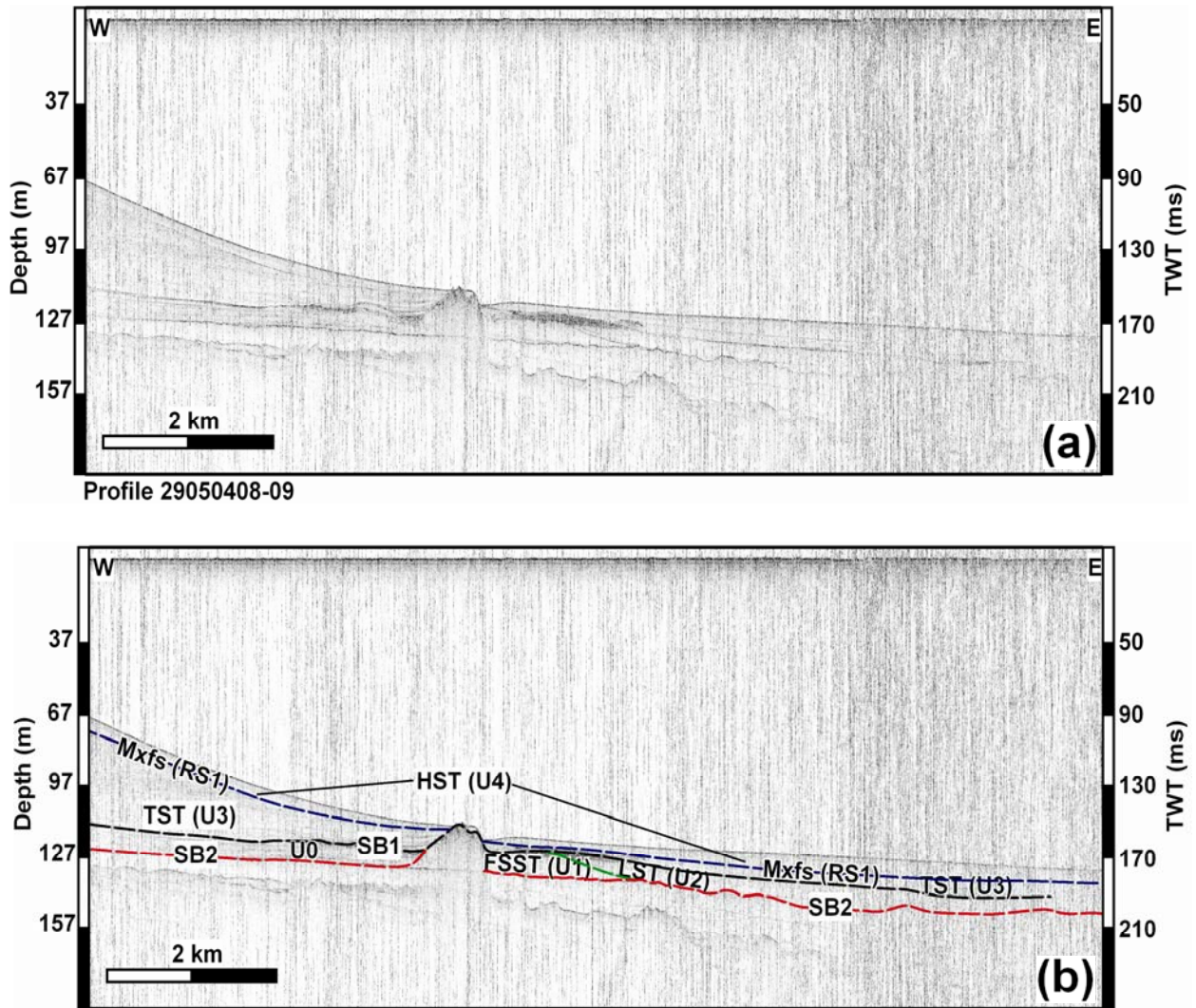


Fig 3.7. Seismic profile (a) and sequence stratigraphic interpretation (b) of the mid and outer shelf of Van Phong Bay. For abbreviations see Table 3-1.

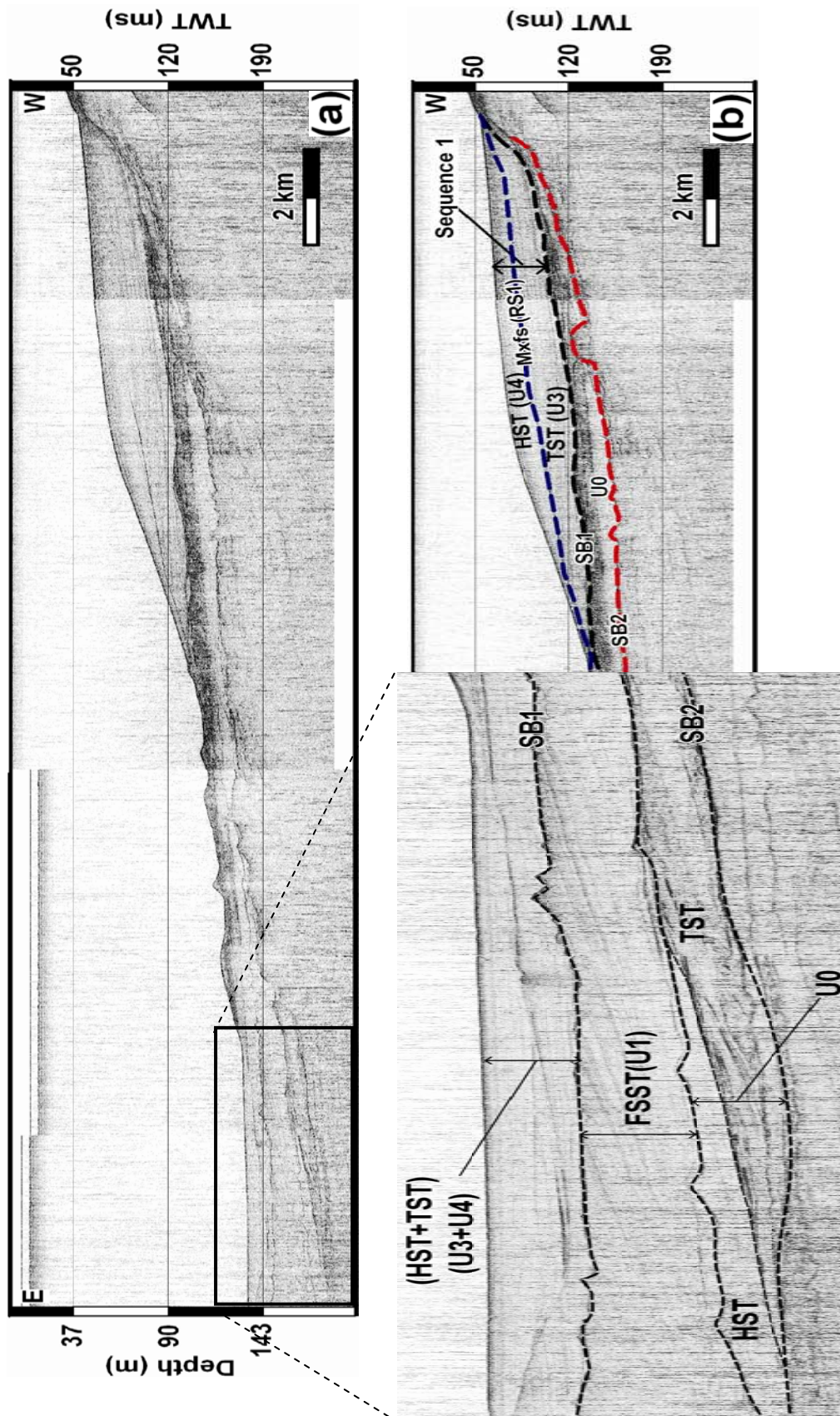


Fig 3.8. Seismic profile (a) and sequence stratigraphic interpretation (b) of the transition from the inner to outer shelf of Nha Trang Bay. For abbreviations see Table 3-1.

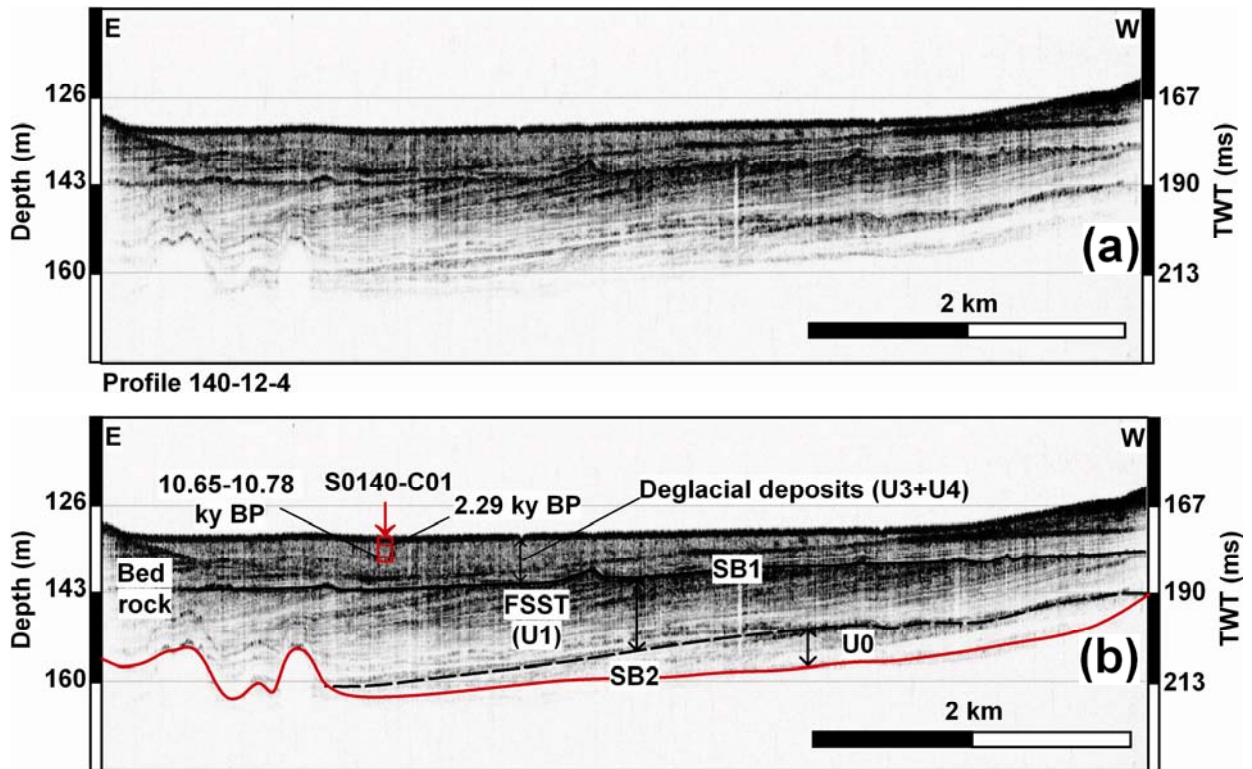


Fig 3.9. Seismic profile (a) and sequence stratigraphic interpretation (b) offshore Nha Trang Bay. Regressive unit (U1) is toplap truncated by the lowstand surface (SB1) and overlain by deglacial/Holocene deposits (U3 and U4). Core data adapted from Schimanski and Stattegger (2005).

3.4.3 Sequence stratigraphic interpretation

➤ LGM lowstand surface SB1

The seismic reflection SB1 surface is interpreted as sequence boundary forming the base of the deglacial sequence 1. This surface has probably experienced multi-phases of the sea-level fall (regression stage), sea-level lowstand and was reworked again during transgression. No direct dating is available for this surface on the SE Vietnam Shelf area, however the formation of SB1 surface in our research can be correlated to the late Pleistocene soil surface dated as 25 to 30 ky BP on the outer Sunda Shelf (Hanebuth and Stattegger 2004). An interpolation map derived from seismic profiles of LGM lowstand surface SB1 is shown on Fig 3.11. In general, the LGM surface shows a high-gradient ($\sim 0.64^{\circ}$) in the middle part between 50-100 m water depths. Especially, in the area off Hon Gom Peninsula the shelf gradient between 50-100 m water depths reaches up to 1.6° . To the the inner part (< 50 m

deep) and outer part (100-150 m deep), the lowstand surface gradient is decreasing very fast. From northern to southern part of study area, the LGM surface gradient becomes gentler.

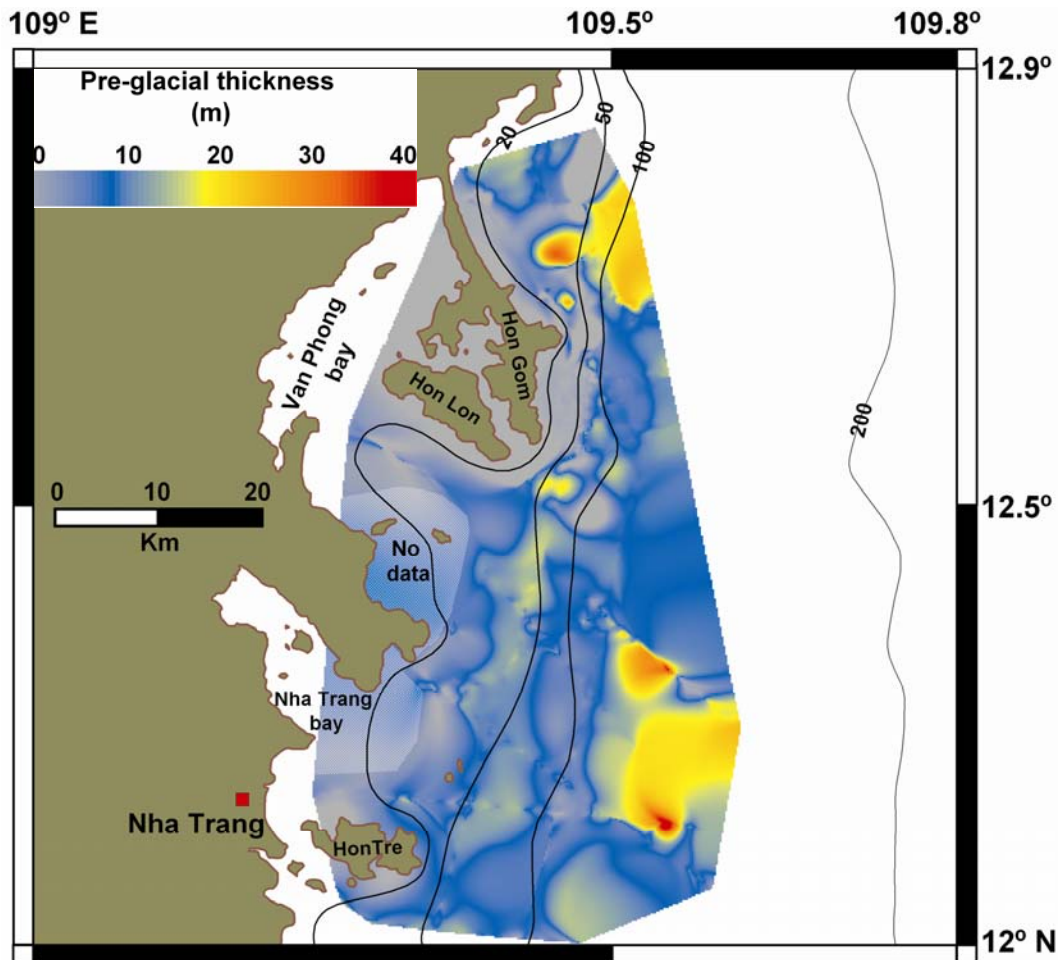


Fig 3.10. Total sediment thickness map of sequence 2 (U0, U1 units) and U2 unit. Thick deposits on the outer shelf resulted from well developed regressive units (U1 and U2) which are pinching out landward at water depth of 100-120 m.

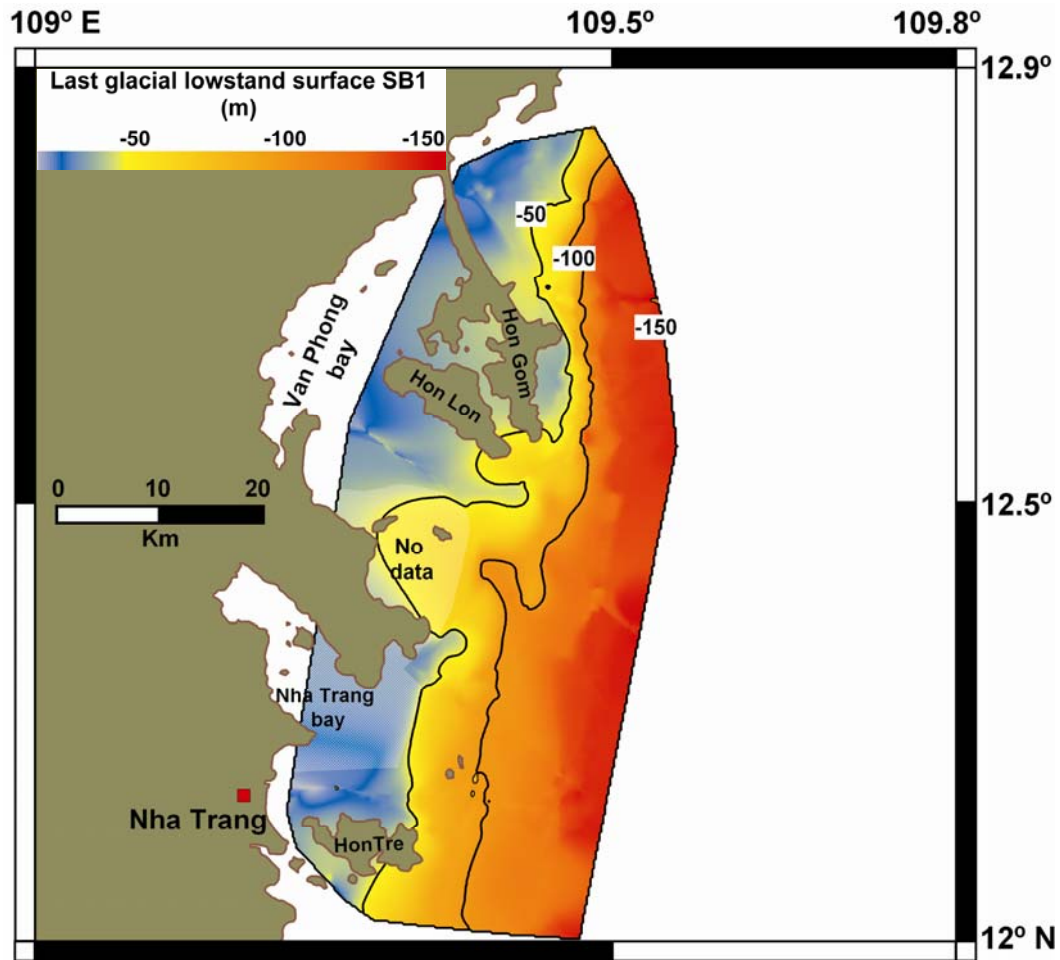


Fig 3.11. Contour map of the LGM surface SB1 with reference to the modern sea-level constructed from seismic profiles. Basically the lowstand surface was blocked at the LGM sea-level around -125 to -130 m and its seaward extension was merged with the transgressive surface (TS).

➤ **Falling stage systems tract (FSST), Lowstand systems tract (LST) and older deposits**
 The steep and seaward dipping strata of unit U1 and U2 were truncated by the lowstand erosional surface SB1 and therefore are related to the regressive deposits. U1 unit is mostly recorded on the outer shelf. Its oblique-tangential geometry allows for an interpretation as forced regressive unit formed entirely in falling stage of sea-level. The sigmoid-wedge shape with tangential clinofolds of U2 unit (Fig 3.5) suggests that it was developed in the period of sea-level stillstand or little rise (Vail 1987). U2 unit is interpreted as lowstand wedge deposits formed during the sea-level lowstand and slow sea-level rise. On the nearby Sunda Shelf, Hanebuth et al. (2003) revealed three types of forced regressive units according to their location and patterns. These units showed seaward rejuvenation (*sensu* Hanebuth et al., 2003) trend of depositional ages as a result of the MIS 3 falling sea-level. U1 unit in our research

are well correlated with the outer shelf regressive wedge (third type) in Hanebuth's classification with similar location and internal patterns of seismic facies. The concave boundary between U1 and U2 units is probably a beach shoreface developed under strong influences of wave (Fig 3.5). Some beach-ridge structures found at water depth of 130 m below modern sea-level give a question about the minimum sea-level lowstand on the Nha Trang Shelf (Fig 3.5). On the Sunda Shelf, the minimum lowstand sea-level reported was around 123 ± 2 m below modern water depth (Hanebuth et al., 2009). Previous research of Schimanski and Stattegger (2005) has indicated the lower trend of sea-level on the central Vietnam Shelf in comparison with data from Sunda Shelf and they explained this as a result of strong subsidence caused by high sedimentation rate on this narrow shelf. Other possibility might relate to the neotectonic movements of the East Vietnam Fault (Fyhn et al., 2009).

Deposits and age of the basal unit U0 remains uncertain since no direct core data as well as correlation with neighboring shelf areas are available for this unit. The interpretation of this unit is therefore speculative based on its seismic reflection patterns, location and correlation to the sea-level curve (Fig 3.14). The transparent-horizontal seismic facies of this unit suggest it could be formed in the aggradational phase of the preceding transgression to highstand period between MIS 6 and MIS 5e. Similarly on the Adriatic basin, plane and parallel seismic units was revealed at the base of the regressive clinoform deposits and be interpreted as HST and TST deposits (Ridente and Trincardi 2005).

➤ **Transgressive systems tract (TST)**

Unit U3 presents a backstepping layer overlying directly the sequence boundary SB1 and is attributed to transgressive deposits. The distal wedge-shape deposits on the top of LST wedge (Fig 3.5) represent probably the early transgressive healing phase (sensu Posamentier and Allen 1993). They were formed by erosion and seaward transport of shoreface sediments. On the mid shelf, the U3 unit shows backstepping or aggradational stacking patterns onlapping the lowstand erosional surface SB1 (Fig 3.7 and Fig 3.8). These deposits were probably formed under the relative sea-level rise with abundant sediment supply (see more discussions in the next part). The seismic profile on the inner shelf of Van Phong Bay (Fig 3.6) shows clear aggradational stacking patterns with highly continuous, medium amplitude and parallel reflectors covering the lowstand erosional surface SB1. Internal patterns suggest that the units were formed under low-energy and stable depositional environments. Sediment core data is not available, therefore the discrimination between the HST deposits with the lower TST on the inner shelf is really difficult. In that sense, the interpretation of the inner shelf HST relies primarily on the previous researches suggesting that the modern HST sediments are mostly

transported offshore and the surface sediments of the inner shelf are covered by relict sand (Allen 1967; Szczuciński et al., 2005; Szczuciński et al., 2009). Parts or the whole package of these reflections must therefore be attributed to the TST. The thick aggradational stacking patterns of the inner shelf TST deposits (15-30 m in thickness) are an indicator of reducing rate of accommodation spaces/sediment supply during the transgression. The TST deposits can be observed across the shelf with low variability (Fig 3.13b). Exceptions appear only when basement structures come close to the surface and reduce sediment thickness (Fig 3.13b).

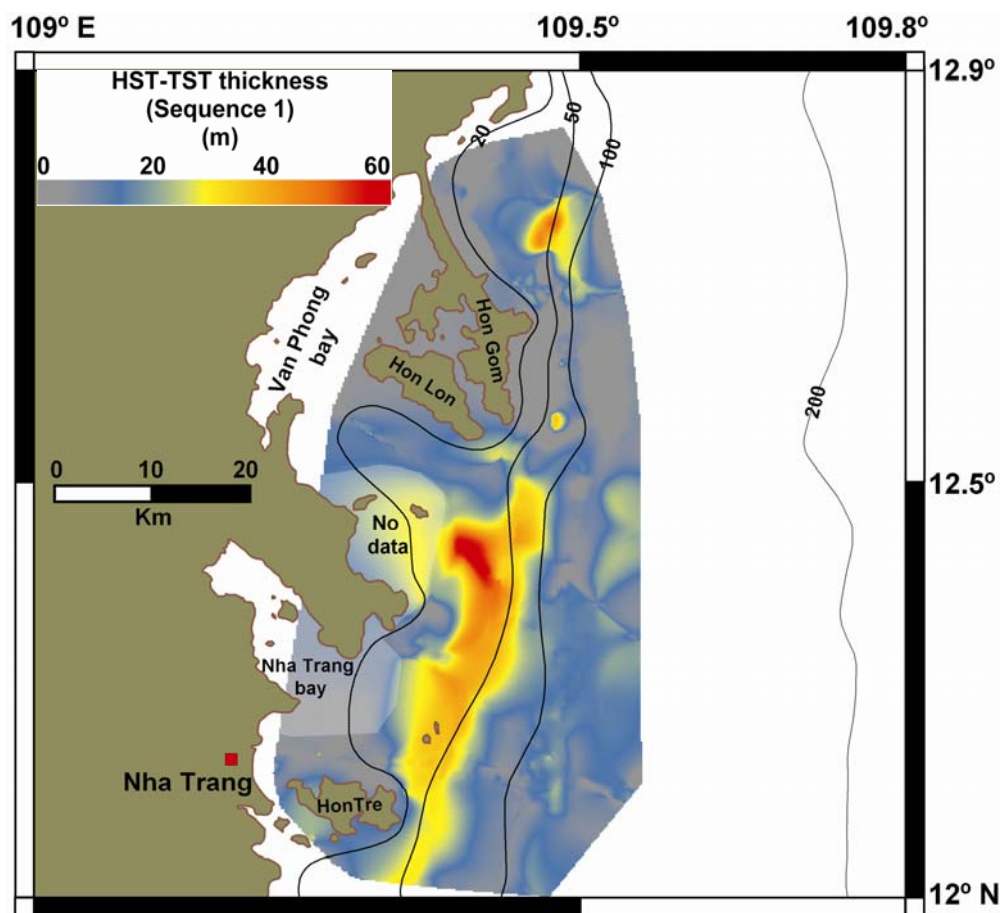


Fig 3.12. Total deglacial/Holocene sediment thickness (sequence 1) including U3 and U4 units. The sediment depocentre is located on the mid shelf.

➤ **Highstand systems tract (HST)**

Unit U4 mostly appears as clinoforms downlapping onto the RS1 surface on the mid shelf. Two radiocarbon ages of this unit taken off Hon Gom Peninsula indicate age of 0.42 to 0.86 ky BP (Fig 3.4). U4 is interpreted as modern highstand deposits. The HST deposits form an elongated mud-belt depocentre of 20 m in thickness developing along the mid shelf which

reduces toward the inner and outer shelf (Fig 3.12; Fig 3.13a). HST thickness is highly variable around Hon Gom Peninsula reflecting the rough morphology of the shelf in this area which is contoured by basement rocks.

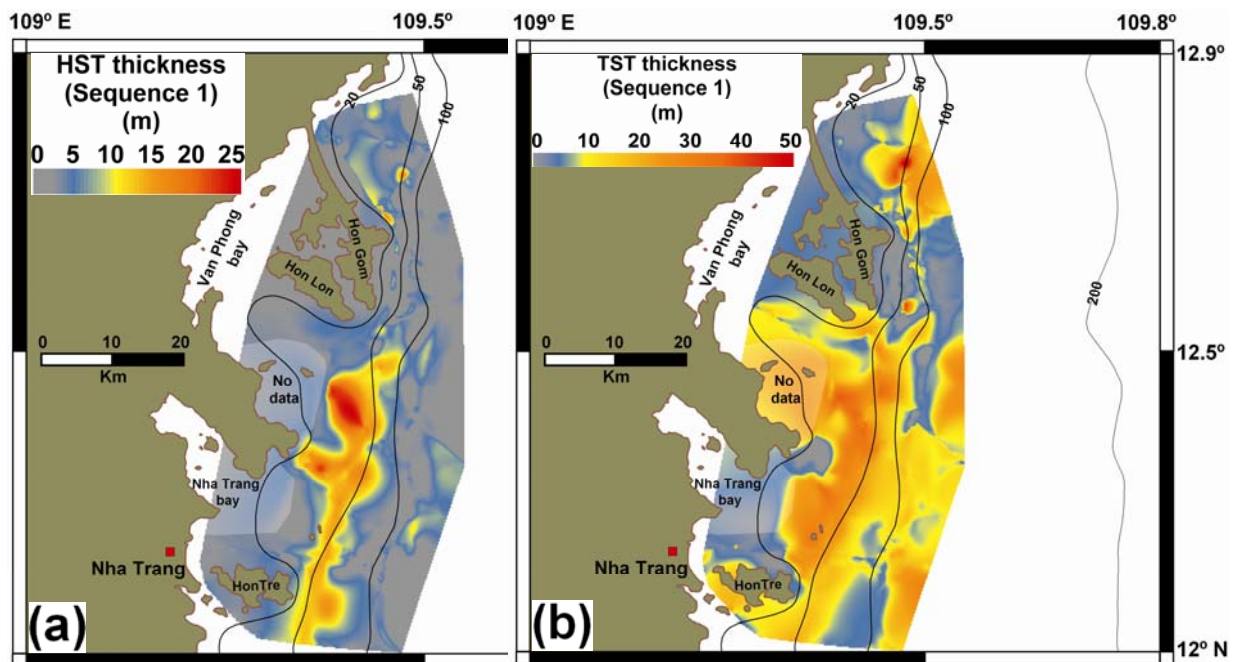


Fig 3.13. Sediment thickness map of HST (a) and TST (b) of sequence 1. HST depocentre is located on the mid shelf in front of Van Phong and Nha Trang Bay. HST deposits are probably transported along-shore southward. The TST deposits develop over the shelf without significant sediment depocentre.

3.5 Proposed sequence stratigraphic model for the Nha Trang Shelf

The Late Pleistocene-Holocene evolution model on the Nha Trang Shelf includes four systems tracts (Fig 3.14). The FSST and LST are well recorded on the modern outer shelf (Fig 3.10). The age of these units are derived by correlation to the regressive deposits on the neighboring shelf areas. Ages of one sediment core taken on the top of the Sunda Shelf regressive wedge at water depth of 152 m were identified as 34 to 31 ky BP (39-36 calibrated) (Steinke et al., 2003). This can probably provide the upper age limit for the FSST deposits on the Nha Trang Shelf area. On the Sunda Shelf, the outer shelf lens-shaped regressive deposits (at ~110 m water depth) were formed around 45 ky BP. Therefore, the forced regressive deposits (FSST) in our research recorded at 120 m water depth must be formed slightly after 45 ky BP. Hence, the FSST on the Nha Trang Shelf was probably

formed during final state of regressive around 45 to 30 ky BP (Fig 3.14b). On the SE Vietnam Shelf, the upper part of the lowstand wedge at water depth of 156 m yielded an age of 24.33 ky BP (Schimanki and Stattegger 2005). This result fits well to the Sunda Shelf data with age of 25-30 ky BP for the late Pleistocene soil surface (Hanebuth and Stattegger 2004) that can be correlated to the SB1 surface on Nha Trang Shelf. Hence, we deduce that LST deposits in our research were probably formed from 30 ky BP to the LGM lowstand termination at 19.6 ky BP (Hanebuth et al., 2009). The separation between FFST and LST could be observed only on the steep gradient off Hon Gom Peninsula (Fig 3.5) but not further south (Fig 3.7, Fig 3.8 and Fig 3.9). The restriction of the LST wedge deposits to Hon Gom Peninsula may be due to low sediment flux (no big river supply indicated by absence of incised-channels) and the low gradient of the outer part (between 100-150 m) of the LGM surface on the southern part (Fig 3.11) that promoted the large accommodation spaces created by early sea-level rise. Therefore, no balance between sediment supply and accommodation space could be reached. On the other hand, the transgressive healing phase deposits were found only in the area off Hon Gom Peninsula (Fig 3.5). This indicates that LST wedge deposits in this area were protected from high wave activity during the early transgression since the healing phase deposits are an indicator of wave base influence limitation (Posamentier and Allen 1993). In the southern part of Nha Trang and Van Phong Bay, LST wedge deposits were probably subjected to stronger hydrodynamic conditions including high wave activity due to the lower-gradient of LGM surface (above the wave base influence) and intense bottom currents (indicated by relic bedforms overlying the LGM surface in Fig 3.8), and this could prevent sediment accretion. The time gap between formation of FSST (~30 ky BP) to TST (~19.6 ky BP) on the southern part of study area is attributed to the development of the marine ravinement surface at the top of distal forced regressive deposits (125-145 m deep in our seismic profiles). Similarly, on the Sunda and Adriatic Shelf, the regressive units were dominated entirely by the forced regressive deposits and the lowstand wedge deposits cannot be identified (Hanebuth et al., 2003; Ridente and Trincardi 2005). Regressive deposits on the Nha Trang Shelf were well preserved on the modern outer shelf (at more than 100 m water depth) and show seaward thickening with average thickness of about 20-30 m (Fig 3.10). This is probably due to the fact that the outer part of the shelf was partly or entirely submerged during sea-level lowstand and therefore was protected from the effects of subaerial erosional processes. Further landward, the FSST deposits are absent in all recorded seismic profiles since the inner and mid shelf regressive deposits were subjected to long term erosional processes during the sea-level fall after MIS 5e highstand and were reworked again during the following transgression. The outer shelf lens-shaped regressive deposits

documented on the Sunda Shelf (Hanebuth et al., 2003) and the SE Vietnam Shelf (Wiesner et al., 2006) cannot be detected on the high-gradient shelf of Nha Trang area. We therefore consider the absence of the seaward dipping regressive deposits on the inner and mid shelf as a result of long-term erosional hiatus (Fig 3.14). The FSST unit is bounded on the top by the unconformity SB1. The SB1 surface in our work is an amalgamated surface which was probably initiated after the MIS 5e, expanded until the LGM sea-level lowstand and was further reworked during the subsequent deglacial transgression (Fig 3.14). SB1 surface is merged seaward with the TS ravinement surface which overlies the LST wedge (U2) (Fig 3.5, Fig 3.8 and Fig 3.9).

The time of maximum flooding on the Nha Trang Shelf remains unclear since the RS1 surface was not dated. However, its formation can be correlated to the initiation of the two nearby deltas Red and Mekong River which have happened around 8.0 ky BP (Hori et al., 2004; Tamura et al., 2007; Tamura et al., 2009). We deduce that the ages of TST on the Nha Trang Shelf can range from 19.6 to 8.0 ky BP. Configurations of the TST deposits show a transition from backstepping on mid-outer shelf to aggradation stacking patterns on the inner shelf that reflects the regime of sea-level rise, sediment flux and the pre-existing LGM lowstand surface gradient. The TST healing phase deposits with wedge shape on the outer shelf (Fig 3.5) probably resulted from slow sea-level rise with intense marine reworking processes at the beginning of transgression. In contrast, The TST deposits on mid shelf (Fig 3.7 and Fig 3.8) were formed during the period of moderate sea-level rise with rate 0.33 to 0.93m /100y (Fig 1.4, chapter 1). An exception happened during the short period of melt water pulse (MWP) 1 A (14.6 to 14.3 ky BP) with high sea-level rise of 5.33m/100y to (Fig 1.4, chapter 1). However the high-gradient of the LGM surface in this part of the shelf (between 50-100m deep) (Fig 3.11) has probably diminished the effects of moderate to high sea-level rise and it resulted in thick backstepping to slightly aggradational stacking TST deposits (Fig 3.7 and Fig 3.8). The high gradient slope often reduced the rate of landward coastline migration during relative sea-level rise and increased the time for marine erosion and reworking sediment processes (Swift 1976; Cattaneo and Steel 2003a). To the inner shelf (at water depth of 30 m) where the LGM surface gradient is more gentle (Fig 3.6 and Fig 3.11), the TST deposits show thick aggradational stacking patterns. The formation of TST deposits in this profile primarily falls in the period of the early Holocene with average rate of sea-level rise of 0.93 m/100y prior to the rapid sea-level rise MWP 1C, as indicated by the regional sea-level curve (Fig 1.4, chapter 1). Hence, the thick aggradational stacking patterns of the TST deposits are attributed to the high sediment supply which can neutralize the effect of the moderate sea-level rise. At similar water depth on the SE Vietnam Shelf (~29 m water

depth), rapid aggradation of TST fluvial sediments in the Mekong River incised-valley before marine flooding around 9.0 ky BP has been documented (Tjallingii et al., 2010).

The HST period on the Nha Trang Shelf began about 8.0 ky BP. At the same time, the Mekong and Red river deltas was initiated. The modern highstand mud deposits observed on the Nha Trang Shelf have been formed following the sea-level highstand of 1.5 m above the modern level reached between 6 and 5.5 ky BP (Michelli 2008). The HST sediment depocentre appears as NE-SW elongated sediment body on the mid-shelf and it is almost absent in the northern part of study area where the river influences are less profound (Fig 3.13a). Location of the HST mud wedge suggests the importance of local rivers as the major sediment sources of the sediment depocentre. Hydrodynamic modeling studies indicate that the surface currents on Nha Trang and Van Phong Bay are mainly oriented offshore during summer and southward along-shore during winter (Barthel et al., 2009). Therefore, the major sediment supply to the shelf during rainy season (account for 70% of sediment supply) is almost coincident with the beginning of winter season (September to December). Sediments will be transported along-shore southward by the dominated NE monsoon effects or they can settle only around the river plume outflow on the inner shelf. Dispersion of fine material directly to the mid and outer shelf by the cross-shore sediment transport during this period is not significant. Since the inner shelf surface sediments are dominated by sands, reasonable sources of the modern fine sediments on the mid and outer shelf are assumed to be redeposited from the inner shelf via advection processes as well as transported along-shore from the northern shelf (Szczeniński et al., 2009).

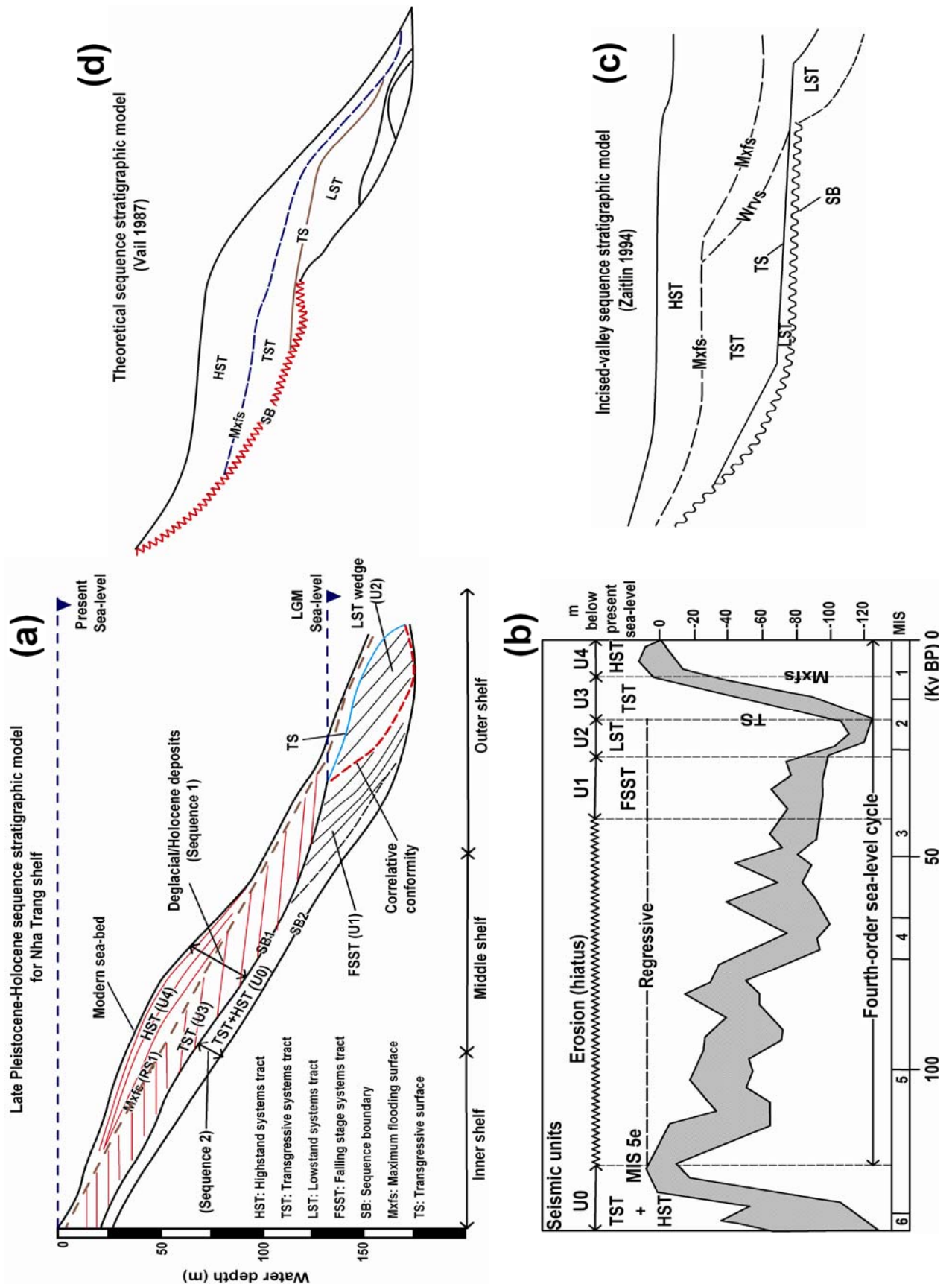


Fig 3.14. Late Pleistocene-Holocene sequence stratigraphic model for the Nha Trang Shelf (a) with regional sea-level curve (b) (Hanebuth et al., 2004; Shackleton 1987; Chappell et al., 1996; Fleming et al., 1998) and comparison to theoretical models of Zaitlin (c) and Vail (d).

3.6 Discussion and conclusions

The late Pleistocene high amplitude of sea-level change during a long fourth-order cycle (100-120 ky) superimposed by several shorter fifth-order cycles is the principal factor in the organization of the Nha Trang continental shelf sequence (Fig 3.14). The proposed sequence-stratigraphic model for the SE Vietnam Shelf basically follows the main features of the theoretical models of Vail (1987) and Zaitlin et al. (1994) (Fig 3.14). However, there still exist differences which are attributed to the local controlling factors. On the Nha Trang Shelf, the thick mud highstand wedge is detached from the sediment source and forms the elongated mid-shelf mud belt. The formation of the mud-belt on the Nha Trang Shelf is probably correlated to the advection-dominated clinof orm-progradation type according to Cattaneo's classification (Cattaneo et al., 2003b). The LST deposits above the LGM surface on the inner and mid shelf are not documented on the Nha Trang Shelf since they were often eroded by subaerial and following marine erosional processes or they are not clearly discriminated by seismic resolution. Besides, the absence of the incised-channels due to transgressive erosional processes in this area did not allow the LST fluvial sediments which were predicted to deposit at the bottom of the incised-channels to be preserved (Zaitlin et al., 1994). Therefore the TS surface in the Nha Trang Shelf's model was mostly merged with the lowstand sequence boundary landward and TST deposits often rested directly on the LGM lowstand surface in the landward part of the LGM coastline. The variable gradient of the LGM surface influences the formation of sequence system tracts: The relative high-gradient in one hand has reduced the effects of the rapid transgression and prolonged the time for sediment reworking with a given amount of sea-level rise. As a result, the TST deposits on the Nha Trang Shelf were stacked thicker than their counterparts on the nearby low-gradient Sunda (Hanebuth and Stattegger 2004) and SE Vietnam (Chapter 2; Bui et al., in prep). On the other hand, the effect of transgression over longer time has also enhanced the marine erosional process of the lower regressive deposits and therefore reduced their preservation. This together with the high wave energy has resulted in the loss of the regressive deposits over the mid and inner part of Nha Trang Shelf.

The late Pleistocene-Holocene stratigraphic architecture on the shelf off Nha Trang area comprises five major seismic units and three bounding surfaces which can be attributed to four systems tracts: FSST, LST, TST and HST.

- The lowermost unit U0 formed as transparent and parallel layer overlying the SB2 surface, and it is interpreted as deposits accumulated during MIS 5e transgression and highstand period of the last glacial cycle. The long gap between U0 and the following FSST unit is attributed to the erosional hiatus.

- The FSST with unit U1 and LST with unit U2 are well preserved on the modern outer shelf but pinch out landward at water depths of 100-120 m. Locations and internal patterns of the deposits suggest that FSST and LST units were primarily formed during the falling stage of sea-level from MIS 3 to the LGM sea-level lowstand of MIS 2. The LST wedge deposits on the central shelf are only recorded in the steep-gradient shelf off Hon Gom Peninsula and they are almost absent in the other parts of study area. The relict beach-ridge deposits identified at water depth of about ~ 130 m below present sea-level indicate that the LGM sea-level lowstand in this area was lower than on the Sunda Shelf in the South. The difference probably resulted from subsidence due to high deglacial Holocene sedimentation and/or neotectonic movements of the East Vietnam Fault System.
- The LGM lowstand surface SB1 was traced by seismic profiles across the shelf. This surface shows relatively high gradient in the middle part and become gentler toward the inner and outer shelf as well as from north to southern part of study area.
- Transgressive deposits (unit U3) were developed across the shelf with significant thickness. The TST shows a clear transition from backstepping to aggradational stacking patterns from outer to inner shelf which reflects the interplay between rate of sea-level rise, LGM surface gradient and sediment supply.
- The thick highstand mud (unit U4) is documented on the mid shelf forming a shore-parallel sediment depocentre and its thickness decreases toward the inner and outer shelf.
- The sequence stratigraphic model for the Nha Trang Shelf reflects the interplay of controlling factors as sea-level fluctuations, sediment supply, shelf morphology and hydrodynamic conditions. The late Pleistocene high amplitude of sea-level change during a long fourth-order and superimposed shorter fifth-order cycle is the principal factor in reorganizing the formation of the Nha Trang continental shelf sequence. Local factors like geometry of the narrow shelf and high sediment supply from the mountainous hinterland provided specific features of the Nha Trang Shelf's sequence stratigraphic model.

References

- Allen SB (1967). Sediments of Nha Trang Bay, South Vietnam. *Am. Asso. Petr. Geol. Bull* 51, 454.
- Badley ME (1985). *Practical seismic interpretation: International Human Resources Development Corporation, Boston, 266 pp.*
- Barthel K, Rosland R and Thai NC (2009). Modeling the circulation on the continental shelf of the province Khanh Hoa in Vietnam. *Journal of Marine Systems* 77, 89-113.
- Bui VD, Dalman R, Weltje G, Stattegger K and Tran TD. Flux and fate of sediments on the Nha Trang Shelf (central Vietnam) since the Last Glacial Maximum (LGM): field measurements and process-based numerical modeling. To be submitted to *Journal of Asian Earth Sciences*.
- Bui VD, Stattegger K, Phung VP and Nguyen TT. Late Pleistocene-Holocene seismic stratigraphy on the South East Vietnam Shelf. To be submitted to *Global and Planetary Change*.
- Cattaneo A and Steel RJ (2003a). Transgressive deposits: a review of their variability. *Earth-Science Reviews* 62 (3-4), 187-228.
- Cattaneo A, Correggiari A., Langone L and Trincardi F (2003b). The late-Holocene Gargano subaqueous delta, Adriatic shelf: Sediment pathways and supply fluctuations. *Marine Geology* 193 (1-2), 61-91.
- Catuneanu O (2002). Sequence stratigraphy of clastic systems: concepts, merits, and pitfalls. *J. Afr. Earth Sci* 35, 1-43.
- Catuneanu O et al. (2009). Towards the standardization of sequence stratigraphy. *Earth-Science Reviews* 92, 1-33.

Chappell J, Omura A, Esat T, McCulloch M, Pandolfi J, Ota Y and Pillans B (1996). Reconciliation of late Quaternary sea-levels derived from coral terraces at Huon Peninsula with deep sea oxygen isotope records. *Earth Planetary Science Letters* 141, 227–236.

Clift P, Lee GH, N Anh Duc, Barckhausen U, H Van Long, and Sun Z (2008). Seismic reflection evidence for a Dangerous Grounds miniplate: No extrusion origin for the South China Sea. *Tectonics* 27, TC3008.

Dam QM, Frechen M, Tran N, Harff J (2010). Timing of Holocene sand accumulation along the coast of central and SE Vietnam. *International Journal of Earth Sciences* 99 (8), 1731-1740.

Douglas IL and Nordstrom CE (1973). Sedimentation in Nha Trang Bay, south Vietnam-*Am. Asso. Petr. Geol. Bull* 57, 786.

Emch M, Feldacker C, Yunus M, Streatfield PK, Thiem VD, Canh DG and Ali M (2008). Local environmental drivers of cholera in Bangladesh and Vietnam. *American Journal of Tropical Medicine and Hygiene* 78, 823-32.

Fleming K, Johnston P, Zwartz D, Yokoyama Y, Lambeck K and Chappell J (1998). Refining the eustatic sea-level curve since the Last Glacial Maximum using far- and intermediate-field sites. *Earth Planetary Science Letters* 163, 327–342.

Fyhn MBW, Nielsen LH, Boldreel LO, Thang LD, Bojesen-Koefoed J, Petersen HI, Huyen NT, Duc NA, Dau NT, Mathiesen A, Reid I, Huong DT, Tuan HA, Hien LV, Nytoft HP and Abatzis I (2009). Geological evolution, regional perspectives and hydrocarbon potential of the northwest Phu Khanh Basin, offshore Central Vietnam. *Marine and Petroleum Geology* 26, 1-24.

Grant J A and Schreiber R (1990). Modern swath sounding and sub-bottom profiling technology for research applications: The Atlas Hydrosweep and Parasound Systems. *Mar.Geophys.Res* 12, 9-19.

Hanebuth TJJ, Statterger K and Saito Y (2002). The stratigraphic architecture of the central Sunda Shelf (SE Asia) recorded by shallow-seismic surveying. *Geo-Marine Letters* 22, 86-

Hanebuth TJJ, Stattegger K, Schimanski A, Lüdmann T and Wong HK (2003). Late Pleistocene forced regressive deposits on the Sunda Shelf (SE Asia). *Marine Geology* 199 (1-2), 139-157.

Hanebuth TJJ and Stattegger K (2004). Depositional sequences on a late Pleistocene Holocene tropical siliciclastic shelf (Sunda Shelf, (SE Asia). *Journal of Asian Earth Sciences* 23, 113-126.

Hanebuth TJJ, Stattegger K, Bojanowski A (2009). Termination of the Last Glacial Maximum sea level lowstand: The Sunda-Shelf data revisited. *Global and Planetary Change* 66, 76-84.

Hori K, Tanabe S, Saito Y, Haruyama S, Nguyen V, and Kitamura A (2004). Delta initiation and Holocene sea-level change: Example from the Song Hong (Red River) delta, Vietnam, *Sediment. Geol* 164, 237–249.

Lee GH and Watkins JS (1998). Seismic stratigraphy and hydrocarbon potential of the Phu Khanh Basin, offshore Central Vietnam, South China Sea. *AAPG Bulletin* 82, 1711-1735.

National Project KC08.12 (2004). Research on the preventative method of flooding processes on the central Vietnam. Final report, Hanoi, 523 pp (in Vietnamese).

Michelli M (2008). Sea-level changes, coastal evolution and paleoceanography of coastal waters in SE - Vietnam since the mid - Holocene. PhD thesis. University of Kiel, 160 pp.

Mitchum JR and Vail PR (1977). Seismic stratigraphy and global changes of sea-level: Part 7. Seismic stratigraphy interpretation procedure. In: Payton, C.E. (Ed.), *Seismic Stratigraphy-Applications to Hydrocarbon Exploration*. AAPG Memoirs 26, 63-81.

Pham VN (Editor) (2003). *Bien Dong Monograph*. Vol. II –Meteorology, Marine Hydrology and Hydrodynamics, Hanoi National University Publisher, Hanoi, 565 pp (in Vietnamese).

Posamentier HW and Allen GP (1993). Variability of the sequence stratigraphic model: effects of local basin factors. *Sediment. Geol* 86, 91–109.

Ridente D and Trincardi F (2005). Pleistocene "muddy" forced-regression deposits on the Adriatic shelf: A comparison with prodelta deposits of the late Holocene highstand mud wedge. *Marine Geology* 222-223(1-4), 213– 233.

Shackleton NJ (1987). Oxygen isotopes, ice volume and sea-level. *Quaternary Science Reviews* 6, 183–190.

Schimanski A and Stattegger K (2005). Deglacial and Holocene Evolution of the Vietnam Shelf: Stratigraphy, Sediments and Sea-level change. *Marine Geology* 214, 365—387.

Steinke S, Kienast M and Hanebuth TJJ (2003). On the significance of sea-level variations and shelf paleo-morphology in governing sedimentation in the southern South China Sea during the last deglaciation. *Marine Geology* 201, 179–206.

Shuttle Radar Topography Mission (SRTM) digital elevation models (<http://srtm.usgs.gov>).

Swift DJP (1976). Continental shelf sedimentation. In: Stanley, D.J., Swift, D.J.P. (Eds.), *Marine Sediment Transport and Environmental Management*, New York, 311–350.

Szczuciński W, Jagodziński R, Nguyen TT, Kubicki A and Stattegger K (2005). Sediment dynamics and hydrodynamics during a low river discharge conditions in Nha Trang Bay, Vietnam. *Meyniana* 57,117-132.

Szczuciński. W, Stattegger K and Schloten J (2009). Modern sediments and sediment accumulation rates on the narrow shelf off central Vietnam, South China Sea. *Geo-Marine Letters*, Volume 29, 1, 47-59.

Tamura T, Saito Y, Sieng S, Ben B, Kong M, Choup S and Tsukawaki S (2007). Depositional facies and radiocarbon ages of a drill core from the Mekong River lowland near Phnom Penh, Cambodia: evidence for tidal sedimentation at the time of Holocene maximum flooding. *Journal of Asian Earth Sciences* 29, 585–592.

Tamura T, Saito Y, Sieng S, Ben B, Kong M, Sim I, Choup S and Akiba F (2009). Initiation of the Mekong River delta at 8 ka: evidence from the sedimentary succession in the Cambodian lowland. *Quaternary Science Reviews* 28 (3–4), 327–344.

Thanh TD, Saito Y, Huy DV, Nguyen VL, Ta TKO and Tateishi M (2004). Regimes of human and climate impacts on coastal changes in Vietnam. *Reg Environ Change* 4, 49–62.

Tjallingii, R, Stattegger K, Wetzel A and Van Phach P (2010). Infilling and flooding of the Mekong River incised valley during deglacial sea-level rise. *Quaternary Science Reviews*, 29 (11-12) 1432-1444.

VAIL PR (1987). Seismic stratigraphy interpretation using sequence stratigraphy, Part 1: seismic stratigraphy interpretation procedure, *in* Bally, A.W., ed., *Atlas of Seismic Stratigraphy*, Vol. 1: American Association of Petroleum Geologists, *Studies in Geology* 27, 1–10.

Veenken P C H (2007). *Seismic Stratigraphy, Basin Analysis and Reservoir Characterisation*, vol. 37, 1st ed., 509 pp., Elsevier, Oxford.

Wiesner M, Stattegger K, Kuhnt W, et al. (1999). Cruise Report SONNE 140 SÜDMEER III, *Reports Institut für Geowissenschaften* 7, 157 pp.

Wiesner M, Stattegger K., Voß M. et al. (2006). *Reports Institut für Geowissenschaften* 23, 99 pp.

Zaitlin BA, Dalrymple RW and Boyd R (1994). The stratigraphic organization of incised valley systems associated with relative sealevel changes. In: Dalrymple, R.W., Boyd, R., Zaitlin, B.A. (Eds.), *Incised-Valley System: Origin and Sedimentary Sequences*, *SEPM Special Publications* 51, 45–60.

Chapter 4

Flux and fate of sediments on the Nha Trang Shelf (central Vietnam) since the Last Glacial Maximum (LGM): field measurements and process-based modeling

Bui Viet Dung¹, Rory Dalman², Gert Jan Weltje², Karl Stattegger¹, Tran Tuan Dung³

¹*Institute of Geosciences, Kiel University, D-24118, Kiel, Germany*

²*Department of Geotechnology, Delft University of Technology, NL-2600 GA Delft, The Netherlands*

³*Institute for Marine Geology and Geophysics, 18 Hoang Quoc Viet, Hanoi, Vietnam*

To be submitted to Journal of Asian Earth Sciences

Abstract

Sediment accumulation and distribution on the Nha Trang Shelf (Central Vietnam) during the post-glacial period (last 20 ky) has been investigated on the basis of process-based numerical modeling simulations and shallow seismic data. Calculation from shallow seismic data indicates that the annual sediment volume stored on the shelf during highstand (HST) period (8.0-0 ky BP) and transgressive (TST) period (19.6-8.0 ky BP) was 2.1 and 5.4 million tons of sediment per year (Mt/y), respectively. Calculation based on empirical equations also suggests that the total sediment supply during HST period of the three main local mountainous river basins (Cai, Dinh and Van Phong) ranges from 1.7 to 4 Mt/y, of which the sediment supply from Cai River is 2 and 6 times larger than that of Dinh and Van Phong River, respectively. Results from numerical modeling sensitivity tests show that with a given amount of sediment input 42.1 to 59.3 % of supplied sediments during HST period are accumulated on the shelf and the rest is mostly transported alongshore southward. Combining these results, we predict that the annual sediment supply to the Nha Trang Shelf during HST period ranges from: 4.1 to 5.1 Mt/y. 50-80 % is contributed from the three main local river basins and the rest is transported alongshore from the north. Assuming that the sediment supply ratios between three local river basins are similar to the HST period, we can predict the annual sediment supply to the Nha Trang Shelf during TST period by 10.9 to 19.8 Mt/y. This means that the sediment supply during TST period is 3 to 4 times higher than that of

HST period. Modeling results show that 30 to 50 % of supplied sediments during TST period were stored on the shelf and significant amount of sediments escaped from the shelf to the continental slope during early transgression as well as were transported alongshore to the south. Sedimentation on the Nha Trang Shelf from the end of the LGM to present has been estimated by a final modeling simulation using the predicted sediment supply to the shelf. Calculated net sediment preserved on the shelf from the final simulation is compatible to the results from seismic data. This indicates that the predicted sediment flux to the shelf is reasonable. The TST thickness map of the model shows similar features in comparison to the seismic results. By contrast, the HST deposits in the model present an alongshore coastline-hugging sediment depocentre that is completely different from the isopach map of seismic data. Differences between model results and seismic data suggest that an improvement of input database as well as model parameter adjustment is needed.

4.1 Introduction

At the global scale, small mountainous rivers are considered to account for half of modern sediment discharge to the ocean (Milliman and Syvitski 1992). Hence, the importance in studying the flux and fate of sediments discharging to the oceans from the mountainous rivers with small drainage basins has been emphasized (Milliman and Syvitski 1992; Milliman 1995; Schimanski and Stattegger 2005b; Liu et al., 2008). These studies indicated that the small river basins have high sediment yields, low sediment storage capacity and they often discharge sediments directly to the neighbouring shelf. Small rivers draining mountainous areas in Papua New Guinea and Taiwan for example discharge annually to the nearby sea 1700 and 100 million tons of sediment per year (Mt/y), respectively. The Vietnamese shelf is symmetric in shape with two wide-low gradient continental shelves including large river deltas in the north and southern part, and a narrow shelf in the centre (Fig 4.1). The Red River in the north discharges 130 Mt/y and Mekong River in the south discharges 160 Mt/y to the South China Sea (SCS) (Milliman and Syvitski 1992). Previous studies suggested that 144 Mt/y and 110 Mt/y are trapped annually on the Mekong and Red river delta, respectively (Ta et al., 2001; Schimanski and Stattegger 2005b). This implies that only ~10% of supplied sediments from these two big rivers are transported to the shelf. The central shelf of Vietnam is drained by numerous small mountainous rivers which annually discharge 40-100 Mt/y to the sea during Holocene period (Schimanski and Stattegger 2005b). Due to the short distance between sediment source and sink, most of the supplied sediments in this region are transported directly to the shelf. Among them, about 20-40 Mt/y are estimated to be stored on the continental shelf and the rest are transported offshore or along-shore (Schimanski and Stattegger 2005b).

In this research, we will concentrate on the Nha Trang Shelf, southernmost central Vietnam where a dense net of shallow seismic profiles is available (Fig 4.1). Sediment supply regime of this area is strongly driven seasonality. Szczuciński et al. (2005) indicated that the sedimentation in dry season is not significant on the Nha Trang Bay. By contrast, the major portions of supplied sediments are delivered to the shelf during the wet season. It is also suggested that significant amount of sediments in this region are transported southwards by longshore currents and only small part is transport offshore (Szczuciński et al., 2005). Sources of sediment supply for the Nha Trang Shelf are therefore considered to be either from the northern shelf by southward along-shore transport or local mountainous rivers. However, quantifying the contributions of each source to the shelf sediment budgets is complex and remains unclear so far. To solve this problem, different numerical forward modeling scenarios will be used to examine the interaction between sediment sources and

sediment sink on the Nha Trang Shelf since the Last Glacial Maximum (LGM). The modeling results are then compared to field measurement data. This will enhance the understanding of flux and fate of sediments discharging into this region. The objectives of this study are therefore:

- Quantifying the contribution of different sediment sources using process-based modeling simulations.
- Estimating the long-term modern sediment supply and store on the shelf by empirical equations and available seismic lines and sediment core data.
- Calculating the general sediment budget for the area after the LGM by model-data comparison.

4.2 Regional setting

The Nha Trang Shelf is located on a passive continental margin which is bordered by the Vietnamese coastline to the west and the SCS to the east (Fig 4.1). The study area is mostly covered by intrusive igneous rock which has been formed since Cretaceous (Nguyen et al., 1994). The continental shelf is ~ 40 km wide in average, steep on the mid-shelf and gentle on the inner and outer part (Fig 4.1). There are two bays in our study area: Van Phong Bay in the northern part and Nha Trang Bay in the central part. The study area is dominated by semi-diurnal to diurnal tide regime with amplitude of 0.4 m in neap and 2.5 m in spring tides (Pham 2003, Szczuciński et al., 2005). Average wave height in this area ranges from 0.5 m and 2.0 m and they can reach up to 7.5 m during storm conditions (Thanh et al., 2004). Most of sediments are supplied to the study area by numerous small and short mountainous rivers which drain the high relief with maximum elevation of 2000 m (Fig 4.1). The amount of sediment discharge to the shelf is strongly driven by the monsoon regime. About 70 % of sediments is contributed during short periods of the rainy season (September to December) and 30 % in the dry season (January to August) (National Project KC08.12 2004). Long-term monitoring data (1985-1995) collected in Nha Trang station indicate average temperature of 27°C (Emch 2008). Maximum rainfall can reach up to 549,2 mm/month during the wet season (Emch 2008).

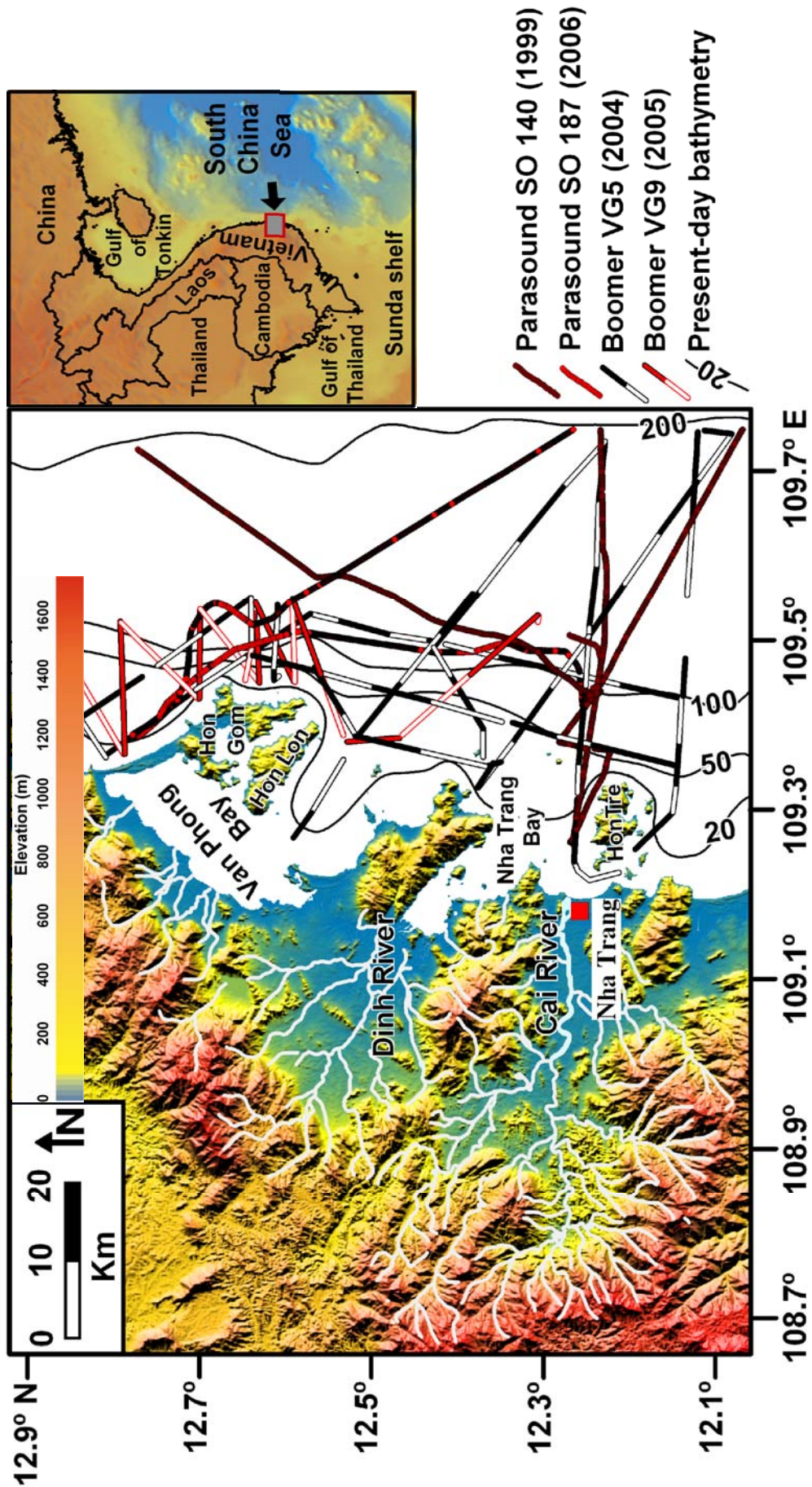


Fig 4.1. Map of the Nha Trang Shelf with modern bathymetry and available seismic profiles. Elevation data of the land part is extracted from Shuttle Radar Topography Mission (SRTM) digital elevation models (<http://srtm.usgs.gov>).

4.3 Numerical modeling

4.3.1 The 3D Simclast model

In this research, we use the SimClast numerical modeling. It is a basin-scale 3D stratigraphic model, which was developed from 2004 to 2008 at Delft University of Technology, Holland. Detailed characteristics of the model are extracted from the published literatures (Dalman and Weltje 2008; Dalman 2009). SimClast is a fully plan view 2D, depth-averaged model, which allows us to study the interaction between fluvial and marine processes. The principal characteristic of the model lies on its multi-scale simulation capacity. In which, the short-term and high-resolution processes model are coupled with the long-term stratigraphic model by implementing sub-grid scale processes into a large-scale basin-filling model. This parameterization refines morphodynamic behaviour and the resulting stratigraphy, while maintaining the computational efficiency. For the purpose of our research, the model uses 1 km scale grid-cell and time steps of 1 year. The model consists of two independent modules: the fluvial and continental shelf. The general outline of each module is summarized below.

➤ Fluvial module

Fluvial processes and stratigraphy in the model are represented by sub-grid parameterisation for application in the large-scale basin-filling model (Fig 4.2). This represents the processes that are too small scale or complex to be explicitly represented in the model by simplified expressions. The discharge routing algorithm of the model combines the steepest descent with diffusive routing method. Creation of the channel is evaluated by comparing the discharge to a threshold value. If the threshold flux is exceeded, an active channel is created. If the flux is lower than the threshold value, discharge is considered to be unconfined and a diffusive routing method will be applied to the water. Channel dimensions are calculated using empirical relationships, which allows us to calculate sediment transport capacity and hence deposition or erosion in each channel segment by evaluating the ratio of sediment load to transport capacity. Channels are unconditionally stable as long as they incise. Aggrading channels and channels that are in equilibrium are conditionally stable and they may be subject to avulsion or bifurcation. The stability of crevasses is calculated based on the cross valley slope and the sediment concentration profile of the main channel. The crevasse will heal if sediment load exceeds transport capacity. Alternately, the crevasse will incise. Once a crevasse system has reached its equilibrium, the threshold discharge controls success or failure of an avulsion or bifurcation. Full avulsion takes place where discharge carried by the original channel is lower the threshold value and it is abandoned. If both the original channel and the crevasse channel discharge exceed the threshold value, a bifurcation (partial avulsion) is formed. If the discharge of the equilibrium crevasse channel is lower than the

threshold value, the avulsion has failed. When the avulsion has partially or fully succeeded, the new channel will follow the path of steepest descent gradient of the neighbor gridcell.

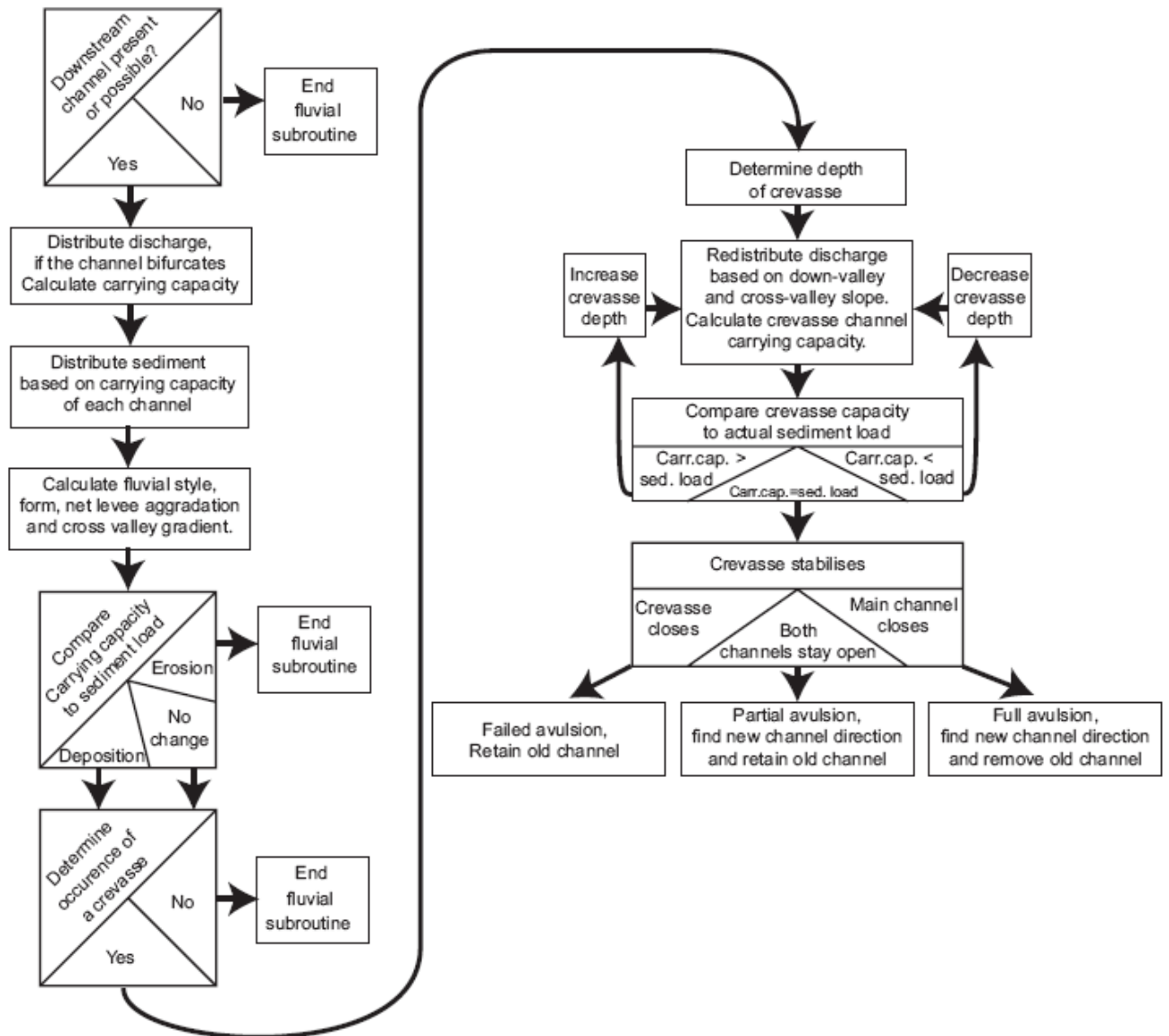


Fig 4.2. Flow chart of the fluvial module (Dalman 2009).

➤ **Continental shelf module**

The continental shelf module will start as soon as the fluvial module has finished avoiding offshore to onshore sediment transport (Fig 4.3). The marine module needs the input data as: the initial bathymetry, initial river plume velocity and sediment discharge. The hydrodynamics in the marine model includes three individual processes. River plumes and large-scale oceanic currents are integrated in one combined algorithm and wave generation and propagation are modeled independently. First the combined currents/plume routine is run, followed by the wave calculations. Next the erosion due to waves and currents is calculated in each grid-cell. Finally the suspended load is iteratively transported and gradually deposited.

The hydrodynamic flow of currents and plumes are simulated using one integrated steady-state potential flow routine. This allows calculating of the deposition of sediments from the river plume and the longshore transportation of the resuspended deposits. In order to calculate the flow field, the model needs the current velocity at the grid boundaries. These boundary conditions can be derived from the oceanographic models or local measurements. The plumes entering the marine domain are dynamically integrated by automatically assigning an inflow point with the channel velocity and direction of flow at the appropriate grid cell.

The model needs the wave height at each point to calculate the sediment resuspension and movement on a wave influenced shelf. As the largest amount of sediment is eroded and consequently deposited during the extreme events (storms), only one event is modelled per time step (one year). Waves at the model boundary can either be provided as input or calculated in the model. As wave height alone is not sufficient for the simulation purpose, the model also uses the linear Airy wave theory and the Stokes equations to calculate the wavelength, wave height and velocity at a certain water depth.

Sediment erosion, transport and deposition are divided into two different routines with differing methods and predominantly different settings. In the offshore and nearshore areas, suspended load transport of fine sediments is dominant and bedload transport is minor (may occur only during storm events). Bedload transport occurs mainly in the surf zone and the upper near shore areas. The model applies the active layer concept to calculate bedload transport under the effect of shoaling wave in the coastal areas. The depth of the active layer at which sediment can be mobilized is determined from the near bed wave orbital velocity. The active bedload layer represents the maximum amount of sediment that can be moved through bedload processes in one gridcell. The net sediment transport over one wave cycle is calculated by intergrating both empirical equation and linearly interpolation. Sediment from the active layer is moved through the model until the active layer is exhausted or the

sediment transport capacity is reduced to zero. Suspended load sediment dynamics as follows: diffusion processes to represent the effect of waves, advective motion of the currents in conjunction with the river-supplied. The suspended particulate matter gradually falls out of suspension during transportation. The initial amount of suspended matter in each gridcell is identified from the erosion routine and the plume input. The model uses a variable time step to evaluate the fluctuation of suspended matter over time in each gridcells. The time step between each gridcells is calculated using the current flow velocity and the size of the gridcells. The model will repeat cycling through the entire model until all suspended matter matter is removed and deposited.

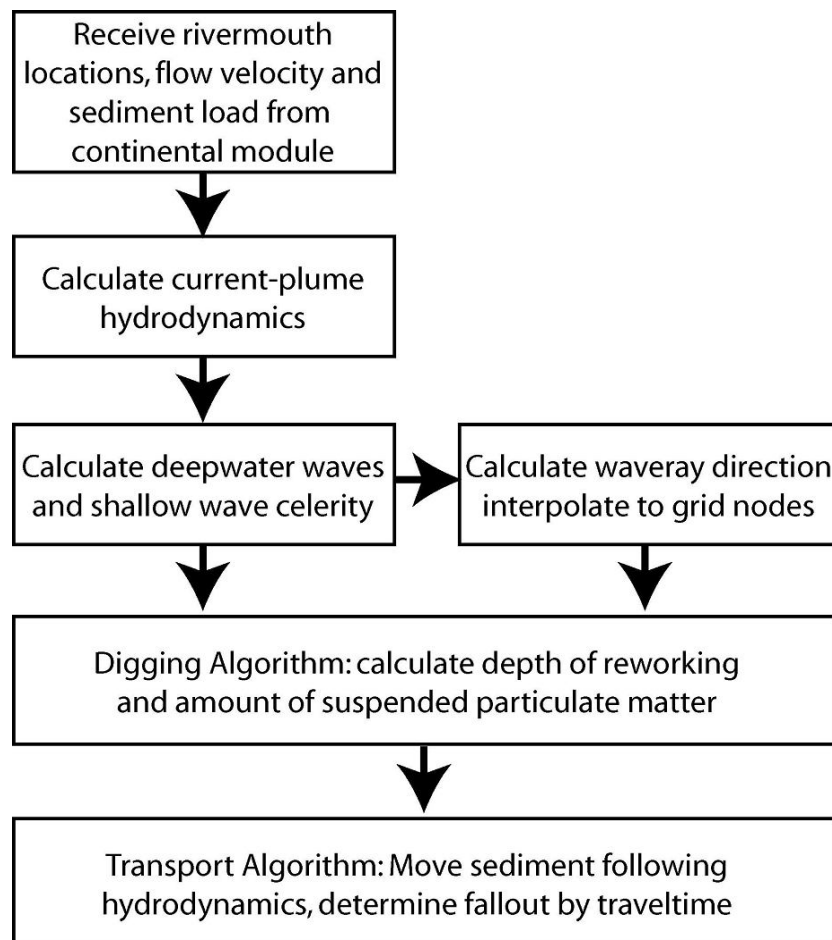


Fig 4.3. Flow chart of the continental shelf module (Dalman 2009).

4.4 Input data

4.4.1 Sediment and water discharge

The river basins surrounding the Nha Trang Shelf are divided into three groups based on the river stream distributions: Cai, Dinh and Van Phong River basins (Fig 4.4).

➤ First approach

Information about sediment flux on the central Vietnam Shelf since the LGM is very seldom. Estimated annual sediment flux for the whole central Vietnam Shelf based on the following equation (1) returned to 40-100 Mt/y (Schimanski and Stattegger 2005b):

$$\text{Sediment flux [t/yr]} = \text{Denudation rate [m/10}^6\text{yr]} * \text{Rock density [t/m}^3\text{]} * \text{Area [10}^4\text{ m}^2\text{]} \quad (1)$$

Applying the same procedure for the Nha Trang area, we can roughly estimate the annual sediment supply for this area of 1.64 to 4.08 Mt/y (Table 4.1).

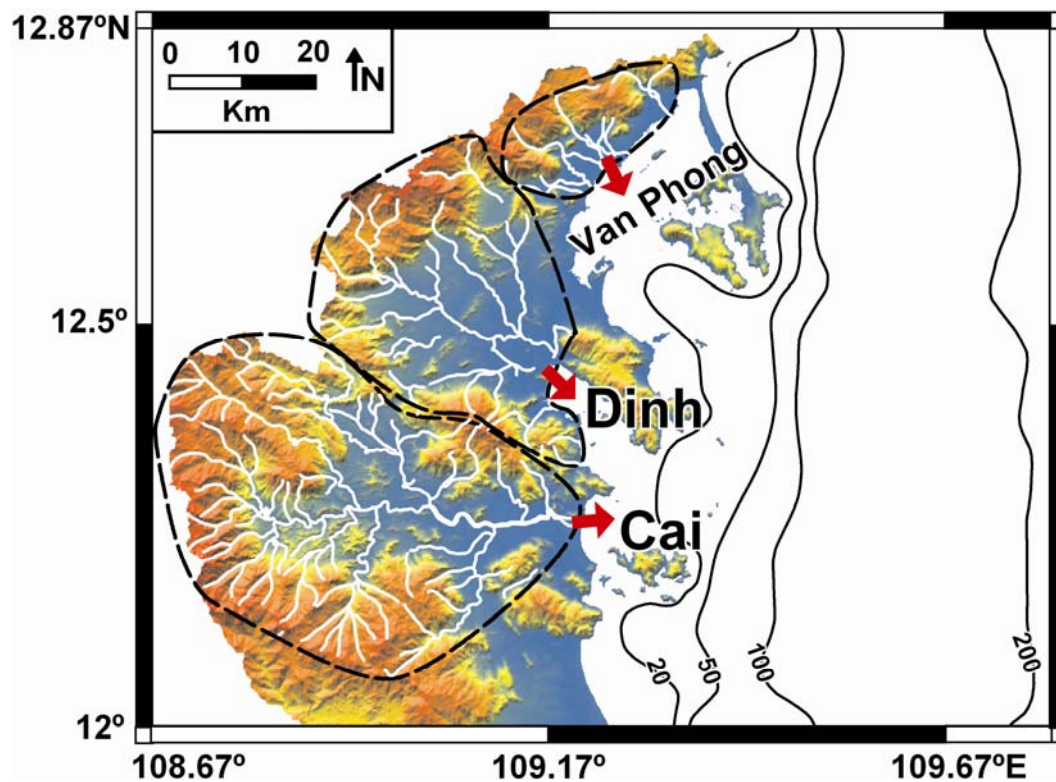


Fig 4.4. Rivers and streams of three main local basins draining into the Nha Trang Shelf.

River basin	Average denudation rate (m/10 ⁶ y)	A (km ²)	Rock density (t/m ³)	Flux (10 ⁶ t/y)
Cai	200-500	1900	2.5	0.95 - 2.37
Dinh	200-500	1100	2.5	0.55 - 1.37
Van Phong	200-500	270	2.5	0.14 - 0.34
Total				1.64 - 4.08

Table 4.1. Input parameters and sediment load of three main basins from denudation rate. Average denudation rate adapted from Einsele (2000).

➤ **Second approach**

In this approach, we calculate long-term average suspended sediment discharge based on the BQART equation (2) for temperature higher than 2°C (Syvitski and Milliman 2007):

$$Q_s = \omega B \left(\frac{Q}{Q_0} \right)^{0.31} A^{0.5} R T B = L(1 - T_e) E_h \quad (2)$$

In which, Q_s is the long-term average sediment load [Mt/y], A is the drainage area [km²], R is the maximum elevation in the drainage basin [km], T is the basin-averaged temperature [°C], Q is the long-term average discharge [km³/yr-1], $Q_0 \equiv 1$ [km³/y] is a reference value introduced to form a nondimensional ratio of long-term average discharge. The constant $\omega = 0.0006 \text{ Mt yr}^{-1} \text{ } ^\circ\text{C}^{-1} \text{ km}^{-2}$. The uncertainty in calculation sediment discharge from this equation is B (variable) which expresses the human impact factor. B depends on lithology erodibility (L), trapping efficient of reservoirs and lakes (T_e) and human impact soil erosion factor (E_h). Each of these parameters shows a wide range of variation depending on both time and space (Syvitski and Milliman 2007). Thus instead of estimating the single parameter, we use the calculation from previous part (Table 4.1) as standard value and vary the B variable till the results from both calculations fit to each other. This procedure has been applied well for the Adriatic Sea (Brommer 2009). As a result, we can derive the B value ranging from 0.6-1.4 (Table 4.2). The average sediment discharge from the Cai and Dinh basins is extracted from published literature (Barthel et al., 2009). Sediment discharge from Van Phong basin is inversely estimated by using the above value of B variable and the calculated sediment load in Table 4.1.

River basin	Q (km ³ /y)	A (km ²)	R (km)	T (°)	W	B	Qs (10 ⁶ t/y)
Cai	2.46	1900	1.8	27	0.0006	0.6-1.4	1-2.35
Dinh	0.68	1100	1.9	27	0.0006	0.6-1.4	0.54-1.27
Van Phong	0.34	270	1.5	27	0.0006	0.6-1.4	0.17-0.4
Total							1.71-4.02

Table 4.2. Input parameters and sediment load of three main basins from BQART equation.

Based on above calculations (Table 4.1 and Table 4.2), we can roughly derive the proportion of 3 rivers in this region as following: Cai: 60 %, Dinh: 30 %, Van Phong: 10 %. These ratios will be applied for all simulations later on.

Information about paleo-river discharge is not available, therefore we use the relationship between modern river discharges and sediment input (average value) (Table 4.2) to establish a rating curve (Fig 4.5). This curve is then used to convert the river discharge to sediment load for the simulations.

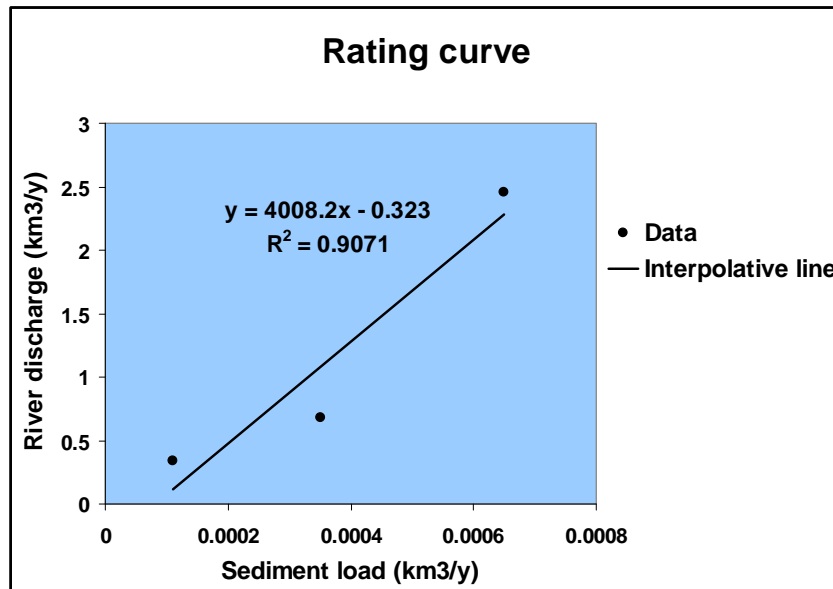


Fig 4.5. Rating curve for sediment load to discharge conversion.

4.4.2 Sediment thickness data from seismic profiles

The average sediment thickness accumulated on the Nha Trang Shelf after the LGM to present are calculated from the two-way travel time isopach thickness map derived from the seismic profiles and validated by sediment cores (Chapter 3, Bui et al., in prep). Average sound velocity of 1550 m/s in subsurface sediments has been applied for time-depth conversion. There are some negative values (as we can observe in the frequency distribution histogram) in the sediment thickness maps which resulted from the irregular of the interpolation data grid (Fig 4.6 and Fig 4.7). These data of course are not real and therefore are neglected in the sediment thickness map.

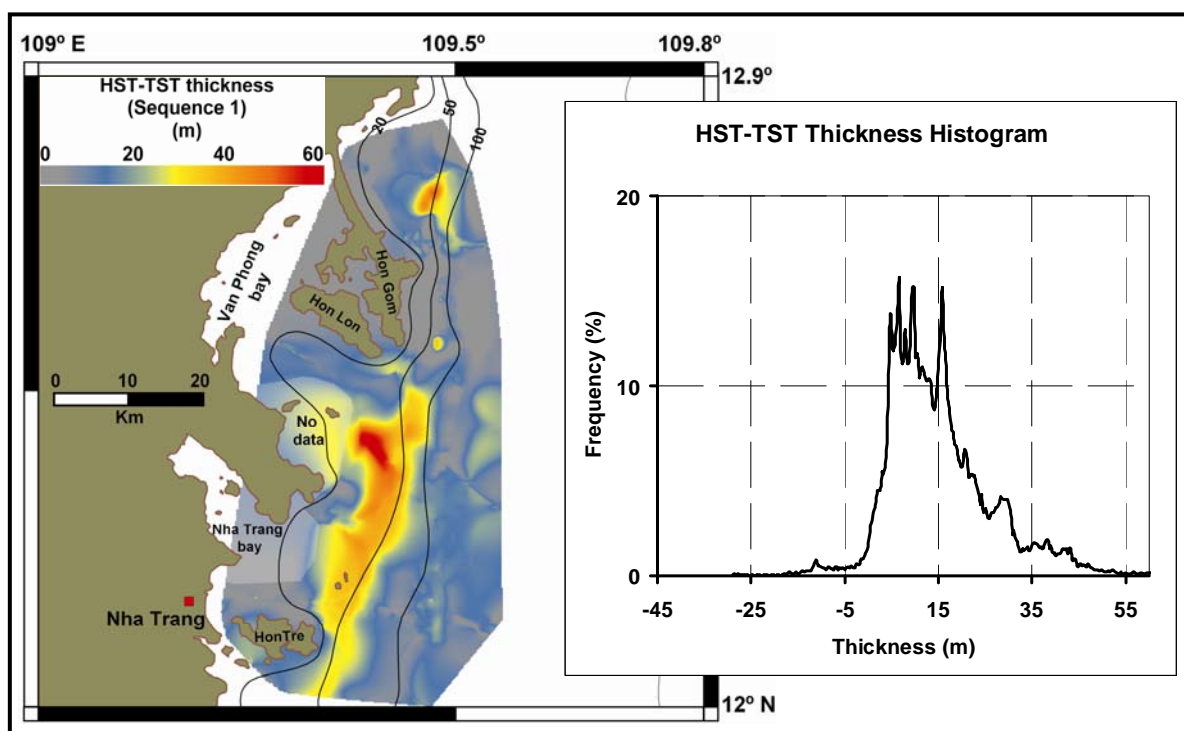


Fig 4.6. Total deglacial sediment thickness and its frequency distribution histogram on the Nha Trang Shelf derived from seismic data (Fig 3.12, Chapter 3, Bui et al., in prep).

We assume that the modern HST period on the studied area is coincident with initiation of the two nearby deltas: Red and Mekong which have been formed around 8.0 ky BP (Hori et al., 2004, Tamura et al., 2009). The HST period is therefore considered to be from about 8.0 ky BP to present. As extracted from the frequency distribution histogram (Fig 4.7), we deduce the average HST thickness of about 3 m. This value is probably lower than published results for the Holocene sediment thickness period on the central Vietnam Shelf (Schimanski and Stattegger 2005a; Schimanski and Stattegger 2005b; Szczuciński et al., 2009). However, data cited above were calculated from sediment cores taken on the mid-shelf sediment

depoecentre or areas where post-Pleistocene sediments are presented. In contrast, our calculation based on seismic data includes as well the exposed bedrock or areas without sediment deposition and therefore resulted in slightly lower values. The histogram frequency distribution of TST is asymmetric. However, TST thickness can be calculated by subtracting the HST thickness from the overall total deglacial sediment thickness (~14m), which both have the symmetry distribution (Fig 4.6 and Fig 4.7). Based on this calculation, we can derive the average TST thickness of about 11 m. The TST period starts with the initial pulse of sea-level rise after the LGM at ~19.6 ky BP (see detail in the next part). Therefore, the TST period in our calculation is considered to last from 19.6 - 8.0 ky BP. Assuming dry bulk density of 1.15 t/m³, we can estimate the volume of sediment stored on the shelf as follow:

$$\text{HST (8.0-0 ky BP): } 5000 \text{ km}^2 * (3 \text{ m}/8000 \text{ y}) * 1.15 \text{ t/m}^3 = 2.15 \text{ Mt/y}$$

$$\text{TST (19.6-8.0 ky BP): } 5000 \text{ km}^2 * (11 \text{ m}/11600 \text{ y}) * 1.15 \text{ t/m}^3 = 5.45 \text{ Mt/y}$$

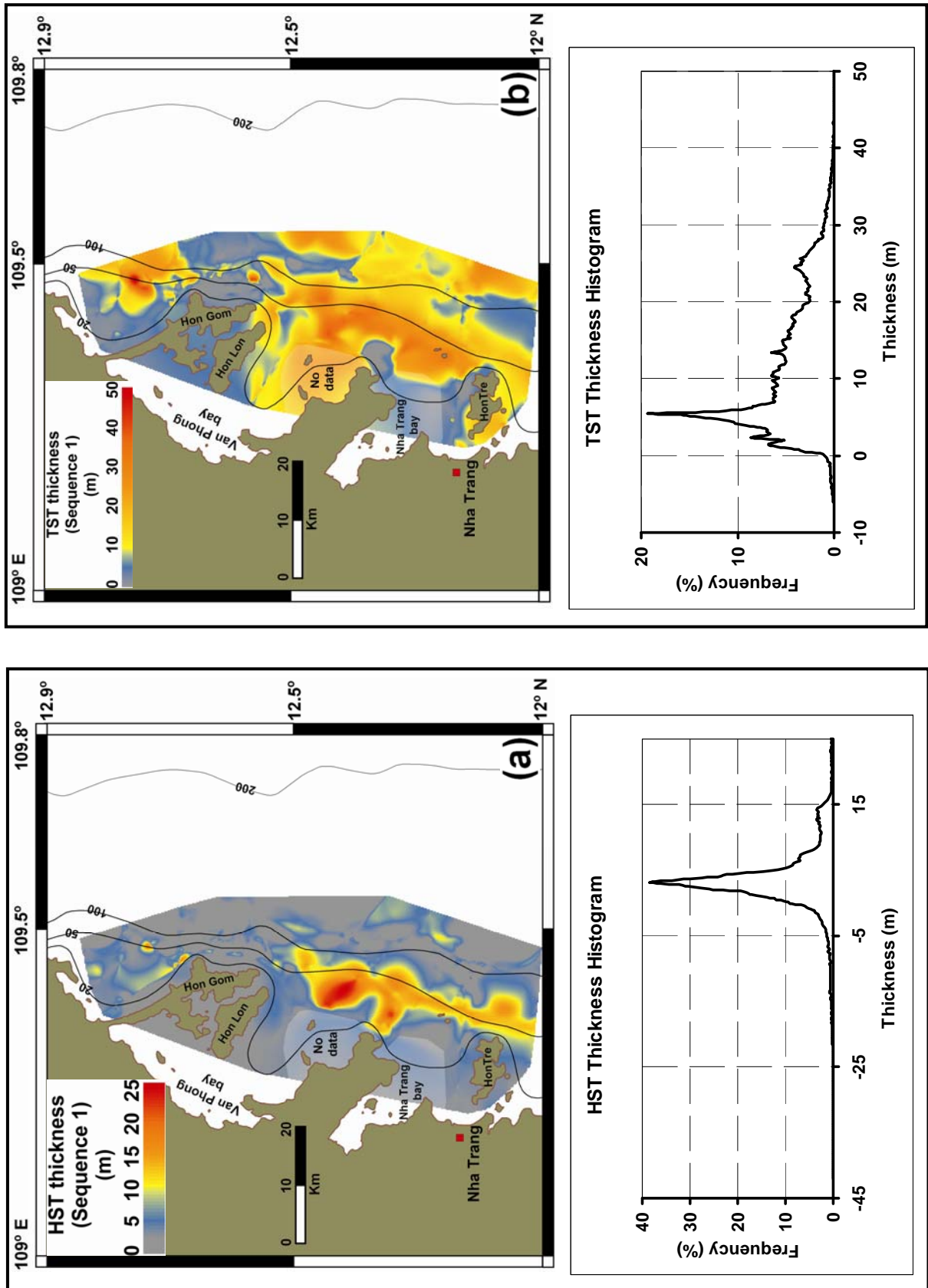


Fig 4.7. Sediment thickness map of HST (a) and TST (b) on the Nha Trang Shelf. Thickness frequency distributions are derived from seismic data (Fig 3.13, Chapter 3, Bui et al., in prep).

4.4.3 Sea-level data

A simplified 26 ky sea-level curve with major data points (Fig 4.8) is extracted from available sea-level data (Hanebuth et al., 2009; Stattegger et al., in prep). The curve between sea-level index points is linearly interpolated 100 y interval.

The termination of the LGM is complex and remains debated topic so far. In general, a slight rise of sea-level from 26 to 19.6 ky BP marking the final phase of the LGM is acceptable. We assume that the sea-level in the study area was linear increasing from the minimum lowstand -125 m to -121 m at 19.6 ky BP. During the following period from 19.4 to 18.7 ky BP, the sea-level rose with amplitude of 1.57m/100y corresponding to the first melt water pulse (MWP). Between 18.7 to 14.6 ky BP, sea-level rose moderate from -109 to -96 m. A highly accelerated sea-level rise from -96 to -80 m is stated between 14.6 and 14.3 kyr BP, corresponding to MWP 1A. The MWP 1A is followed by a more gentle transgression to -27 m at 8.6 kyr BP.

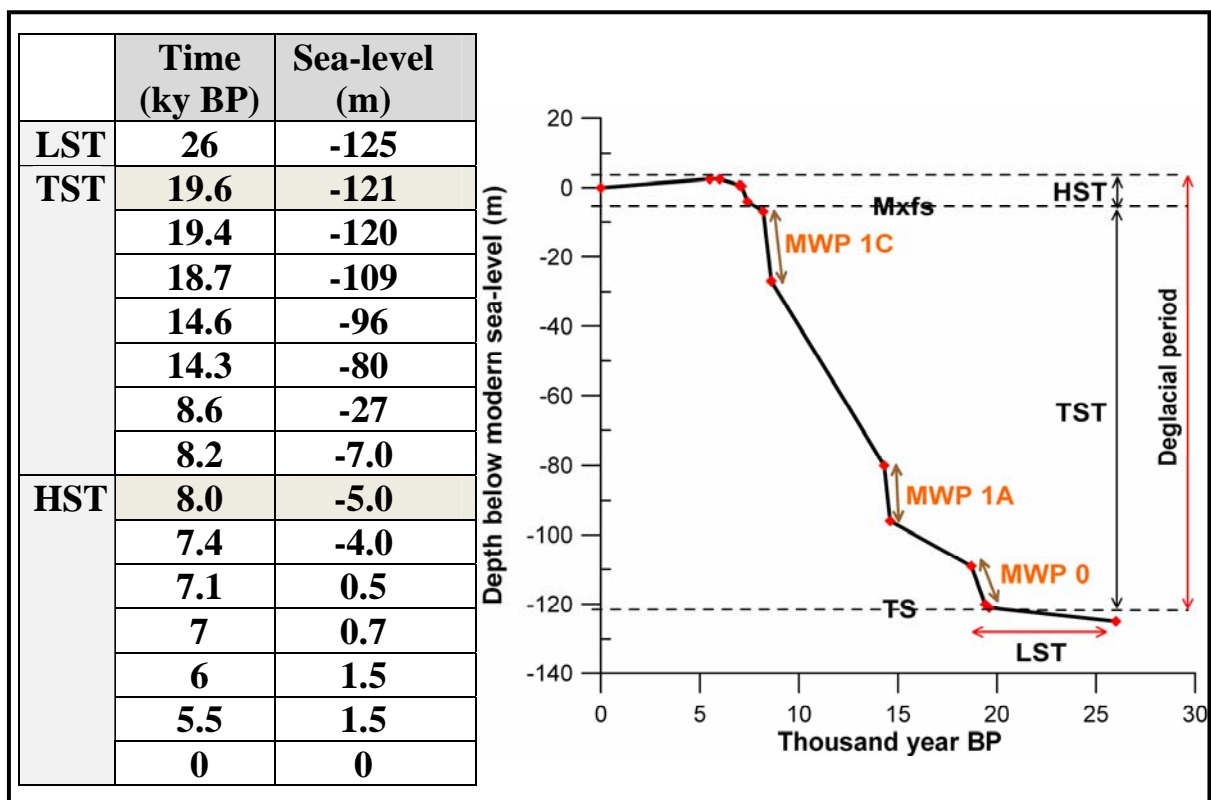


Fig 4.8. Sea-level data and LGM/deglacial sea-level curve for the Sunda and southern Vietnam Shelf (Hanebuth et al., 2000; Hanebuth et al., 2009; Stattegger et al., in prep.).

An acceleration sea-level (MWP 1C) happened at 8.6 to 8.2 kyr BP, with the rapid sea level rise from -27 to -7.0 m. After that, the sea-level rose slowly from -7.0 m to -4.0 m at 7.4 ky BP and slightly accelerated between 7.4 to 7.1 ky BP with rate of 1.5m/100y. Sea-level rise

decelerated until the mid-Holocene sea-level highstand was reached around 6.0-5.5 ky BP by 1.5 m above present-day sea-level. From 5.5 to 0 ky BP is marked by linearly falling of sea-level from 1.5 m to its present-day position.

4.4.4 Initial bathymetry from seismic profiles

The simulation period is starting from the end of the LGM period to present and therefore we deploy the LGM lowstand surface as the initial surface. The lowstand erosional surface is mainly extracted from interpreted seismic data (Fig 3.11, chapter 3, Bui et al., in prep).

Since the main aims of the research focus on the continental shelf and only reference elevation data on land was used. Elevation of the islands and nearby land areas are extracted from the Shuttle Radar Topography Mission (SRTM) digital elevation models with resolution of 90 m (<http://srtm.usgs.gov>). Those data are then corrected by subtracting the average deglaciation/Holocene sediment thickness which is derived from local geological map (Tran 1998) from the modern elevation. In order to adapt the input data format of the modeling software, the final initial surface is then interpolated with grid cell-size of 1 km² resulting in grid size of 87 rows and 57 columns (Fig 4.9)

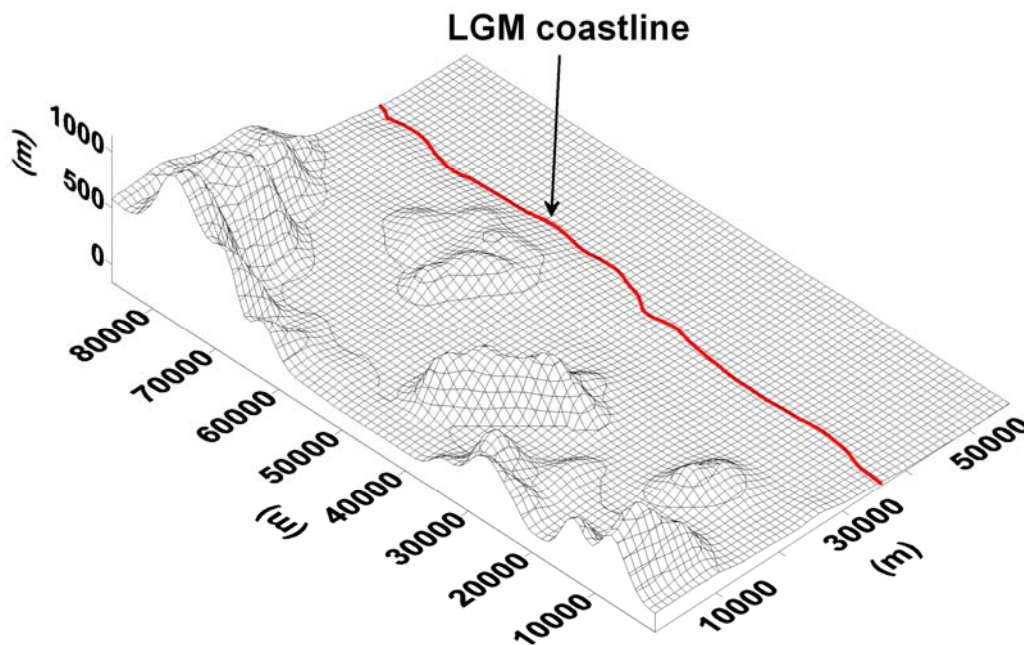


Fig 4.9. The model grid of the LGM lowstand surface with 87 rows and 57 columns of 1 km² cell size and LGM coastline.

4.5 Results and discussion

4.5.1 Sensitivity experiments

In this part, sensitivity tests of the initial and boundary conditions of the numerical model are presented (Table 4.3). The effects of grain size characteristics of the substratum, river input sediments and wave height to the shelf sedimentation will be evaluated. In addition, we will evaluate the interactions of sediment sources to the sediment patterns on the shelf. Besides the sediment discharge to the shelf from the three main river basins (Fig 4.4), we added one more artificial river at the northern edge of the grid. This river was assumed to be the northern sediment source by longshore currents for the study area. In the experiments, net percentage of sediment preserved was deduced from the ratio between the net sediment accumulated on the model's domain to the total fluvially supplied sediments. The difference between the total fluvially supplied sediments and sediment preserved was attributed to the longshore and offshore sediment transport. During all of the experiment tests, the initial surface substratum thickness (subsurface layer) was assumed to be 1 m and an initial longshore southward current of 1m/s was deployed at the inflow boundary (northern boundary).

Input parameters	Experiments	
		Simulation period
Initial flow current (m/s)	1	
Initial substratum thickness (m)	1	
Fluvial fine grain-size fraction (%)	80, 60 and 20	1000 y
Fluvial coarse grain-size fraction (%)	20, 40 and 80	
Substratum fine grain-size fraction (%)	80,60 and 20	1000 y
Substratum coarse grain-size fraction (%)	20,40 and 80	
Deep water wave height (m)	2,4 and 6	1000 y
Fluvial sediment input from the north (%)	0-100	19600 y

Table 4.3. Parameters of sensitivity experiments

➤ Sensitivity tests with fluvial and substratum grain size fraction

The model uses two classes of sediment grain size: coarse fraction (medium sand with grain diameter of 0.5 mm) and fine fraction (clay with grain diameter of 0.002 mm). Six different

scenarios with 20, 50 and 80% (0.2, 0.5 and 0.8 coefficient) of coarse grain fraction in fluvial and shelf substratum sediment have been chosen for evaluation (Fig 4.10).

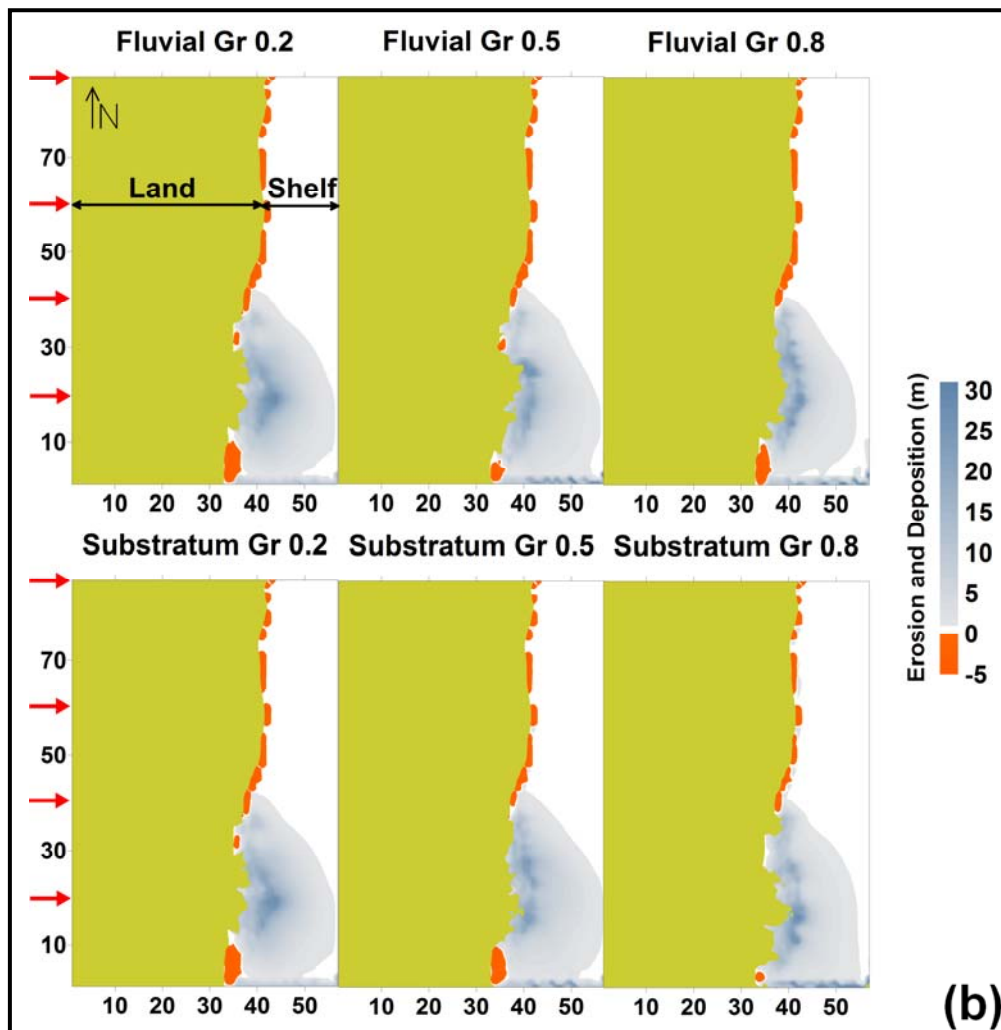
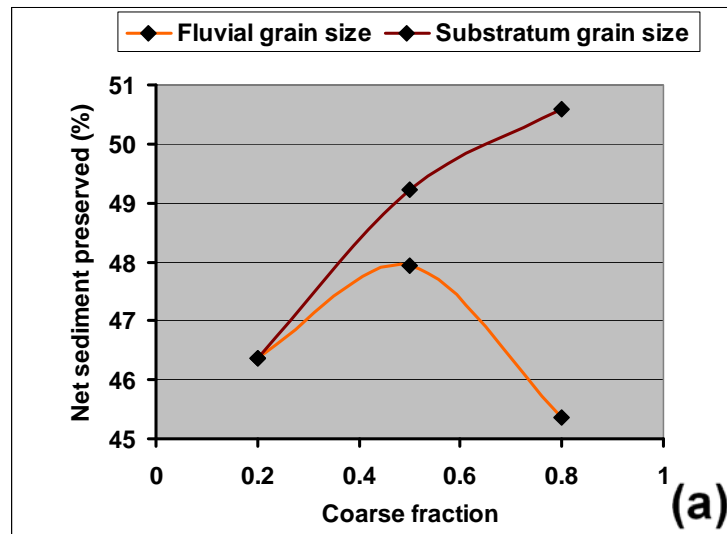


Fig 4.10. Net sediment preservation (a) and erosion/deposition with morphology of the coastline after 1 ky simulation (b) with different coarse fraction of fluvial and substratum sediment. Red arrows indicate river entries.

During all of the simulations, we used constant deep water wave height of 6m as extreme conditions and waves are running parallel to the coastline from E to W. In both cases, an increasing coarse fraction input retains most of supplied sediment around the river plume entry, sediment depocentre seems to be elongated alongshore and offshore sediment transport has reduced significantly (Fig 4.10b). Net sediment preserved on the shelf is proportional to the increasing coarse grain fraction in the substratum sediment and it is fluctuant in case of fluvial sediment supply grain size (Fig 4.10a). However the differences in percentage of net sediment preserved between these scenarios are minor (less than 5 %) (Fig 4.10a). By reducing coarse fraction, erosional processes increase slightly on the shallow shelf near the coastline (Fig 4.10b).

➤ **Sensitivity test with deep water wave height**

Similar analyses are carried out with deep water wave height of 2, 4 and 6m (Fig 4.11). Waves are running parallel to the coastline from E to W.

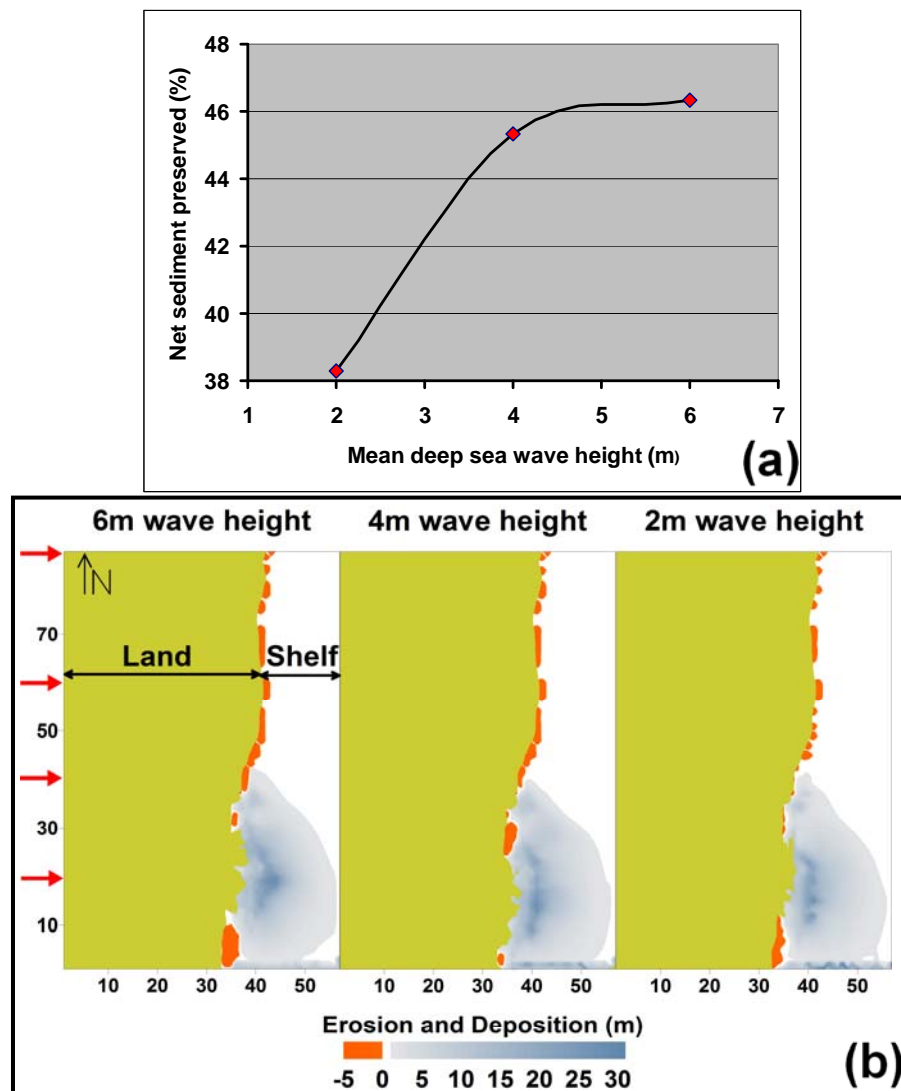


Fig 4.11. Net sediment preservation (a) and erosion/deposition with morphology of the coastline after 1 ky simulation (b) with different deep water wave heights. Red arrows indicate river entries.

Wave heights of 4 and 6 m have almost similar impact on the net sediment preserved on the shelf (Fig 4.11a). By reducing wave height, less sediment is retained in front of the river plume entry and sediment depocentre is elongated by alongshore transport (Fig 4.11b). Alongshore sediment transport is increasing with reduced wave height (thicker formation of deposits at southern grid boundary) (Fig 4.11b). Wave height variations have minor influences on offshore sediment transport. The net sediment preserved on the shelf is decreasing by reducing wave height input (Fig 4.11a). Erosional processes are enhanced on the shallow shelf near the coastline by increasing wave height input (Fig 4.11b).

➤ **Sensitivity test with river sediment input**

11 numerical experiments have been carried out to evaluate the interaction of supplied sediment sources to the shelf sedimentation patterns (Fig 4.12 and Fig 4.13). In all of these simulations, the total amount of sediment supply to the model is the same but we adjust the portions of sediment sources at different simulations. It means that the percentage of sediment discharging to the model from the northern artificial river is increased from 0 to 100 % in the amount of supplied sediments. Fluvial sediment supply is assumed to consist of 20 % of coarse fraction and 80 % of fine fraction. During all of the simulations, we used constant deep water wave height of 6m and waves are running parallel to the coastline from E to W.

Scenario	Total	HST	TST
0	52.0185	59.3177	50.0279
10	52.6398	58.3275	51.0886
20	50.642	54.7385	49.5248
30	47.1999	50.1923	46.3837
40	40.1639	43.9517	39.1309
50	33.5192	43.4885	30.8003
60	30.6122	42.1013	27.4788
70	20.8296	22.308	20.4264
80	18.0295	22.2592	16.8759
90	16.242	32.5483	11.7948
100	15.0993	34.0926	9.91933

Table 4.4. Simulation scenarios and percentage of sediment preserved on the shelf.

The initial surface substratum (subsurface layer) is assumed to contain 20 % of coarse fraction. We use the volume of the stored sediments as a first approach of sediment supply by rivers: 5.45 Mt/y for TST (19.6-8.0 ky BP) and 2.15 Mt/y for HST (8.0-0 ky BP). These

values are derived from the estimated sediment thickness stored on the shelf during HST and TST period in the previous section (section 4.4.2). A general correlation between percentage of sediment supply from the north and net sediment preserved on the shelf is shown on Table 4.4 and Fig 4.14. A linear trend of decreasing in TST thickness when increasing sediment supply from the north can be clearly observed. HST thickness shows steady decrease from the scenarios with 0-60 % sediment supply from the north. HST thickness reaches the lowest value at 70 and 80 % sediment supply from the north and its thickness is increasing with the rising of sediment supply from the north.



Fig 4.12. Erosion/deposition during HST (8.0-0 ky BP) and morphology of the coastline at 0 ky BP with different percentage of sediment supply from the north. Red arrows indicate river entries.

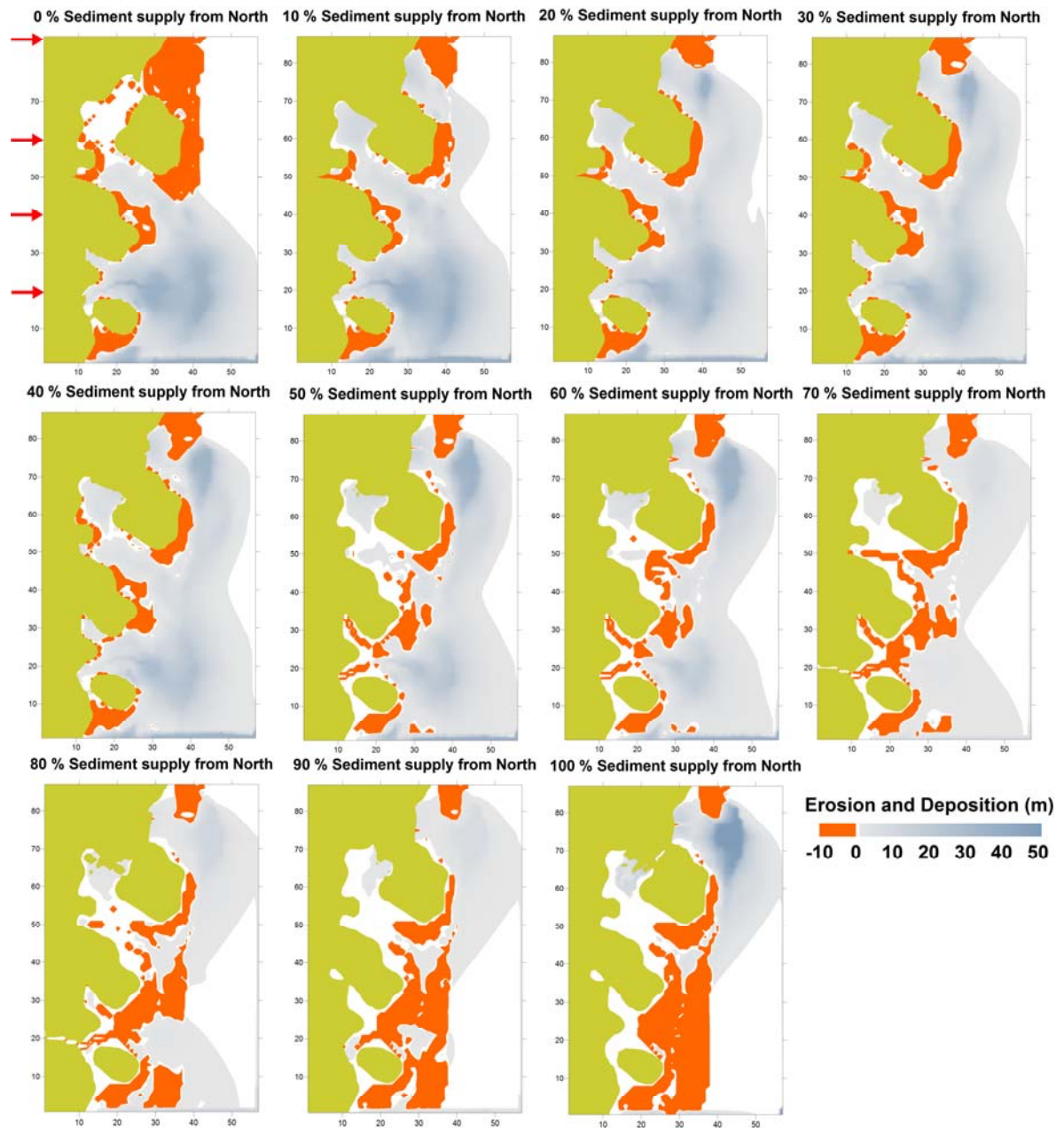


Fig 4.13. Erosion/deposition during TST (19.6-8.0 ky BP) and morphology of the coastline at 8.0 ky BP with different percentage of sediment supply from the north. Red arrows indicate river entries.

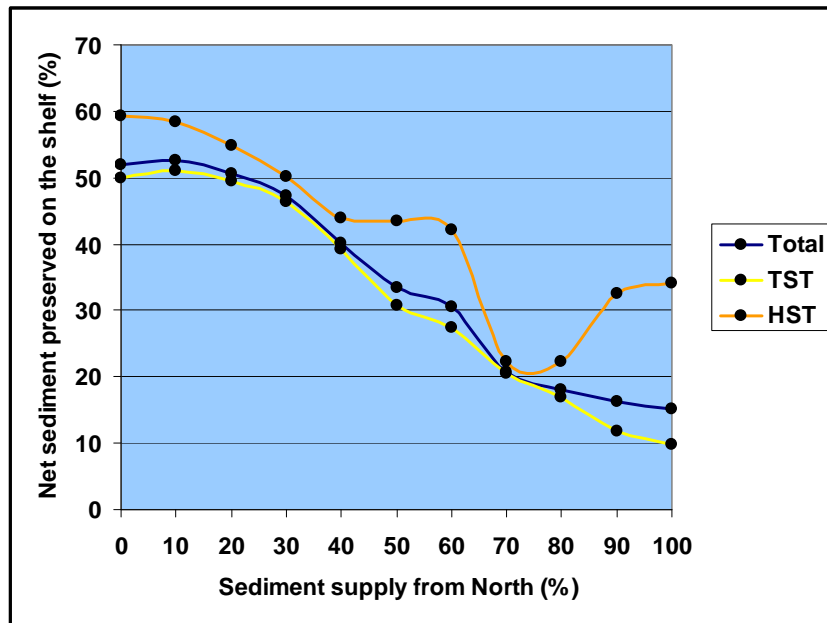


Fig 4.14. Correlation between percentage of sediment supply from the north and net sediment preserved on the shelf.

4.5.2 Predicted sediment supply to the shelf during HST and TST period

Average calculation for the whole central Vietnam Shelf suggest that approximately 40-50 % of supplied sediment are stored on the shelf for the period of 7.6 ky BP to present (Schimanski and Stattegger 2005b). If that is true, only the first six scenarios (0 to 60 % sediment supply from the north) of the above simulations are taken into account. The annual sediment volume stored on the shelf during HST and TST was derived from seismic data (section 4.4.2). Results from numerical modeling sensitivity tests indicate that 42.1-59.32 % of the supplied fluvial sediments have been preserved on the shelf (the first 6 scenarios in Table 4.4). From inverse calculation based on percentage of net sediment preserved on the shelf and the total sediment thickness stored on the shelf, we can predict the annual sediment supply to the Nha Trang Shelf during highstand period (8.0 ky BP to present) as follow: $(2.15 \times 100) / (59.32 - 42.1) = 3.62 \text{ to } 5.1 \text{ Mt/y}$. Comparison between sediment flux from the three local river basins (1.71-4.02 Mt/y) to the estimated amount of supplied sediment to the area (3.62 to 5.12 Mt/y) indicates that the local rivers can account for about 50-80 %. The rest comes from other rivers in the north by alongshore transport. On the other hand, the HST sediment thickness distribution map shows the elongated sediment depocentre located in front of the local river mouths (Fig 4.7), which enhances the importance of the local rivers acting as the primary sediment supply sources for the shelf during the HST period. As observed in the modeling results (Fig 4.12 and Fig 4.13), the offshore sediment transport during HST period rarely reached the outer shelf. Therefore, the major gap between sediment

supply and storage on the shelf during this period is attributed for the alongshore transport parts. The estimated sediment supply from above empirical equations (Tab 4.1 and Table 4.2) is basically based on the present-day parameters of the drainage basins as temperature and basin areas. As deduced from the sea-level curve, shortly after 8.0 ky BP the paleo-coastline reached nearly its modern position (~ -5m below modern level) and its maximum retrogradation occurred around 6.0-5.5 ky BP with sea-level highstand of 1.5 m above modern level. Hence, the difference in river basin areas during HST period was not so significant in comparison to the present-day value. Besides, previous researches on the SCS suggest that the sea surface temperature (SST) was more or less stable since the last 8.0 ky BP (Shintani et al., 2008) or slightly higher during the period of the mid-Holocene highstand (Michelli 2008). Our calculation can therefore represent the average value over the HST period. The uncertainty of calculation with BQART equation (section 4.4.1) lies on the variation of discharge and human impact factors (e.g river damming and deforestation) which have not been investigated so far. Therefore at this stage of the research, these are not included in the calculation.

Calculations from modeling results indicate slightly low TST sediment preservation potential (27.5-50 %). Similarly, inverse calculation of TST sediment supply from the percentage of net sediment preserved on the shelf and the total sediment thickness stored on the shelf will result to: $(5.45*100)/(50-27.5) = 10.9 \text{ to } 19.82 \text{ Mt/y}$. These results suggest that annual sediment supply during TST period is 3 to 4 time higher than that of HST period. The TST thickness map (Fig 4.7) shows only moderate variation suggests from possibly different sediment sources. Since no data about sedimentation during TST period are available for this region so far, a qualitative validation for the estimation results is not done. As a result, the estimated sediment budget for the transgressive (TST) period shows a wide range of variation. Modeling results from previous section show a lower percentage of sediment stored on the shelf during TST period than that of HST period (Fig 4.14). This is reasonable since during the early transgression when the coastline located on the outer shelf, significant amount of sediment from the river mouths were transported to the deep sea as well as transport alongshore to the south (Fig 4.13).

4.5.3 Final simulation of sedimentation on the Nha Trang Shelf

4.5.3.1 Input data

In order to evaluate the above estimations of sediment supply to the shelf, a final simulation has been carried out. Results of shelf sedimentation and coastline evolution over the deglacial period from this simulation are discussed in detail. In the final simulation, sediments enter

the model from the three local river basins (Cai, Dinh and Van Phong) and one artificial river at the northern edge of the grid (Fig 4.15, Fig 4.16 and Fig 4.17). During the simulation, we deploy the above estimated total sediment supply of 5.1 Mt/y for the HST period and 10.9 Mt/y for the TST period.

Input parameters	TST (19.6-8.0 ky BP)	HST (8.0-0 ky BP)
Fluvial coarse grain-size fraction (%)	20	20
Fluvial fine grain-size fraction (%)	80	80
Substratum coarse grain-size fraction (%)	20	20
Substratum fine grain-size fraction (%)	80	80
Deep water wave height (m)	6	6
Initial flow current (m/s)	1	1
Initial substratum thickness (m)	1	1
Cai River discharge (km ³ /y)	7.7	3.3
Dinh River discharge (km ³ /y)	3.7	1.6
Van Phong River discharge (km ³ /y)	1.04	0.28
Nothern River discharge (km ³ /y)	3.04	1.32
Cai River sediment flux (10 ⁶ t/y)	5.23	2.46
Dinh River sediment flux (10 ⁶ t/y)	2.62	1.23
Van Phong River sediment flux (10 ⁶ t/y)	0.872	0.41
Nothern River sediment flux (10 ⁶ t/y)	2.18	1.02

Table 4.5. Input parameters of the final simulation.

Sediment discharge from the local river basins Cai, Dinh and Van Phong is assumed to account for 80 % of total sediment release and the rest is supplied from the northern artificial river. This ratio is applied for both HST and TST simulation period. River water discharges input the model is derived from the rating curve (Fig 4.5). The calculation for the TST period comes out with the assumption that the relative contributions of the three local rivers are similar to HST period. All the other input parameters are kept the same like in the river sediment input sensitivity tests (Table 4.5).

4.5.3.2 Sedimentation over 19.6 ky (Deglaciation/Holocene)

During the early transgression (19.6-14.6 ky BP), sediment was accumulated across the outer shelf due to slow to moderate sea-level rise (0.32-1.57 m/100y) (Fig 4.15). A shore hugging

sediment depocentre can be observed and sediments transport to the deep sea (continental slope) was also very prominent during this period. The abrupt sea-level rise between 14.6-14.3 ky BP (MWP 1A) reduced significantly the sediment deposited on the shelf and coastline was migrated landward approximately 5-10 km during 300 y (Fig 4.15 and Fig 4.16). Slight sediment deposition near the Cai and Dinh River mouths can still be observed.

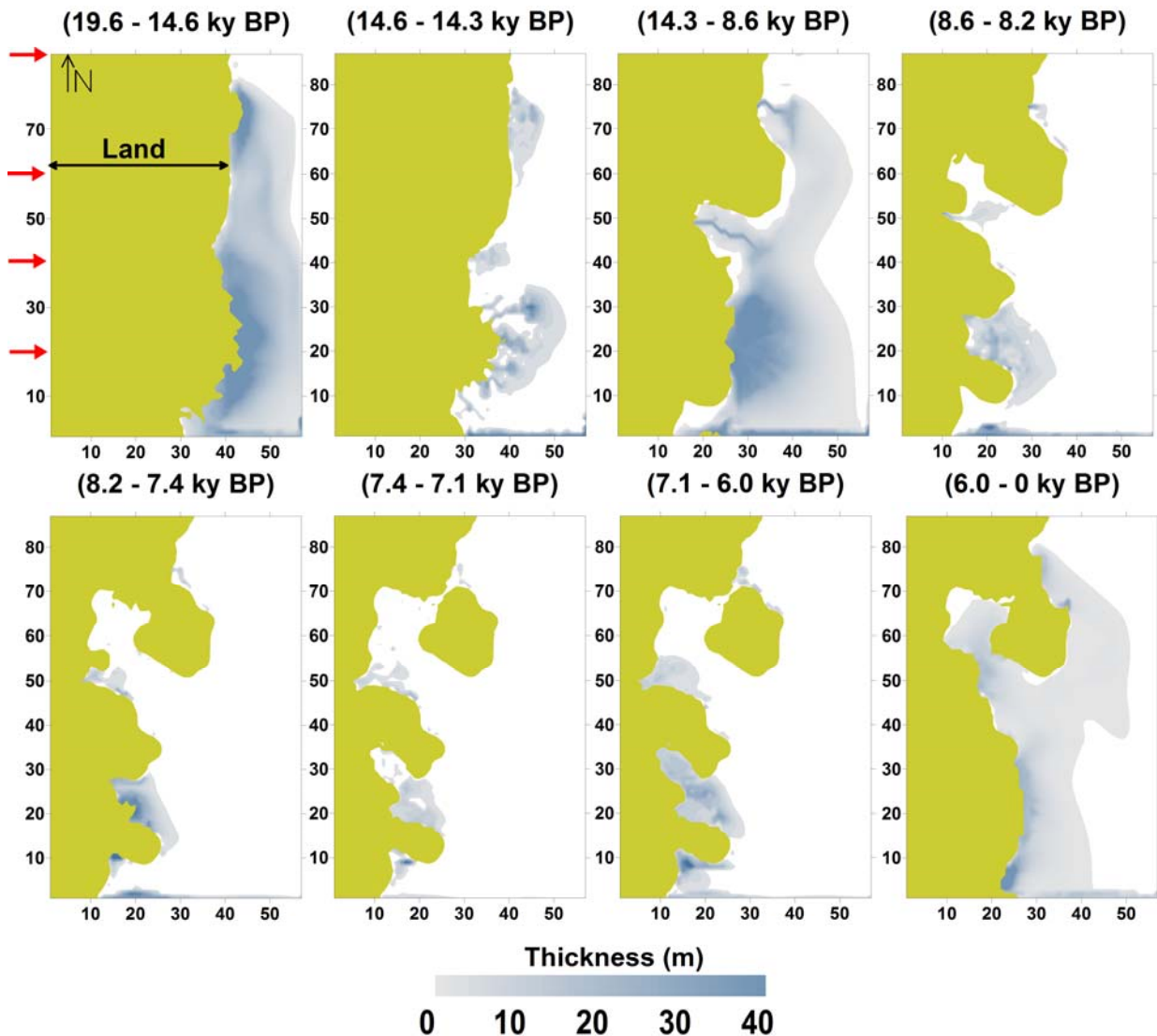


Fig 4.15. Sediment thickness distribution at different periods from 19.6-0 ky BP (Deglaciation/Holocene) with reference to the coastline evolution (Fig 4.16).

However the offshore sediment transport was strongly reduced. The following period (14.3-8.6 ky BP) was marked by high rate of sediment progradation as a result of low sea-level rise resulting in thick sediment accumulation on the mid-shelf. Sediment accumulation was restricted only around Cai and Dinh River mouths during the rapid sea-level rise between 8.6-8.2 ky BP (MWP 1C) and the following period between 8.2 and 7.4 ky BP. Sediment supply from the north and Van Phong River was not significant during those periods. The

short rapid sea-level rise period between 7.4 and 7.1 ky BP has submerge most of Van Phong and Nha Trang and reduced sedimentation over the shelf. In general, both alongshore and offshore sediment transport were strongly reduced during the early HST period. The final sea-level rise period between 7.1 and 6.0 ky BP was marked by high sedimentation around Cai, Dinh and Van Phong River mouths (Fig 4.15). During the period after the sea-level highstand (6.0-5.5 ky BP) to present, sedimentation was increased over the inner and mid shelf due to slight drop of sea-level (Fig 4.15). An elongated shore-hugging sediment depocentre was developed in front of Cai, Dinh and Van Phong River mouths.

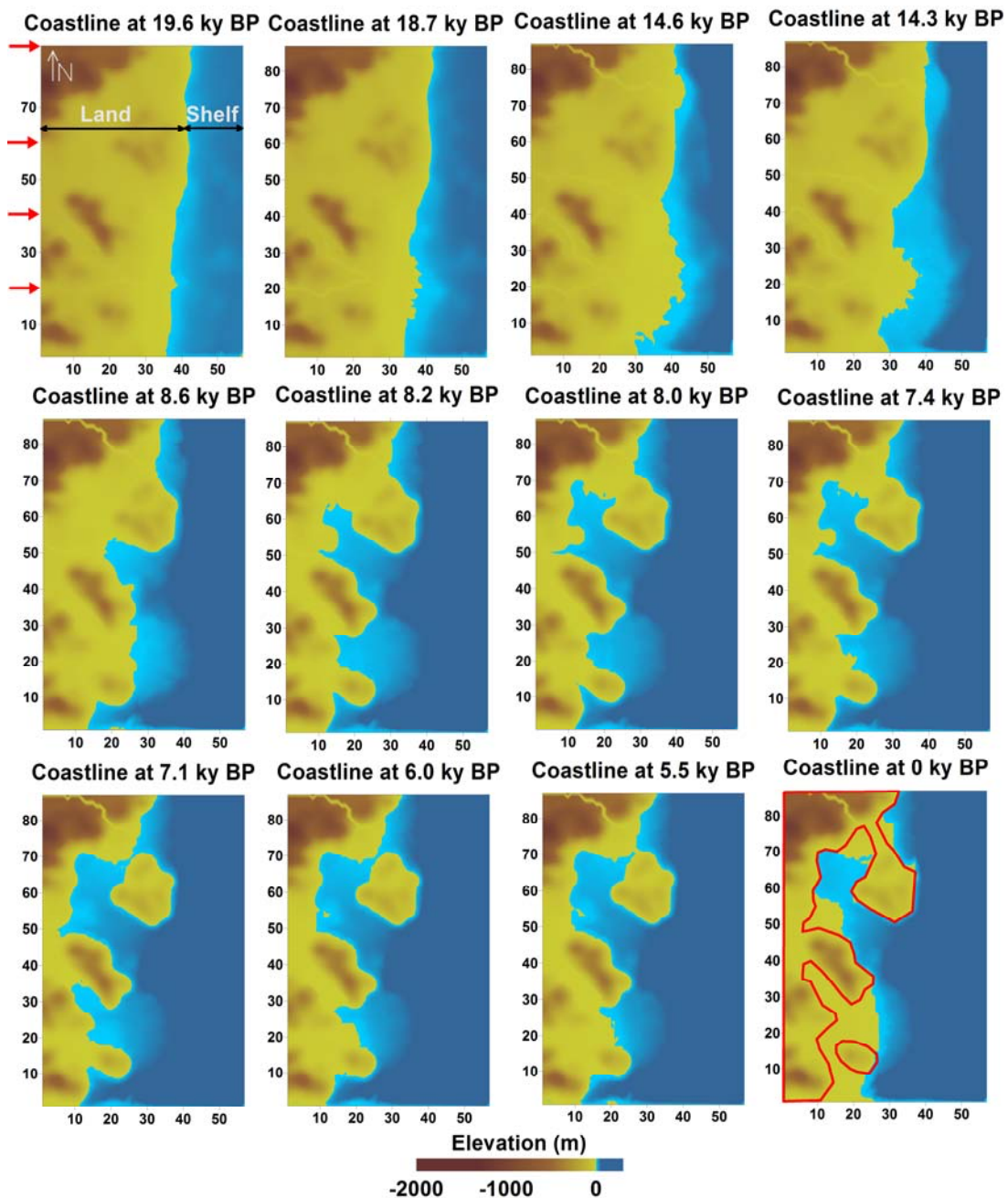


Fig 4.16. Coastline (yellow color) evolution over 19.6 ky (Deglaciation/Holocene) from final simulation. The real modern coastline is shown by red line. Negative values indicate the elevation on land and positive values indicate water depth at sea.

4.6 Discussion

Calculation from the final modeling simulation (Fig 4.15 and Fig 4.17) shows that about 2.9 and 5.6 Mt/y of sediment were stored on the shelf during HST and TST period, respectively. These values are compatible to the results that are derived from seismic data (see section 4.4.2). This suggests that the predicted sediment flux to the shelf is reasonable. The TST thickness map of the model (Fig 4.17) shows quite similar features in comparison to the seismic result (Fig 4.7b). In both TST isopach maps, the sediment thickness is characterized by a low variability over the shelf and reaches the maximum values in the mid-shelf. However, the distribution of HST deposits in the model and seismic data are quite different. The HST isopach map derived from seismic data (Fig 4.7a) shows a clear alongshore mid-shelf sediment depocentre and sedimentation on the inner-outer shelf during HST period is not significant. By contrast, results from the model indicate that most of sediment during HST period is accumulated on the inner shelf (Fig 4.15 and Fig 4.17). Nha Trang and partly Van Phong Bay have been filled up during the HST period (after 6.0-5.5 ky BP) and this results in the difference between model results and existing topography (Fig 4.16).

In general, results of the model simulation are well compatible to field data. Differences between these two approaches suggest that some parameters within the model need to be further adjusted. As shown on the sensitivity tests (Fig 4.10b and Fig 4.11b), wave regime and sediment grain-size of substratum and river input have strong influences on shallow shelf sedimentation but their impacts on deeper shelf sediment deposition are less profound. Alongshore sediment transport is more sensitive to variation of input wave height than offshore transport (Fig 4.11b). The river sediment plume entering the shelf is mostly settling close to the coastline and forms an alongshore-hugging sediment depocentre forced by the marine hydrodynamic processes (Fig 4.10b, Fig 4.11b, Fig 4.15 and Fig 4.17). In order to imitate the detached type of sediment depocentre (similar to the case of HST deposits on the Nha Trang Shelf), the offshore sediment transport algorithm (wave diffusion processes) in the continental module of the model needs to be enhanced. Besides, the Nha Trang Shelf is drained by short and steep-gradient rivers (Fig 4.1) which normally have high plume velocity. Therefore, it is also necessary to increase the input river plume velocity and this can probably spread the sediment depocentre further offshore (Dalman 2009). On the other hand, we use a constant sediment and water discharge from the rivers over the HST and TST period for the final simulation (Table 4.5). However, the variations of water and sediment discharge during the HST period may be influenced by human impacts and may significantly influence the model results. To increase the significance of the model results, an improvement of input database (especially the paleo-river discharge and sediment load) should be considered. This problem can

be solved by coupling the SimClast to other models (e.g Hydrotrend Model, Kettner and Syvitski 2008). Alternatively, it would be interesting to extend the model grid further landward to capture the influences of land topography to the model results during the mid-Holocene sea-level highstand.

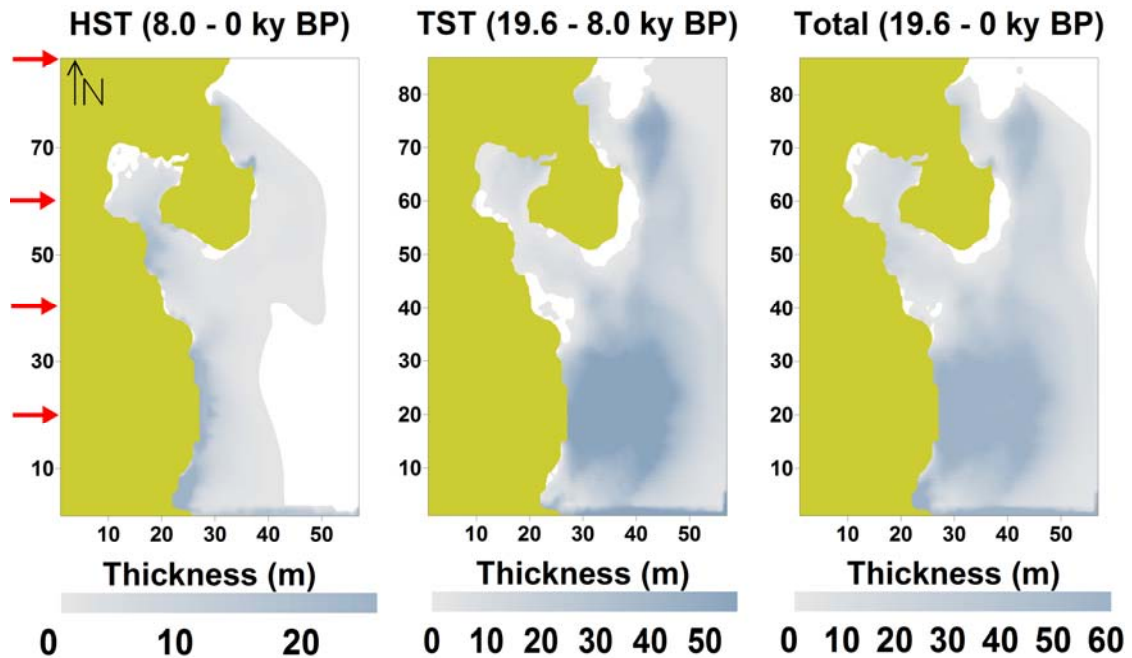


Fig 4.17. Sediment thickness distribution over 19.6 ky (Deglaciation/Holocene) from final simulation with reference to modern coastline.

4.7 Conclusions

The data-modeling approach was carried out to examine the sedimentation on the Nha Trang Shelf from the end of the Last Glacial Maximum (LGM) onward. The results can quantify the sediment budget in this area since the LGM. Some conclusions from the research can be made:

- The annual sediment supply to the Nha Trang Shelf during HST period (8.0 ky BP to present) was predicted by 3.6 to 5.1 Mt/y. Half of total supplied sediments were stored on the shelf. The local river basins Cai, Dinh and Van Phong contributed 50-80% of supplied sediments and the rest was added by alongshore transport from the northern part. Calculation based on empirical equations also suggests that the annual sediment supply during HST is dominated by Cai River which contributes 2 to 6 times more sediment than Dinh and Van Phong River, respectively. During the early HST period, sediment accumulation was retained mainly around the Cai and Dinh River mouths and their rapid seaward progradation over the inner and mid shelf was initiated only after the mid-Holocene sea-level highstand. In general, the major gap between sediment supply to and

storage on the shelf during this period is the southward alongshore transport parts since the sediment is rarely transported to the outer shelf.

- Estimated sediment supply for TST period (19.6-8.0 ky BP) is 3 to 4 times higher than that of HST period. About 30 to 50 % of supplied sediments during TST period were stored on the shelf. The low percentage of sediments stored on the shelf during this period is attributed to significant sediment escape to the continental slope during early transgression as well as to alongshore transport southward. During TST period, high sedimentation rates appear across the shelf and were interrupted only by melt water pulses 1A and 1C.
- Calculated net sediment volume preserved on the shelf using the predicted sediment supply to the shelf is compatible to the results that are derived from seismic data. This suggests that the predicted sediment flux to the shelf is reasonable. The TST thickness map of the model shows quite similar features to the seismic result. However, the distribution of HST deposits in the model and seismic data show several inconsistencies. This suggests that an improvement of input database as well as model calibration is needed.

References

- Barthel K, Rosland R and Thai NC (2009). Modeling the circulation on the continental shelf of the province Khanh Hoa in Vietnam. *Journal of Marine Systems* 77, 89–113.
- Brommer M (2009). Mass-balanced stratigraphy Data-model comparison within a closed sedimentary system (Adriatic Sea, Italy). PhD thesis. University of Delft, 155 pp.
- Bui VD, Stattegger K and Phung VP (in prep). Late Pleistocene-Holocene seismic stratigraphy of Nha Trang Shelf, Central Vietnam.
- Dalman R and Weltje G (2008). Sub-grid parameterisation of fluvio-deltaic processes and architecture in a basin-scale stratigraphic model. *Computers and Geosciences* 34, 1370-1380.
- Dalman R (2009). Multi-scale simulation of fluvio-deltaic and shallow marine stratigraphy. PhD thesis. University of Delft, 156 pp.
- Einsele G (2000). *Sedimentary Basins: Evolution, Facies, and Sediment Budget*. Springer-Verlag, Berlin, Heidelberg, New York, London, Paris, Tokyo, Hong Kong, Barcelona, Budapest, 792 pp.
- Emch M., Feldacker C, Yunus M, Streatfield PK, Thiem VD, Canh DG and Ali M (2008). Local environmental drivers of cholera in Bangladesh and Vietnam. *American Journal of Tropical Medicine and Hygiene* 78, 823–32.
- Hanebuth TJJ and Stattegger K, Grootes PM (2000). Rapid flooding of the Sunda Shelf: A Late Glacial Sea-Level record. *Science* 288, 1033-1035.
- Hanebuth TJJ, Stattegger K, Bojanowski A (2009). Termination of the Last Glacial Maximum sea-level lowstand: The Sunda-Shelf data revisited. *Global and Planetary Change* 66, 76-84.
- Hori K, Tanabe S, Saito Y, Haruyama S, Nguyen V, and Kitamura A (2004). Delta initiation and Holocene sea-level change: Example from the Song Hong (Red River) delta, Vietnam. *Sediment. Geol* 164, 237–249.

Kettner AJ and Syvitski, JPM (2008). HydroTrend version 3.0: a Climate-Driven Hydrological Transport Model that Simulates Discharge and Sediment Load leaving a River System. *Computers & Geosciences* 34(10), 1170-1183.

Liu JP, Liu CS, Xu KH, Milliman JD, Chiu JK, Kao SJ and Lin SW (2008). Flux and Fate of Small Mountainous Rivers Derived Sediments into the Taiwan Strait. *Marine Geology* 256, 65-76.

Michelli M (2008). Sea-level changes, coastal evolution and paleoceanography of coastal waters in SE - Vietnam since the mid - Holocene. PhD thesis. University of Kiel, 160 pp.

Milliman JD and Syvitski PM (1992). Geomorphic/tectonic control of sediment discharge to the ocean: The importance of small mountainous rivers. *J. Geol* 100, 525-544

Milliman JD (1995). Sediment discharge to the ocean from small mountainous rivers: The New Guinean example. *Geo-Marine Letters* 15, 127–133.

National Project KC08.12 (2004). Research on the preventative method of flooding processes on the central Vietnam. Final report, Hanoi, 523 pp (in Vietnamese).

Nguyen XB, Tran DL and Huynh T (1994). Geological Map of Vietnam on 1:500 000 scale. Geological Survey of Vietnam (in Vietnamese).

Pham VN (Editor) (2003). *Bien Dong Monograph. Vol. II –Meteorology, Marine Hydrology and Hydrodynamics*, Hanoi National University Publisher, Hanoi, 565 pp (in Vietnamese).

Schimanski A and Stattegger K (2005a). Deglacial and Holocene Evolution of the Vietnam Shelf: Stratigraphy, Sediments and Sea-level change. *Marine Geology* 214, 365-387.

Schimanski A and Stattegger K (2005b). A conceptual sediment budget for the Vietnam Shelf. *Meyniana* 57, 101–115

Shintani T, Yamamoto M, and Chen MT (2008). Slow warming of the northern South China Sea during the last deglaciation. *Terr. Atmos. Ocean. Sci* 19, 341-346.

Shuttle Radar Topography Mission (SRTM) digital elevation models (<http://srtm.usgs.gov>).

Stattegger K, Tjallingii R, Phung VP and Wetzel A (in prep). Holocene sea-level history of SE Asia and its global implications. To be submitted to *Global and Planetary Change*.

Syvitski JPM and Milliman JD (2007). Geology, geography, and humans battle for dominance over the delivery of fluvial sediment to the coastal ocean. *Journal of Geology* 115, 1-19.

Szczuciński W, Jagodziński R, Nguyen TT, Kubicki A and Stattegger K (2005). Sediment dynamics and hydrodynamics during a low river discharge conditions in Nha Trang Bay, Vietnam. *Meyniana* 57, 117–132.

Szczuciński. W, Stattegger K and Schloten J (2009). Modern sediments and sediment accumulation rates on the narrow shelf off central Vietnam, South China Sea. *Geo-Marine Letters* 29 (1), 47-59.

Ta TKO, Nguyen VL, Tateishi M, Kobayashi I and Saito Y (2001b). Sedimentary facies, diatom and foraminifer assemblages in a late Pleistocene-Holocene incised-valley sequence from the Mekong River delta, Bentre Province, southern Vietnam; the BT2 core. *Journal of Asian Earth Sciences* 20(1), 83-94.

Tamura T, Saito Y, Sieng S, Ben B, Kong M, Sim I, Choup S and Akiba F (2009). Initiation of the Mekong River delta at 8 ka: evidence from the sedimentary succession in the Cambodian lowland. *Quaternary Science Reviews* 28 (3–4), 327–344.

Thanh TD, Saito Y, Huy DV, Nguyen VL, Ta TKO and Tateishi M (2004). Regimes of human and climate impacts on coastal changes in Vietnam. *Reg Environ Change* 4, 49–62.

Tran T (1998). Tuy-Hoa D-49-XXVI geological and mineral resources map of Vietnam on 1:200.000, Department of Geology and Minerals of Vietnam (in Vietnamese).

Chapter 5

General conclusions

The late Pleistocene-Holocene sedimentary architecture on two different geological setting areas along the Vietnam Shelf have been investigated on the basis of shallow seismic data, sediment core data, sequence stratigraphic concepts and numerical modeling. From the results, important overall conclusions can be summarized (Fig 5.1):

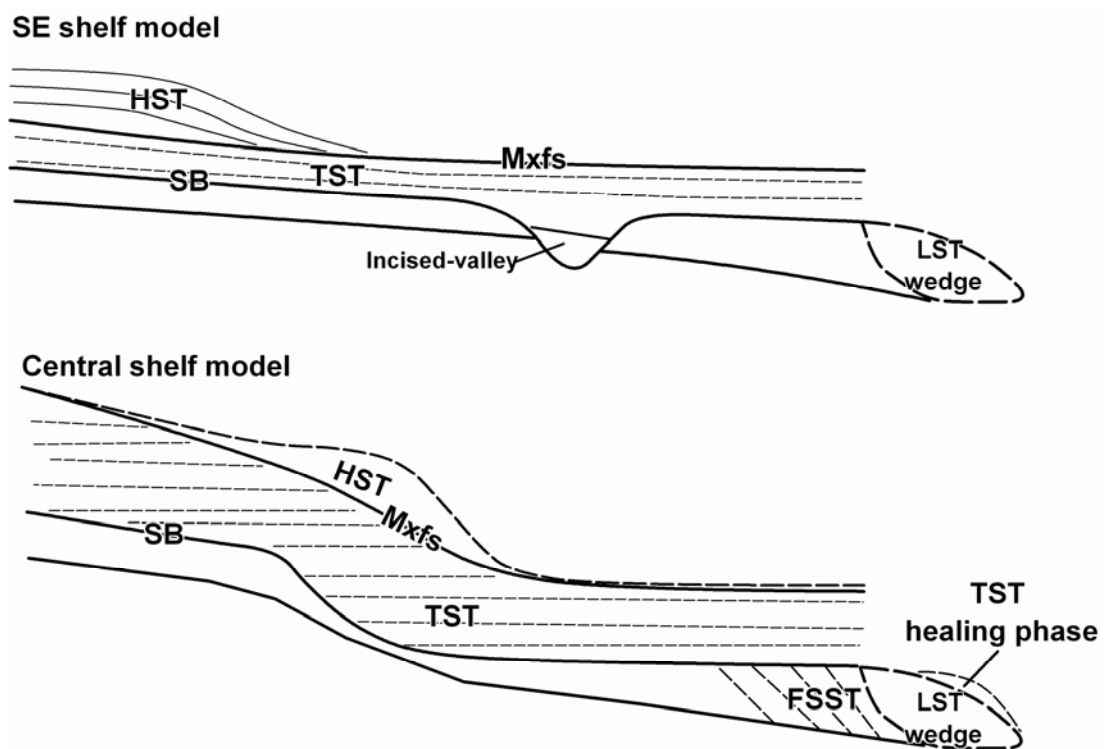


Fig 5.1. Late Pleistocene-Holocene sequence stratigraphic model for the SE and Nha Trang Shelf.

- The SE Vietnam Shelf architecture from the LGM to present (25 ky) is composed of three systems tracts and a prominent seismic reflection surface forming the base of the sequence. This lowstand surface has probably experienced multi-phases of the sea-level fall (regression stage), sea-level lowstand and was reworked again during transgression. An interpolation map of this surface is compiled from seismic profiles and sediment core data revealing the W-E to N-S oriented incised-channel system of the paleo-Mekong river. The incised-channels can be traced from 20 to 60 m of modern water depth and

show a clear change from north to south. The northern incised-channels branch off Vung Tau appears as narrow and deep V-shape in cross-section (<5 km wide and tens of meters deep) which probably resulted from the steep and more accentuated morphology of the shelf. By contrast, the southern paleo-channels show an N-S orientation with a trend of decreasing depth of incision (< 15 m deep) in comparison to the northern ones due to the lower gradient of shelf morphology. LST deposits on the SE Vietnam Shelf consist of a prograding delta wedge and a lowstand erosional surface. The TST was dispersed across the shelf as a layer overlying the sequence boundary SB1. The TST is mostly preserved from marine erosional processes in the incised-valley depressions. The HST is primarily composed of thick prograding mud clinofolds of the modern Mekong subaqueous delta. The HST wedge is pinching out at modern water depths of 20-30 m resulting in a veneer HST layer on the mid and outer shelf which is locally mixed with the lower transgressive deposits.

- Evolution of the Nha Trang Shelf over 120 ky includes four systems tracts: FSST, LST, TST and HST. The FSST and LST were well preserved on the modern outer shelf and they were pinching out landward at water depths of 100-120 m. The LST wedge deposits on the central shelf are only found in the steep gradient shelf off Hon Gom Peninsula and they are almost absent in the other parts of study area. The relict beach-ridge deposits identified at water depth of about ~ 130 m below present sea-level indicate that the LGM sea-level lowstand in this area was lower than on the Sunda Shelf in the South. The difference probably resulted from subsidence due to high deglacial Holocene sedimentation and/or neotectonic movements of the East Vietnam Fault System. The LGM lowstand surface could be traced by seismic profiles across the shelf. This surface shows a relatively high gradient in the middle part and becomes gentler toward the inner and outer shelf as well as from northern to the southern part of study area. TST deposits on the Nha Trang Shelf were accumulated across the shelf with significant thickness. The TST shows a clear transition from backstepping to aggradational stacking patterns from outer to inner shelf which reflects the interplay between rate of sea-level rise, LGM surface gradient and sediment supply. The HST is formed as a shore-parallel mid-shelf clinofold and its thickness decreases toward the inner and outer shelf.
- The late Pleistocene-Holocene sequence stratigraphic models of the SE Vietnam and Nha Trang shelves show distinctive features which result from the differences in sediment supply regime, shelf morphology and hydrodynamic conditions between the two areas (Fig 5.1). On the SE Vietnam Shelf, the thick HST wedge is confined to the inner shelf leaving the mid and outer shelf in starving condition. The HST depocentre on the Nha

Trang Shelf is located on the mid shelf forming a clinoform and it is thinning toward the inner and outer shelf. Such clinoforms are often found in the down-drift direction of river mouths and may extend over several hundred kilometres (Liu et al., 2004, Pratson et al., 2007). The TST deposits on the SE Vietnam Shelf are often thin and widely dispersed over the shelf. By contrast, the TST deposits on the Nha Trang Shelf are stacked much thicker than their counterparts on the low-gradient shelf of the SE Vietnam Shelf. Incised-channels are almost absent on the Nha Trang Shelf but they are well recorded on the SE Vietnam Shelf. LST wedge deposits are recorded in both areas below 100 m water depth on the outer shelf. The LST wedge deposits on the SE Vietnam Shelf are thicker than on the Nha Trang Shelf.

- Calculation from shallow seismic data indicates that the annual sediment volume stored on the Nha Trang Shelf during highstand (HST) period (8.0-0 ky BP) and transgressive (TST) period (19.6-8.0 ky BP) was 2.1 and 5.4 million tons sediment per year (Mt/y), respectively. Calculation based on empirical equations also suggests that the total sediment supply during HST period of the three main local mountainous river basins (Cai, Dinh and Van Phong) ranges from 1.7 to 4 Mt/y, of which the sediment supply from Cai River is 2 and 6 times higher than that of Dinh and Van Phong River, respectively. Results from numerical modeling show that with a given amount of sediment input 42 to 59 % of supplied sediments during HST period are accumulated on the shelf and the rest is mostly transported alongshore southward. Combining these results, we predict that the annual sediment supply to the Nha Trang Shelf during HST period ranges from: 4.1 to 5.1 Mt/y. Among them, about 50-80 % is contributed from the three main local river basins and the rest is transported alongshore from the north. Assuming that the sediment supply ratios between three local river basins are similar during TST period, we can predict the annual sediment supply to the Nha Trang Shelf during TST period by 10.9 to 19.8 Mt/y. This means that the sediment supply during TST period is 3 to 4 times higher than that of HST period. Modeling results show that 27 to 50 % of supplied sediments during TST period were stored on the shelf and significant amount of sediments escaped from the shelf to the continental slope during early transgression as well as were transported alongshore to the south. Sedimentation on the Nha Trang Shelf since the LGM has been estimated by a final modeling simulation using the predicted sediment supply to the shelf. In general, the results of the model simulation are compatible to the field data. Some differences between these two approaches suggest that an improvement of input database as well as model calibration is needed.

References

Liu JP, Milliman JD, Gao S and Cheng P (2004). Holocene development of the Yellow River's subaqueous delta, North Yellow Sea. *Marine Geology* 209, 45–67.

Pratson LF et al. (2009). Seascape Evolution on Clastic Continental Shelves and Slopes, in *Continental Margin Sedimentation: From Sediment Transport to Sequence Stratigraphy* (eds C. A. Nittrouer, J. A. Austin, M. E. Field, J. H. Kravitz, J. P. M. Syvitski and P. L. Wiberg), Blackwell Publishing Ltd., Oxford, UK, 339-384.

Curriculum Vitae

Personal Information

Name: Bui Viet Dung

Gender: Male

Date of Birth: November 19, 1979

Nationality: Vietnamese

- **2007 - 2011** PhD at Sedimentology, Coastal and Continental Shelf Research group, University of Kiel, Germany
- **2006 – 2007** Researcher at Institute for Marine Geology and Geophysics, Vietnamese Academy of Science and Technology, Vietnam
- **2004 – 2006** M.Sc in Coastal Geosciences and Engineering, University of Kiel, Germany
- **2001 – 2004** Researcher at Institute for Marine Geology and Geophysics, Vietnamese Academy of Science and Technology, Vietnam
- **1996 – 2000** B.Sc in Exploration Geophysics at Oil and Gas Department, Hanoi University of Mining and Geology, Vietnam
- **1993 – 1996** Hanoi-Amsterdam High School Specialized in Math, Vietnam